FOULING BEHAVIOR DURING ULTRAFILTRATION OF SKIM LATEX

HO KAR WEI

FACULTY OF ENGINEERING

UNIVERSITY OF MALAYA

KUALA LUMPUR

2013

FOULING BEHAVIOR DURING ULTRAFILTRATION OF SKIM LATEX

HO KAR WEI

THESIS SUBMITTED IN FULFILLMENT OF THE REQUIREMENTS FOR THE DEGREE OF MASTER OF ENGINEERING SCIENCE

FACULTY OF ENGINEERING

UNIVERSITY OF MALAYA

KUALA LUMPUR

2013

UNIVERSITI MALAYA

PERAKUAN KEASLIAN PENULISAN

Nama: (No. K.P/Pasport:)

No. Pendaftaran/Matrik:

Nama Ijazah:

Tajuk Kertas Projek/Laporan Penyelidikan/Disertasi/Tesis ("Hasil Kerja ini"):

Bidang Penyelidikan:

Saya dengan sesungguhnya dan sebenarnya mengaku bahawa:

(1) Saya adalah satu-satunya pengarang/penulis Hasil Kerja ini;
(2) Hasil Kerja ini adalah asli;
(3) Apa-apa penggunaan mana-mana hasil kerja yang mengandungi hakcipta telah dilakukan secara urusan yang wajar dan bagi maksud yang dibenarkan dan apa-apa petikan, ekstrak, rujukan atau pengeluaran semula daripada atau kepada mana-mana hasil kerja yang mengandungi hakcipta telah dinyatakan dengan sejelasnya dan secukupnya dan satu pengiktirafan tajuk hasil kerja tersebut dan pengarang/penulisnya telah dilakukan di dalam Hasil Kerja ini;
(4) Saya tidak mempunyai apa-apa pengetahuan sebenar atau patut semunasabahnya tahu bahawa penghasilan Hasil Kerja ini melanggar suatu hakcipta hasil kerja yang lain;
(5) Saya dengan ini menyerahkan kesemua dan tiap-tiap hak yang terkandung di dalam hakcipta Hasil Kerja ini kepada Universiti Malaya ("UM") yang seterusnya mula dari sekarang adalah tuan punya kepada hakcipta di dalam Hasil Kerja ini dan apa-apa pengeluaran semula atau penggunaan dalam apa jua bentuk atau dengan apa juga cara sekalipun adalah dilarang tanpa terlebih dahulu mendapat kebenaran bertulis dari UM;
(6) Saya sedar sepenuhnya sekiranya dalam masa penghasilan Hasil Kerja ini saya telah melanggar suatu hakcipta hasil kerja yang lain sama ada dengan niat atau sebaliknya, saya boleh dikenakan tindakan undang-undang atau apa-apa tindakan lain sebagaimana yang diputuskan oleh UM.

Tandatangan Calon Tarikh

Diperbuat dan sesungguhnya diakui di hadapan,

Tandatangan Saksi Tarikh

Nama:
Jawatan:

UNIVERSITI MALAYA

ORIGINAL LITERARY WORK DECLARATION

Name of Candidate: Ho Kar Wei (I.C/Passport No: [redacted])

Registration/Matric No: KGA090018

Name of Degree: Master of Enginering Science

Title of Project Paper/Research Report/Dissertation/Thesis ("this Work"):

Fouling behavior during ultrafiltraztion of skim latex

Field of Study: Purification and separation processes

I do solemnly and sincerely declare that:

(1) I am the sole author/writer of this Work;
(2) This Work is original;
(3) Any use of any work in which copyright exists was done by way of fair dealing and for permitted purposes and any excerpt or extract from, or reference to or reproduction of any copyright work has been disclosed expressly and sufficiently and the title of the Work and its authorship have been acknowledged in this Work;
(4) I do not have any actual knowledge nor do I ought reasonably to know that the making of this work constitutes an infringement of any copyright work;
(5) I hereby assign all and every rights in the copyright to this Work to the University of Malaya ("UM"), who henceforth shall be owner of the copyright in this Work and that any reproduction or use in any form or by any means whatsoever is prohibited without the written consent of UM having been first had and obtained;
(6) I am fully aware that if in the course of making this Work I have infringed any copyright whether intentionally or otherwise, I may be subject to legal action or any other action as may be determined by UM.

Candidate's Signature Date 2013 MAY 25

Subscribed and solemnly declared before,

Witness's Signature Date

Name:
Designation:

Abstract

Natural field latex with about 30% dry rubber content (DRC) needs to be further concentrated to about 60% DRC for further downstream processing into a variety of products. A large volume of skim latex (consists of 6-8% DRC) is produced as by-product during centrifugation of natural field latex. Membrane separation process can be used to recover the skim rubber particles as well as the by-product serum from the skim latex stream leading to zero discharge. Current practice requires a wastewater treatment plant to treat the waste to meet the legal requirement before discharging to the environment. As such a study has been initiated to gain an understanding of the fouling behavior of skim latex in terms of permeate flux and fouling resistances during the ultrafiltration of skim latex in order to increase membrane life as well as optimizing cleaning procedure. A bench scale crossflow ultrafiltration unit using single channel tubular ceramic membrane with pore size 0.05µm was used in this study. The effect of operating conditions, i.e. crossflow velocity (1.3 cm/s to 4.6 cm/s) and transmembrane pressure (0.3 bar to 1.0 bar) were investigated. The overall filtration performance showed a similar trend, i.e. initial permeates fluxes start up high and then decreases rapidly. Finally, permeate flux attained pseudo steady state where permeate flux was almost constant at this stage. At crossflow velocity 4.6cm/s, initial permeate flux and permeate flux at pseudo steady state decreased with the increase in transmembrane pressure. At crossflow velocity 1.3 cm/s, permeate flux at pseudo steady state is reduced by about 38% as transmembrane pressure increased from 0.6 bar to 1.0 bar. However, permeate flux at pseudo steady state is increased drastically (263%) as transmembrane pressure increased further to 1.3 bar. This behavior occurred due to the change in the microstructure of fouled membrane as shown in scanning electron microscope images.

Keywords: Ultrafiltration; skim latex; ceramic membrane; fouling

Abstrak

Lateks mentah dari ladang getah dengan kandungan getah hampir 30% kandungan getah kering (DRC) perlu dipekatkan sehingga kandungan getah mencapai 60% DRC sebelum diproses selanjutnya. Semasa process pemekatan, skim lateks (DRC 6-8%) akan dihasilkan sebagai produk sampingan dalam kuantiti yang besar. Proses penurasan dengan menggunakan membran merupakan cara yang ideal untuk memperoleh semula getah dan elemen farmaseutikal dalam skim latek. Amalan yang digunakan dalam industri getah sekarang memerlukan loji rawatan untuk merawat air sisa supaya memenuhi keperluan undang-undang sebelum dilepas ke alam sekitar. Dengan itu, kajian atas kesan parameter operasi kepada proses penapisan adalah sangat penting untuk memahami tingkah laku pengotoran dari segi kadar resapan dan rintangan pengotoran untuk meningkatkan hayat membrane dan mengoptimumkan prosedur pembersihan. Unit penapisan skala makmal dengan membran seramik dengan saiz liang 0.05µm digunakan dalan kajian ini. Kesan halaju aliran dan tekanan dalam proses penurasan membrane telah dikaji. Secara keseluruhan, kadar resapan adalah tinggi semasa permulaan. Kadar resapan kemudian berkurang dengan masa dan menjadi stabil selepas masa penurasan 2000s. Pada halaju 4.6 cm/s, kadar resapan pada permulaan dan semasa stabil berkurang dengan penambahan tekanan dalam membran. Pada halaju 1.3 cm/s, kadar resapan semasa stabil berkurang sebanyak 38% semasa tekanan bertambah dari 0.6 bar ke 1.0 bar. Kadar resapan semasa stabil bertambah pula sebanyak 263% semasa tekanan dalam membran bertambah melebihi 1.3 bar. Hal ini adalah disebabkan oleh pengotoran permukaan membran telah mengubah struktur kotoran pada permukaan membran. Lapisan kotoran pada permukaan membran mempunyai poros yang lebih besar pada tekanan yang lebih tinggi membenarkan resapan yang lebih tinggi. Kajian

juga menunjukkan kadar resapan bertambah dengan halaju aliran. Ini adalah disebabkan oleh tegasan ricih pada permukaan membran dapat melambatkan kesan pengotoran.

Kata kunci: Penurasan ultra; skim lateks; membran seramik; pengotoran

Acknowledgement

I would like to thank my supervisors, Professor Dr. Nik Meriam Nik Sulaiman. She provided me a lot of advices and ideas to keep me moving forward.

I would also like to present my appreciation to University Malaya Research Grant (UMRG Projec#RG007-09AET) & Fundamental Research Grant Scheme (FRGS Project#FP049-2010A) as this research is funded by them. I would also like to thank those people that have helped me during my time of study in the Membrane Lab, Department of Chemical Engineering, Faculty of Engineering, University of Malaya, Malaysia. Without their support and help, to finish the study is impossible. I would also like to thanks Associate Professor Dr. Che Rosmani Binti Che Hassan for giving me advices and help during the research.

Last but not least, I would also present my appreciation to the support and encouragement from my family and friends all along the way.

TABLE OF CONTENT

List of figures

List of tables

List of symbols

ΔP	Transmembrane pressure (bar)
A	Cross sectional area (m^3)
A	Membrane effective surface area (m^2)
BOD	Biological oxygen demand
C_b	Concentration of solute in the bulk
C_m	Concentration of solute on membrane surface
C_p	Concentration of solute in the in the permeate solution
COD	Chemical oxygen demand
I	Fouling potential / resistivity (m^{-2}).
J	Permeates flux (cm^3/s)
J_w	Water permeate flux (cm^3/s)
k	Permeability of the medium (m^3)
k	Permeability of the medium (m^3)
l	Membrane thickness (m)
L_p	Liquid permeability of the membrane
L_{p0}	Initial membrane permeability
Q	The rate of permeate volume (m^3/s)
Q	The rate of permeate volume (m^3/s)
R	Hydraulic resistance (cm^{-3})
R''_m	Membrane resistance after fouling and cleaning
R'_m	Membrane resistance after fouling
R_c	Cake layer fouling resistance (cm^{-3})
R_f	Reversible fouling resistance (cm^{-3})
R_{if}	Irreversible fouling resistance (cm^{-3})
R_m	Membrane resistance (cm^{-3})

R_{rej}	Rejection coefficient
R_t	Total filtration resistance
SS	Suspended solids
T	Filtration time (s)
TDS	Total dissolved solids
v	Filtrate volume (m^3)
μ	Dynamic viscosity (Pa.s)
μ_w	Water dynamic viscosity (Pa.s)
η	Apparent viscosity (Pa.s)

List of abbreviations

Al_2O_3	Alumina/Aluminium oxide
BOD	Biochemical oxygen demand
CFV	Cross flow velocity (cm/s)
COD	Chemical oxygen demand
DRC	Dry rubber content (%)
MFI	Membrane fouling index ($s.cm^{-6}$)
MWCO	Molecular weight cut off
SDI	Silt density index
SS	Suspended solids
TDS	Total dissolved solids
TSC	Total solid content (%)

CHAPTER 1

INTRODUCTION

1.1 Background

Thailand, Indonesia and Malaysia are the three largest rubber producer countries in the world. These countries produced around 70-90% of the world natural rubber production (Table 1.1). Table 1.1 showed that natural rubber production for Indonesia had increased about 26.7% from year 2006 to 2010. Malaysia as the third largest natural rubber producer, produced about 20-23% of the world natural rubber production (*Annual Rubber Statistics Malaysia 2010*; "Malaysian Rubber Export Promotion Council," 2003-2011).

According to Department of Statistics Malaysia, in 2010, Malaysia had exported more than 800 000 tonnes rubber products since year 2000 as shown in table 1.2 (*Annual Rubber Statistics Malaysia 2010*).

Table 1.1: Natural rubber production from 2006 to 2010 (*Annual Rubber Statistics Malaysia 2010*)

	Production of the years ('000 tan metric)									
Countries	2006	%	2007	%	2008	%	2009	%	2010	%
Malaysia	188.0	23.0	153.3	23.0	156.4	22.8	161.2	23.4	142.4	20.5
Indonesia	140.9	17.2	191.0	28.7	208.0	30.3	208.0	30.1	305.0	43.9
China	74.8	9.1	91.0	13.7	69.3	10.1	69.3	10.0	67.0	9.6
Thailand	251.9	30.8	230.4	34.6	251.7	36.7	251.7	36.5	180.4	26.0
Others	163.1	19.9	-		-		-		-	
Total	**818.7**	**100**	**665.7**	**100**	**685.4**	**100**	**690.2**	**100**	**694.8**	**100**

`

Table 1.2: Summary of rubber exports for year 2000-2010 (*Annual Rubber Statistics Malaysia 2010*)

Year	Export	
	'000 tonnes	RM million
2000	978.0	2571.3
2001	820.9	1886.4
2002	887.0	2491.9
2003	946.5	3581.5
2004	1109.1	5210.5
2005	1128.0	5786.6
2006	1137.6	8234.6
2007	1018.1	7335.2
2008	915.5	8111.3
2009	697.6	4459.5
2010	900.9	9210.1

Natural rubber is gaining economic importance in terms of sustainability issues. Large scale natural rubber producers are also prone to the volatile nature of the commodity price movement. According to NST Business Times in September 2012, Malaysia and Thailand are looking at the possibility to develop a joint large-scale rubber and rubber based industries located in the Kedah-Thai border. This effort is taken to stabilize the falling rubber prices as well as to protect the rubber smallholders who are dependent on the commodity for their living.

Natural rubber latex is the main industrial raw material for natural rubber latex products. Natural rubber is a naturally occurring substance obtained from the exudations of *Hevea brasilienesis* rubber tree. Natural rubber is either exported as latex concentrates or processed into dry solid rubber (in sheet, crepe, or block forms).

If solid rubber is required, natural rubber latex is collected and undergoes further processing. In this process, heat is applied to destroy many of the proteins and solid rubber is produced. The industry classifies solid rubber based on its method of

processing and the final purity of the material. It is referred as technically specified rubber (TSR) or sometimes sheet rubber.

In the market, about 10% of all natural rubber is processed into latex concentrate by removing some of the water. Latex concentrate containing about 60% DRC is made from freshly tapped field latex, un-coagulated ("Market Information in the Commodities Area," 2011). During the concentration process of natural rubber latex, large amounts of skim latex with DRC of 6-8% are produced as a byproduct (Thongmak et al., 2009). Rubber particles in the skim latex are recovered through coagulation. Coagulation is the process of destabilization of rubber particles. Acetic acid and formic acid are generally used for coagulation. In practice, the quantity of acid used for coagulation of the latex especially skim latex after centrifuging process is generally found to be higher than the actual requirement. Insufficient acid during coagulation results in incomplete coagulation and cause the rubber particles to enter the effluent stream along with skim serum. The usage of excess acid not only causes acidic effluent but also causes difficulties in coagulation.

1.2 Problem statement

Skim latex is a by-product during concentration process of natural rubber latex with dry rubber content of only 6-8%. It is economically and environmentally desirable to recover these remaining rubber particles in skim latex. However, rubber particles in skim latex are highly stabilized and it is difficult to recover them. The conventional practice by most rubber mills is to use industrial grade sulfuric acid to coagulate the remaining rubber particles. The quantity of acid used is generally in excess of the actual requirement (Van et al., 2007). Acidic skim rubber produced fetches a low price in the market. Furthermore, highly acidic effluent is discharged as waste and released acidic

gas into the environment, posing a series of environmental problems such as malodor and polluting the waterways. In a survey of Vietnam Rubber Factory (Table 1.3), it was shown that about 25m^3 of acidic effluent was released per ton of product produced. The effluent is even more than during latex concentration process. Table 1.4 shows the content of hydrogen sulfite in gaseous emission during processing of natural rubber latex. These data shows that most of the hydrogen sulfite is released at the reception tank. In the centrifuging process, about 0.008-0.012 mg/m^3 was released, an average of about 1.38% of total gaseous emission.

Table 1.3: Wastewater /Effluent discharged per ton of products (Van et al., 2007)

Product	Effluent (m^3)
Skim latex	25
Latex concentrate	18
Miscellaneous	35
Total flow rate	10^6 m^3/ year

Table 1.4: Concentration of ammonia and hydrogen sulfite in gaseous emission from latex processing (Van et al., 2007)

Process	H_2S (mg/m^3)
Reception tank	0.022 – 0.03
Rolling	0.019 – 1.27
Centrifuging	0.008 – 0.012
Drying	0.001 – 0.021
Packaging	0.005 – 0.016

Membrane separation process provides an alternative method of recovery of skim rubber. The main purpose of filtration of skim latex is to concentrate skim latex to about 30% which is almost similar to the rubber content of field latex. Concentrated skim latex can be added into the new batch of field latex for the following centrifugation process or it can be blended for other purposes. Filtration of skim latex

can produce clear serum which is free of rubber as a by-product. The single largest component of the serum is a water soluble carbohydrate which is about 23% by weight of the total non-rubbers. This carbohydrate is an important chemical feed stock for the synthesis of a range of bioactive material (Deng & Deng, 2000). If all the serum from skim latex processing can be exploited, the income from biochemical extraction may well exceed the sales of latex concentrate. The studies by Veerasamy shows that field latex can be concentrated from DRC 30% to 46% using membrane separation technology with a suitable preservation system (Veerasamy et al., 2003).

However, application of membrane separation process in filtration of skim latex has drawback due to fouling problem (Shah & Sulaiman, 2009; Veerasamy et al., 2003; Veerasamy et al., 2009). This phenomenon affects membrane separation efficiency and incurs higher costs in term of membrane replacement and the need for cleaning. Membrane fouling is defined as the accumulation of particles of feed inside or in the pores of the membrane surface. Formation of fouling layers on membrane surface will change the properties on the membrane and thus increase the resistance to permeate flow. Fouling is governed by factors such as membrane pore size, solute loading and size distribution, membrane material and other operating conditions. Understanding the behavior of fouled membranes can lead to optimization of the process system in terms of the flux-fouling relationship. However, there is presently limited study and resources on the fouling behavior during ultrafiltration of skim latex.

`

1.3 Objectives of study

This study focused on the fouling behavior during the ultrafiltration of skim latex. The objectives of this investigation are as follows:

a. To investigate the effects of transmembrane pressure on fouling.
b. To investigate the effects of crossflow velocity on fouling.
c. To investigate the relationship between crossflow velocity and transmembrane pressure on filtration performances.
d. To characterise membrane fouling using various techniques
e. To identify fouling mechanisms of skim latex on membrane surface.

1.4 Significance of study

As mentioned previously, one of the major limitations of membrane separation process of skim latex is membrane fouling. One of the key elements to develop an effective prevention or cleaning methods is to gain understanding of the fouling behavior. A sound characterization protocol can determine the predominant membrane fouling mechanism at different stages of the filtration operation. The complex nature and structure of fouling layers present additional challenges in the study of fouling. Experimental data obtained from the characterization of fouling layer can also be used to develop a protocol to clean the used membrane and assess the effectiveness of various membranes cleaning method; and to optimize the operation of the process.

`

1.5 Outline of dissertation

As shown in Table 1.5, the dissertation is presented in five chapters. Chapter 1 gives a brief overview of the thesis. The problem statement and the significance of the research are also presented in this chapter. In Chapter 2, a review on previous studies and works related to this investigation is presented in order to provide fundamental understanding on the area of research. Research methodology including materials and equipments used in the study is discussed in Chapter 3. In the following Chapter 4, experimental results are presented and analyzed. The fouling behavior during ultrafiltration of skim latex is discussed as a result of different operating parameters. Finally, conclusion derived from the results obtained is summarized in Chapter 5. Additional information is presented in the appendix.

Table 1.5: Summary for dissertation outline

Chapter	Description
Chapter 1: Introduction	Research background and problem statement.
Chapter 2: Literature review	Review on previous works and provide fundamental understanding.
Chapter 3: Methodology	Materials and experimental approaches used in the study.
Chapter 4: Results and discussions	Experimental results and data interpretation.
Chapter 5: Conclusion	Summary on research finding.

`

CHAPTER 2

LITERATURE REVIEW

2.1 Natural rubber latex

2.1.1 Characteristics of natural rubber latex

Currently, almost all fresh natural rubber as the main industrial raw material for rubber products is obtained from Brazilian (*Hevea brasilienesis*) rubber trees. Fresh latex tapped from the rubber tree, known also as field latex, is a cloudy, white liquid, similar in appearance to cow's milk. It is basically a polydispersed biopolymer colloid suspension of rubber particles in an aqueous phase. Dispersed rubber particles consist of isoprene units $(C_5H_8)_n$ arranged as cis-1,4-polyisoprene as shown in Figure 2.1 (Beilen & Poirier, 2007). The mean diameter of natural rubber latex particles from *Hevea brasiliensis* varies from 0.2μm to 3μm (Cornish, 2001). The molecular weight of isoprene monomer in natural rubber latex is a 68Da. Rubber particle of *Hevea brasiliensis* has at an average molecular weight of 1200kDa (Beilen & Poirier, 2007).

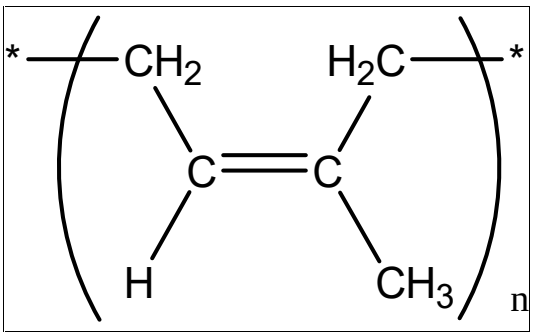

Figure 2.1: Chemical structure of cis-1, 4-polyisoprene in natural rubber

Due to its high molecular weight (>1 million Da), natural rubber possesses high performance properties which include resilience, elasticity, abrasion and impact resistance, and efficient heat dispersion which cannot be matched by synthetic rubber. As shown in Figure 2.2, in natural rubber latex, the particles consist of a rubber core surrounded by a layer of highly specific protein and lipid composition which act as a membrane (Nawamawat et al., 2011). This layer usually carries positive charges at normal pH 6.5. The phospholipids with some positive charges attract proteins which having lower isoelectric points than 6.5 to form a lipid bilayer with hydrophilic heads facing out. The glycosylated moieties and hydrophilic groups of the phospholipids group enable the particles to interact with the aqueous cytosol (Cornish, 2001). This may cause the rubber particles to obtain a net negative surface charge and caused repulsive force between rubber particles and prevents the collision between rubber particles ("All About Natural Rubber Latex," 2009). This phenomenon had improves the latex colloidal stability.

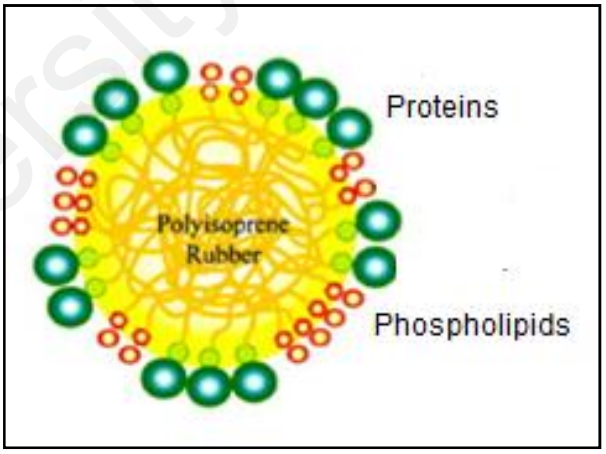

Figure 2.2: Cross section of rubber particles (Nawamawat et al., 2011)

Natural rubber latex consists of about 30% rubber and about 5% non rubber materials such as proteins, minerals, carbohydrates and lipids (Beilen & Poirier, 2007; Danwanichakul et al., 2011). A summary of natural rubber latex composition is shown

in Table 2.1. The study of Cornish also stated that proteins associated with rubber particles of *Hevea brasiliensis* contain of 80 different proteins across a size range of 5 to over 200kDa (Cornish, 2001).

Table 2.1: Composition of natural rubber latex (Heinisch, 1974)

Component	Composition (%)
Rubber	30-40%
Proteins	1.5-3.0%
Resins	1.5-2.0%
Sugars	1.0-2.0%
Ash	0.5-0.1%
Water	55.0-70.0%

As a biological liquid, latex will coagulate within a few hours after tapping due to naturally occurring agents. Spontaneous coagulation of latex is mostly due to the hydrolysis of the lipid substances in the latex which produce fatty acid anions. As a biological liquid, microbial activities in latex during storage produce volatile fatty acids. The presence of divalent metal ions such as calcium and magnesium tend to neutralize the negative charges adsorbed on rubber particles surface. Such reactions reduce the stabilizing layer and thus caused spontaneous coagulation of latex. To prevent such coagulation, a short term preservative, called anticoagulant, is added. Anticoagulants prevent coagulation by offsetting the enzymatic and bacterial influences. The most widely used preservative is ammonia. Presence of ammonia in latex causes hydrolysis of phospholipids and protein retained on rubber particles surface. Hydrolysis of phospholipids produces glycerol, fatty acids anion, phosphate anions and organic base. Every molecule of phospholipids produces two higher fatty acids anions enhancing the net negative charge on rubber particles surface and thus improve its colloidal stability. Proteins also undergo hydrolysis in the presence of ammonia, producing protein with lower molecular weight. Decrease of molecular weight causes the increase in their

solubility in water. Proteins are displaced from the rubber-serum interface causing the reduction in net negative charge on rubber particles surface. This can reduce the colloidal stability of latex. However, hydrolysis of phospholipids is a relatively fast reaction compared to hydrolysis of protein. Therefore, in the presence of ammonia, colloidal stability of latex is improved.

Natural rubber latex exhibits pseudoplastic rheological behavior (Doneva et al., 1998; Krusteva et al., 1999; Sridee, 2006). It has shear thinning properties, i.e. latex viscosity decreases with the increase of shear rate. A plot of viscosity versus shear rate of natural rubber latex at various total solid contents from the study of Sridee was shown in Figure 2.3. The plot proved that viscosity of natural rubber latex was reducing with shear rate. At low shear stress, rubber particles interactions between them make its viscosity high. When shear rate is applied, rubber particles slide and align in the shear direction. As shear rate increases, the interactions between particles can be overcome, and the viscosity of the latex will decrease. Besides shear rate, colloidal system viscosity is also highly dependent on particle size distribution. Viscosity will increased as particle size increase (Sridee, 2006). Total solid content and temperature will also affect latex viscosity. High total solid content increases the interaction between the particles and thus increases its viscosity (Krusteva et al., 1999)

`

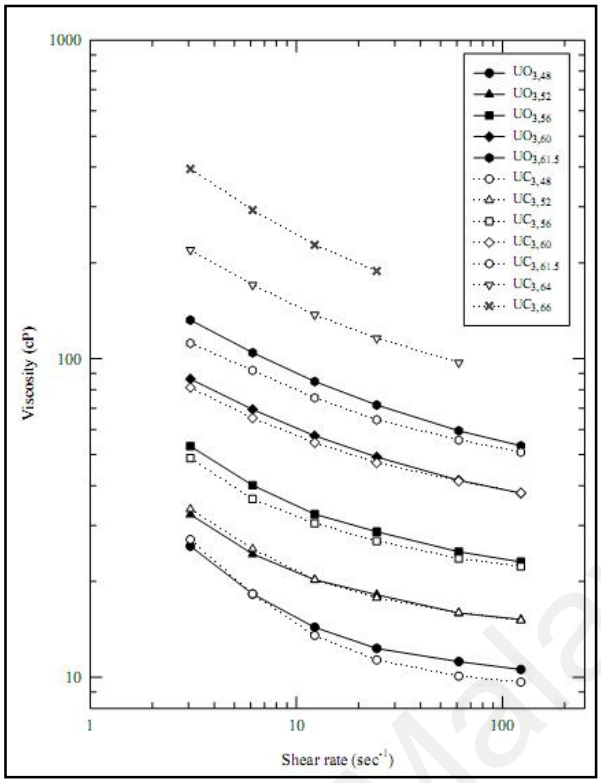

Figure 2.3: A plot of viscosity at 25°C versus shear rate of natural rubber latex at various total solid contents (Sridee, 2006)

2.1.2 Natural rubber processing

As shown in Figure 2.4, natural rubber is either exported as latex concentrates or processed into dry solid rubber (rubber sheet, crepe, or block forms). In the industry, about 10% of natural rubber latex is exported as latex concentrate (Kumar, 2012; Tekasakul & Tekasakul, 2006). Latex concentrate is usually used to make gloves, coating, adhesives and other applications. As mentioned previously, fresh tapped natural rubber latex usually consists of only 30% dry rubber content and it is not economic to produce rubber products at this concentration. It needs to be further processed and concentrated to about 60% dry rubber content before undergoing further product development. Centrifugation, creaming, evaporation and electro decantation are

methods that can be used to concentrate field latex. Two common methods used are creaming and centrifugation. Concentration by creaming uses creaming agents (ammonium alginate and tamarind seed powder) that cause the lighter rubber particles to swell and rise to the top and form cream while the dispersion medium remain at the bottom and form a skim layer. The lower layer is then removed to obtain concentrate latex with about 50-55% DRC. However, it is a slow process and the colloidal stability of properties of the films form is highly affected.

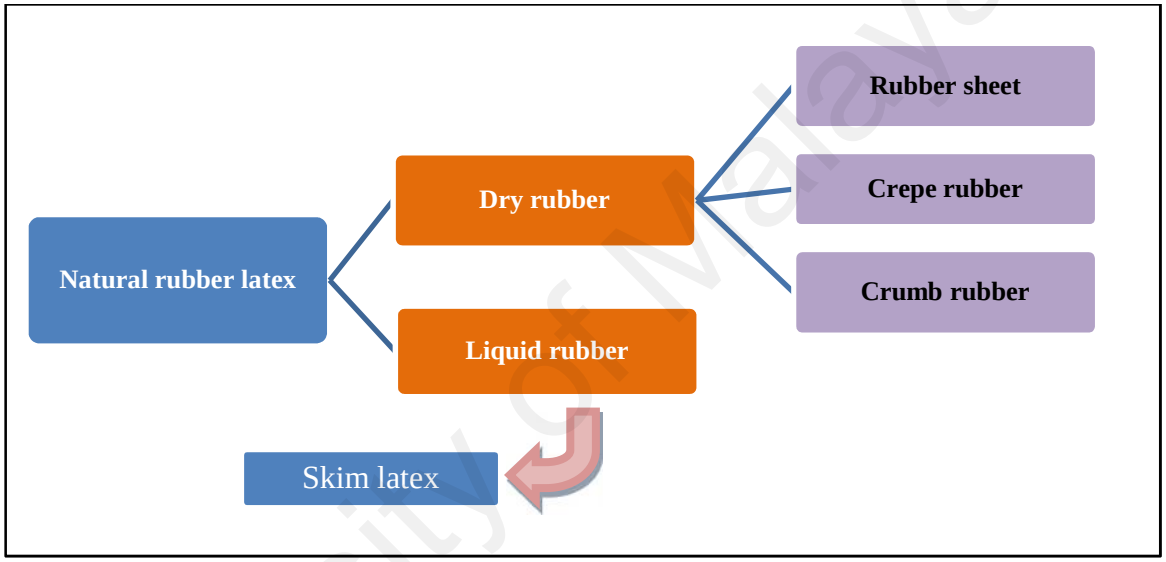

Figure 2.4: Typical natural rubber processing and manufacturing

In Malaysia, about 85 to 90% of latex concentrate is obtained through centrifugation (Veerasamy et al., 2003). In this method, field latex is spun at very high speed. Centrifugal force generated can separate the rubber from serum. The rubber particles will raise to the surface due to its density that is lower than the serum. Centrifugation of field latex produces cream (60% DRC) and skim latex (6-8%DRC) ("How Products Are Made," 2006-2011). One of the best centrifuges used in concentration of field latex is the de Laval centrifuge. In the process, latex is fed into the machine through the center and enters into a number of conical shells within a bowl which rotates at high speed (6000rpm). Rubber particles are separated from the aqueous

phase serum by the means of centrifugal force due to differences in density. Rubber particles with lower densities will rise to the surface as a cream gully (Figure 2.5). However, a portion of small rubber particles are difficult to be effectively separated from the aqueous phase and usually come out together with the serum to produce skim latex. As shown in Figure 2.5, in centrifugation process, only a small portion of proteins, carbohydrates and lipids remained in concentrated latex with the remainder being retained in skim latex.

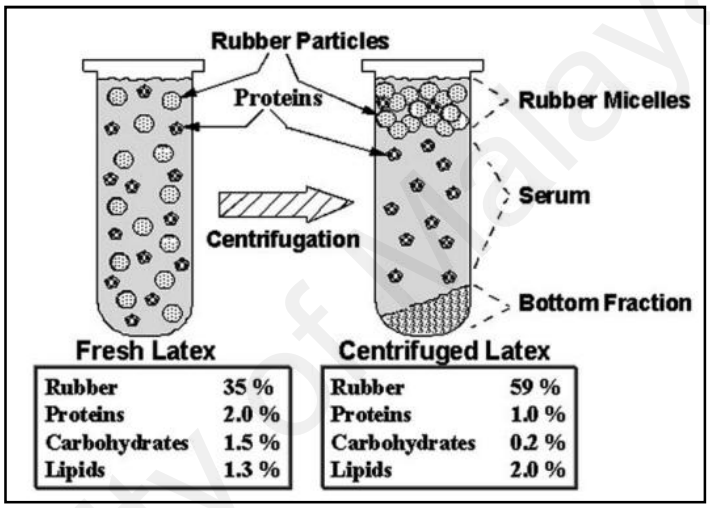

Figure 2.5: Fresh latex and centrifuged latex compositions and its structure (Perrellaa & Gaspari, 2002)

The concentrated latex will be collected, ammoniated and stored for further manufacturing processes. Meanwhile skim latex obtained was deammoniated, coagulated with acid, creped and dried to produce cheap grade rubber block.

2.1.3 Environmental problems and wastewater practice in natural rubber processing

As rubber industry grows with time, the consequence of rubber processing has also lead to a serious environmental problem. The rapid growth in natural rubber products had caused high volume of polluted effluent being released during the processing operations. Typical environmental problems in rubber industry are acidic wastewater with high BOD, COD, SS, high concentration of ammonia and nitrogen compounds, and emit high level of odor. The composition of wastewater from rubber industry also provides a favorable condition for pathogenic bacteria (Van et al., 2007). As comparison, effluent from creaming process is less acidic than effluent from centrifugation process. However, BOD and COD level of the effluent from centrifugation process is much higher. From Table 2.2, effluent from creaming process is more acidic than effluent from centrifuging process.

Table 2.2: Typical characteristics rubber processing wastewater (Van et al., 2007)

Process	pH	BOD (mg/l)	COD (mg/l)	SS (mg/l)	TDS (mg/l)	Sulfide (mg/l)
Latex concentrate (Creaming)	8.95	34900	58752	14142	28307	-
Latex concentrate (Centrifuging)	5.3	3645	5873	1962	13597	-
Ribbed smoked sheet rubber	5.05	4080	8080	-	4120	-

To overcome pollution problem of rubber industry, waste water treatment is introduced to make sure it meets the Malaysian Environment Laws (Environment Quality Act 1974, Act 127). Table 2.3 shows the summary of wastewater treatment practices in the rubber industry. The purpose of the treatment is to remove the remaining rubber particles and solid wastes in the wastewater and to neutralize the

wastewater. However, long retention time and sufficient space are required to carry out all these treatments.

Table 2.3: Summary of waste water treatment practices in the rubber industry (Van et al., 2007)

Wastewater treatment	Description	Constrains
Pretreatment	✓ Rubber trap is installed to trap solid waste by reducing solid waste by 40-60%. ✓ Equalization tanks were used to retain solid waste.	✓ Adequate detention time is required. ✓ Suitable coagulants are required.
Primary treatment	✓ Waste water was neutralized using lime. ✓ Suspended solids were retained using coagulants with adequate retention time. ✓ Sludge obtained will be dried and removed.	✓ Sufficient retention is required.
Secondary treatment	✓ Biological treatment to reduce the quantity of pollutants and suspended solids.	✓ Constrained on land area. ✓ Primary treatment steps need to be incorporated. ✓ Detention time of 2-3days may require.
Tertiary treatment	✓ To remove the remaining residual in the waste.	

2.2 Skim latex

2.2.1 Characteristics of skim latex

During centrifugation of field latex, mainly rubber particles are removed while leaving other components in the serum. Besides rubber particles, proteins and other non-rubber components with higher density than rubber particles will precipitate in the serum during centrifugation process. Skim latex which is produced as a by-product during concentration process of natural rubber latex consists of dry rubber content (DRC) about 6 -8% and total solid content (TSC) of about 7% (Paiphansiri & Tangboriboonrat, 2005). Most of the rubber factories tend to discard skim latex due to its high ratio aqueous phase in the skim. Wastewater from rubber factory need to be treated before released to the environment.

One of the important concerns in natural rubber products is the protein allergenic problem due to the presence of proteins in rubber. Low protein skim rubber has high potential to be used in protective products such as gloves and masks, and other medical related products. Furthermore, the fluidity and interfacial morphology of skim rubber can form smoother films (Rippel et al., 2003). Thus, it is economically desirable to recover the remaining rubber particles in skim latex. On the other hand, it is also environmentally desirable to do so as it can prevent rubber particles to be discharged in the waste stream.

However, it is relatively a difficult task to coagulate the remaining finely dispersed rubber particles in skim latex due to its high colloidal stability. Previous studies show that the average diameter of rubber particles in skim latex (297nm) was 36.4% smaller than the size of rubber particles in the cream latex (467nm) (Danwanichakul et al., 2011; Rippel et al., 2003). Skim latex also contains dissolved ammonia added as preservative making skim serum slightly alkaline (pH 9-10)

(Jayachandran & Chandrasekaran, 1998). High content of protein substances (9-11% w/v) is also present in skim latex (Jayachandran & Chandrasekaran, 1998). The high content of ammonia and proteins had further enhanced the stability of these finely dispersed rubber particles and affect the following coagulation process. Further, these non-rubber components will affect the skim rubber recovered and it's pricing in the market (Haris et al., 2010).

Similar to fresh tapped natural rubber latex, skim latex possesses shear thinning behavior which is referred as pseudoplastic material (Liang & Kai, 2011). Hence, viscosity of skim latex decreases with increasing shear rate. However, viscosity of skim latex is lower than natural rubber latex as the particles size smaller and rubber content in skim latex is much lower. Viscosity of skim latex is dependent on concentration, storage time and temperature (Liang & Kai, 2011).

2.2.2 Processing of skim latex

The conventional method to recover skim rubber is by coagulation with industrial grade sulfuric acid instead of acetic acid and formic acid. Coagulation is the process of destabilization of rubber particles. Usage of acid produces acidic skim rubber and fetched a low price in the market. In acid coagulation, the acid content of the coagulated rubber could reduce rubber quality. The quantity of acid used for coagulation of the latex especially skim latex after centrifuging process generally is found to be higher than the actual requirement. Insufficient acid during coagulation results in incomplete coagulation with in escape of rubber particles into the effluent along with skim serum. The use of acid in skim latex coagulation also leads to generation of highly acidic effluent being discharged from latex rubber industries (~pH 5-6) (Van et al., 2007). The usage of excess acid not only causes acidic effluent but also

redistribute the rubber protein and causes difficulties in coagulation ("Pollution Control Implementation Division - III," 2011). Release of this acidic gas into the environment will cause a series of environmental problems such as malodor and will also affect health. Figure 2.6 shows the typical latex processing in rubber industry. In skim latex processing, skim latex is coagulated with 10% sulfuric acids following by neutralization with 3% NaOH. Crepe rubber produced also need to soak in 0.15% sulfuric acid and 1% phosphoric acid.

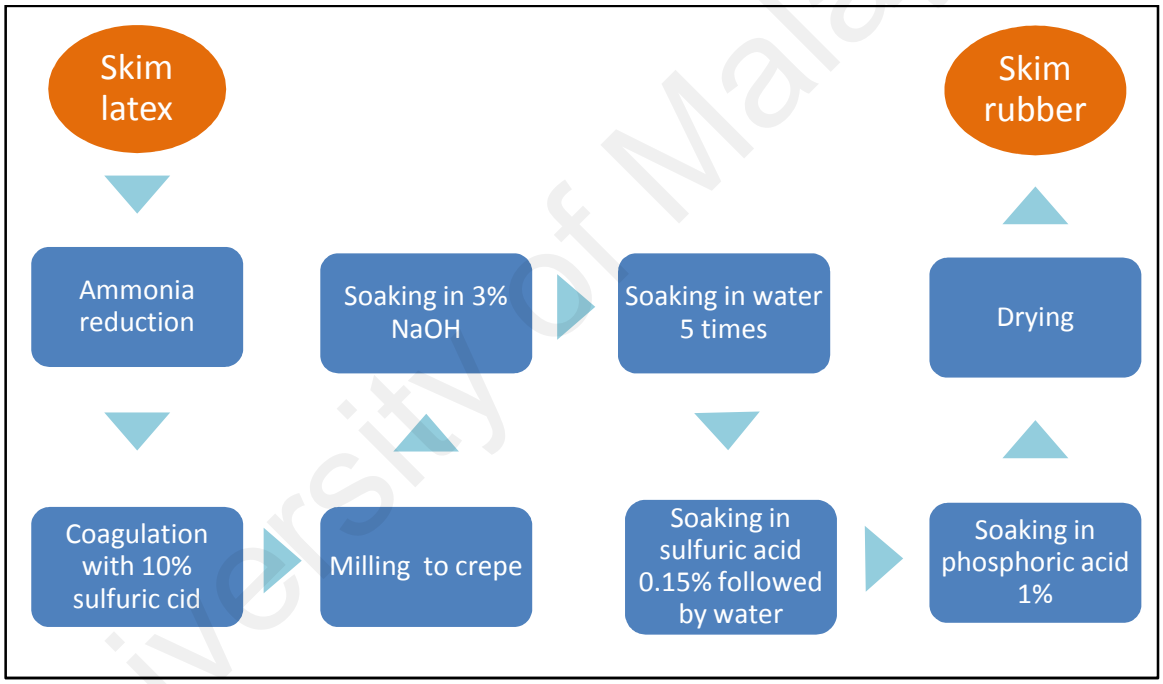

Figure 2.6: Typical processing of skim latex (Haris et al., 2010)

2.2.3 Coagulation of skim rubber

2.2.3.1 Biological method

Coagulation can also be carried out without the addition of acid using biological methods. However, biological method is not commonly used due to various reasons. Skim rubber may normally is of lower quality and is usually associated with offensive smell. Furthermore, biological method usually takes longer time than acid coagulation. Previous study to coagulate skim rubber using Acinetobacter derived from latex centrifugation effluent (Jayachandran & Chandrasekaran, 1998). The results showed that significant amount of coagulation is only observed after incubation of 48 hours. However, COD of residual effluent for biological coagulation is about 80% lower than that of chemical coagulation using sulfuric acid.

Rubber Research Institute Malaysia (RRIM) tends to improve the assisted biological coagulation method by adding sugar from pineapple juice. The results showed that nearly complete coagulation can be achieved in 16 hours. However, the skim rubber produced contains bubbles and is more suitable to convert to block rubber instead of RSS sheet (Cecil & Mitchell, 2005).

Chitosan and polyacrylamide have also been used to coagulate skim latex instead of sulfuric acid (Danwanichakul et al., 2011). The study showed that chitosan can be a promising alternative by giving coagulation-flocculation efficiency as high as 80%. The serum after coagulation with chitosan has a pH closer to 7. Both the skim rubber and serum properties from chitosan system were comparable to the sulfuric acid system but the quality of the serum was better than sulfuric acid. Effluent produced was 69% lower in BOD and 16.9% lower in COD.

`

2.3 Membrane separation technology

2.3.1 Introduction

2.3.1.1 Classification of membrane separation technology

Membrane filtration has emerged as a separation technology which is competitive in many ways with conventional separation techniques, ranging from distillation, adsorption, absorption and extraction. It is more and more widely used in various industries, such as medical application, food industries to waste treatment. Membrane separation process has gained wide acceptance because it is a low energy consumption process, and has no secondary contamination. Four industrial scale membrane separation processes have been developed, i.e. reverse osmosis, nanofiltration, ultrafiltration, and microfiltration.

In simply term, membrane separation process is a process where solids are separated from solution by a semi-permeable membrane which allows the passage of one or more of the components (Porter, 1990). The driving force in all these processes is pressure driven. Figure 2.7 summarizes the separation process relative to common materials that would be filtered out through each process. Separation processes are classified based on the membrane filters pore size and also the approximate particles molecular weight that can be filtered. Table 2.4 shows the types of particles that can be removed for different types of filters. From the summary in Table 2.4, microfiltration membranes allow most of the substances except bacteria and suspended solids to pass through, while reverse osmosis shows the lowest permeability.

`

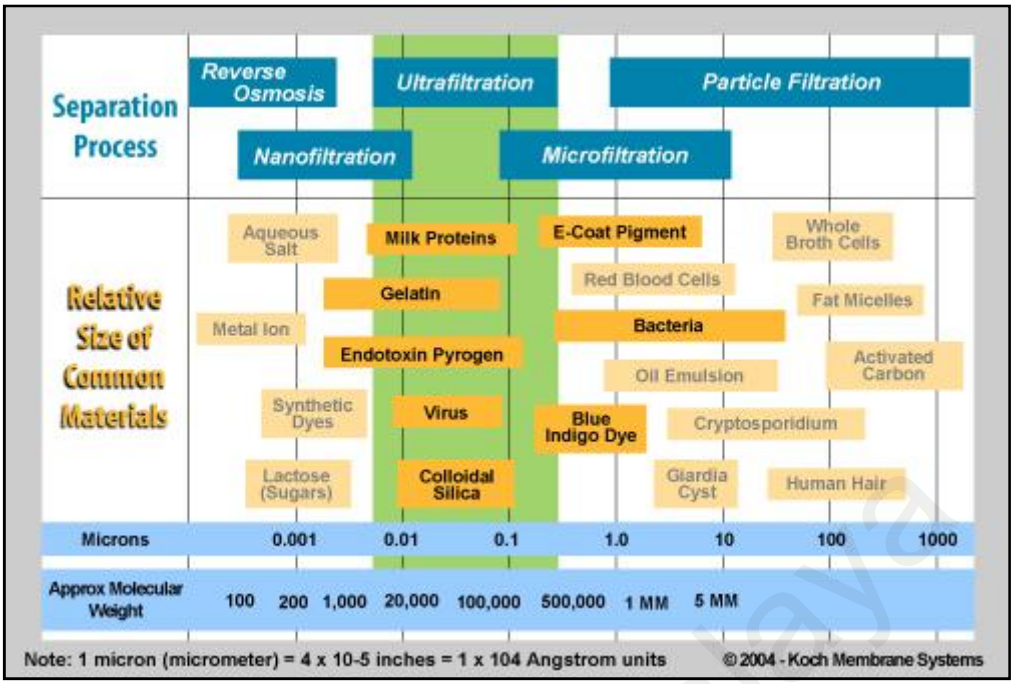

Figure 2.7: Characterization of filtration process based on filtered particles sizes and approximate molecular weight (Jebamani et al., 2009)

Table 2.4: Permeability of various substances in water by membrane filtration processes (Jebamani et al., 2009)

Membrane process	Permeability of particles					
	Water	Monovalent ions	Multivalent ions	Viruses	Bacteria	Suspended solids
Microfiltration	√	√	√	√	χ	χ
Ultrafiltration	√	√	√	χ	χ	χ
Nanaofiltration	√	√	χ	χ	χ	χ
Reverse osmosis	√	χ	χ	χ	χ	χ

Selections of membrane separation processes and membranes are mostly based on the molecular weight cut off. In addition to molecular weight, there are several other factors such as molecule shape and pH that affect permeation through the membrane. Microfiltration can only filter colloidal particles and bacteria in the range of 0.1 to 10µm in diameter. In ultrafiltration, microporous membranes with pore diameter between 1-100nm are commonly used. Therefore, in ultrafiltration, not only colloidal particles and bacteria can be removed, viruses also can be filtered out; with particle

sizes in the range of 0.005 to 0.1 microns or molecular weight cut off (MWCO) ranging from 300000 to around 200 Daltons for dissolved materials. Ultrafiltration membranes usually are classified in term of MWCO, rather than membrane pore size.

2.3.1.2 Modes of Flow (Dead end and crossflow modes)

Membrane separation process can be operated in dead end mode or crossflow mode. In dead end, feed solution flows perpendicularly onto the membrane surface (Figure 2.8). The solution passes through the membrane which is the only exit from the filtration module and solutes which are larger than the pore size are retained on the surface. Particles accumulate and start to build up a cake layer on the surface of the membrane, which will deteriorate the efficiency of the filtration process. Filtration rate decays as the cake layer build up immediately as filtration starts.

`

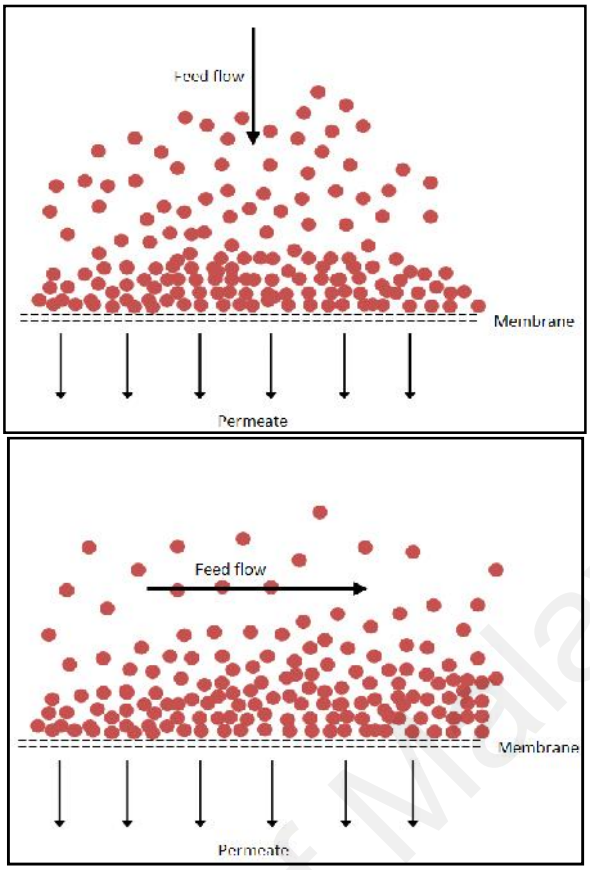

Figure 2.8: Illustration of particles motion in dead end and crossflow filtration

Crossflow filtration, also known as tangential flow filtration, is a process of filtration where by the feed flows parallel to the membrane surface as shown in Figure 2.8. Crossflow filtration is more efficient for separation of colloidal solution and can minimize the fouling layer compared to conventional dead end mode filtration. In crossflow filtration, a feed solution, under pressure, is forced through the center of a porous tube where pressure differential is established between the inside and outside of the membrane. The pressure differences force some of the feed solution and dissolved molecules, which are smaller than the membrane pore size, to pass through the membrane as permeate. Particles that are larger than the pore are retained in the feed solution. Feed solution flows in parallel induces turbulence and creates a continuous scouring action. This force of flow can sweep away particles that accumulate on

membrane surface and re-directed to the bulk solution. Thus, concentration polarization, pore blocking and formation of fouling layer can be reduced

(Cotterill, 1996; "Crossflow Microfiltration ", 2002; Sulaiman & Aroua, 2002; Vyas et al., 2002). The scouring effect in crossflow filtration reduces fouling, maintain the permeate flux for a longer period of use, thus enhances the membrane efficiency and capacity compared to filtration in dead end mode. Further, membranes in crossflow filtration usually can be reused after cleaning and thus reducing production cost.

2.3.1.3 Membrane Materials

A variety of materials has been used for commercial ultrafiltration membranes. It can be made of organic polymers or inorganic materials such as ceramic, glass, metal or organic materials. Among all these materials, polymeric membranes, such as polysulphone and cellulose acetate are the most common. However, cellulose acetate membranes are sensitive to acid or alkaline hydrolysis, high temperature and biological degradation. Thus, various techniques such as polymer blending, surface modifications are used to improve their performance and reduce fouling (Akoum et al., 2005; Belfer et al., 1999).

2.3.1.4 Membrane Properties

2.3.1.4.1 Pore size or molecular weight cut off (MWCO)

Membranes actually do not have a specific value for pore size due to its material and processing conditions. In membrane separation processes, membranes are characterized by membrane pore sizes or molecular weight cut-off. In ultrafiltration,

membranes are characterized in term of molecular weight cut off rather than membrane pore size. Molecular weight cut-off is defined as the molecular weight of the globular protein that is 90% rejected by the membrane. Flux reduction decreases as membrane molecular cut off increase (Howell, 1995). The main reason is that protein forms a monolayer in large pores while in small pore size, protein molecules tend to plug the pores (Howell et al., 1993). It had been proved that permeate flux decays slowly for membrane with large pore size because large pore size leads to lower membrane resistance (Hwang & Huang, 2009).

2.3.1.4.2 Porosity

Porosity is the pore volume divided by the volume of the material. Porosity can be measured by analyzing image of membrane obtained from microscopic analysis (Kennedy et al., 2008).

2.3.1.4.3 Membrane permeability

In order to assess the membrane permeability, Carman-Kozeny equation can be used to describe the convection transport in term of volume flux as a function proportional to applied pressure.

$$J = L_p \,.\, \Delta P \qquad \text{(Equation 2.1)}$$

Where J is the water permeate flux, L_p is the liquid phase permeability of the membrane and ΔP indicates the transmembrane pressure. The initial microfiltration and ultrafiltration membrane permeability, L_{p0}, can be characterized from the pure water

flux. Initial membrane permeability is then estimated through Carman-Kozeny equation. Pure water flux is highly dependent on membrane pore size and its size distribution.

2.3.1.4.4 Surface / pore charge

Membrane surface charge is very difficult to measure. However, membrane surface charges can be estimated through measurement of zeta potential. The zeta potential of membrane surface was calculated from the measured streaming potentials using the Helmholtz-Smoluchowski equation (Cho et al., 2000; Costa et al., 2006; Hong & Elimelech, 1997). Zeta potential is the electric potential at the shear plane of a particle. In colloidal system, zeta potential can be related to the stability of colloidal suspension. The surface charge implies different fouling tendencies. The zeta potential of membrane depends on the nature of ions present in the solution, i.e. pH of the solution (Hong & Elimelech, 1997; Mart et al., 2003). In previous study, membranes become less negative with increasing divalent cation concentration (Hong & Elimelech, 1997). At high ionic concentration, membrane surface charges had been reduced. This had caused the decrease in electrostatic repulsion between the membrane surface and feed solution, which eventually leads to more severe fouling layer (Hong & Elimelech, 1997; Seidel & Elimelech, 2002) . Thus, the zeta potential of membrane is actually depends on the ions present in the feed solution (Seidel & Elimelech, 2002). Negatively charged feed solution is more effectively separated with negatively charged membrane (hydrophilic) than solution with positive charges. Since most solutions tend to be negatively charged, hydrophilic membranes are preferred for separation process (Ernst et al., 2000). More hydrophilic membranes can lead to less adsorption and fouling during separation process. Particles adsorption is highly affected by the zeta potential and the solution pH (Ernst et al., 2000).

The isoelectric point is the pH at which a particular molecule or surface carries no net charges (Mart et al., 2003). Isoelectric point of a solution is highly affected by the change of electrolyte concentration in the solution. This point is very important as it is normally the point where the colloidal system is least stable ("Zetasizer Nano series technical notes,").

2.3.2 Fouling in membrane separation process

2.3.2.1 Fouling mechanisms

In membrane filtration, fouling is referred to the blocking of membrane pores by the deposition and adsorption of particles on membrane surface or within the membrane pores (Kennedy et al., 2008). Fouling is a general term to describe the deterioration of membrane performance.

In dead end filtration process, the solution flows normally to the membrane surface. Particles passed through the membrane when subject to the driving force. While in crossflow filtration, the feed flows tangentially to the surface of membrane. Particles are pushed through the membrane when transverse driving force is applied at the feed side. Thus, particles move in pressure driven crossflow filtration as a result of the balances of transverse flow and tangential flow forces (Song & Elimelech, 1995). Transverse flow is determined by the combination of applied pressure, membrane resistance and the extent of concentration polarization (Song & Elimelech, 1995). Feed solution is continuously supplied into the system in order to maintain the pressure gradient. Permeate is obtained at the other side of membrane. Retentate is removed at further downstream. Rejected particles are either diffused back into the bulk solution or deposited on the membrane surface. Tangential flow tends to reduce the accumulation of particles on membrane surface by sweeping away the accumulated particles.

As filtration continues, the concentration gradient of rejected particles on membrane surface increases and form a concentration polarization layer. The layer acts as a second resistance layer to permeation and reduce permeate flux. This had attributed to the rapid decrease in permeate flux at the initial stage of filtration process. In previous studies of the application of membranes separation technology in latex suspensions, a typical flux performances with time was obtained as shown in Figure 2.9 (Doneva et al., 1998; Krusteva et al., 1999). Experimental results show that initial pore blocking can be occurred during the first few minutes of filtration and does not increase further later on (Mourouzidis-Mourouzis & Karabelas, 2006). The fast initial pore blocking is usually irreversible.

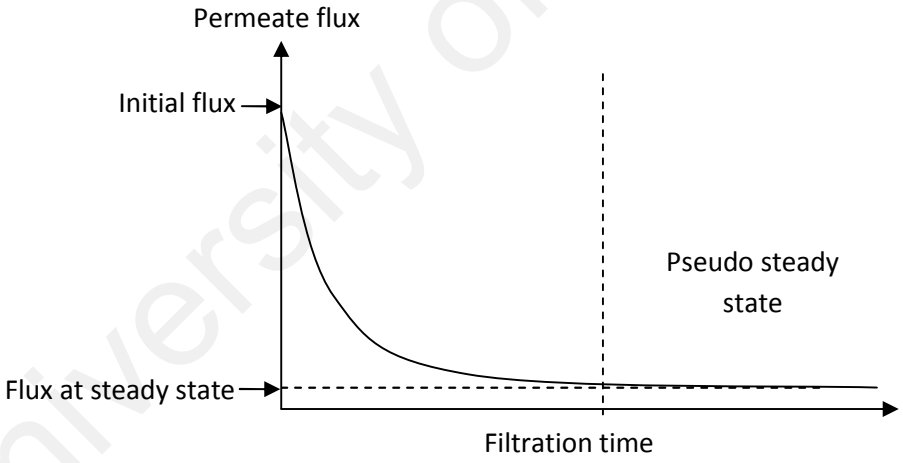

Figure 2.9: A typical flow of permeate flux as a function of filtration time

The rate of particle deposited onto the polarized layer is the result of balance between the convection motion of the permeate through the membrane and the particle back transport mechanism away from the surface (Mondor & Moresolib, 2002). A cake or gel layer starts to form when filtration is prolonged. When the rate of deposition is almost equal to the rate of particles inertial lift back to the bulk solution, a pseudo

steady state is reached (Hwang & Huang, 2009). At steady state, the concentration polarization layer reached a thickness that is about constant with time. The properties of the cake layer formed in turn determine the performance and characteristics of the filtration process.

In membrane separation process, the process performances are characterized by flux and its selectivity. Flux indicates the productivity of the process and is defined as the rate of flow of fluid through the membrane per unit area of the membrane. Selectivity is the ability of the membrane to select one or more components to pass through the membrane while rejecting the others. It can be expressed in terms of retention or separation factor. Both selectivity and productivity are highly dependent on membrane and feed solution characteristics.

Fouling can be classified into washable (reversible) and non-washable (irreversible) phenomenon. Reversible fouling usually is easily removed by hydraulic flushing or backwashing after filtration. Reversible fouling usually points to the deposition of particles on membrane and in the membrane pores. On the other hand irreversible fouling refers to fouling due to strong physical or chemical adsorption of particles onto the membrane surface and pores (Faibish & Cohen, 2001). Thus, irreversible fouling is difficult to remove through physical backwashing (Kennedy et al., 2008). Reversible and irreversible fouling are major obstacles in membrane separation technology. Severe fouling can deteriorate the filtration performance causing a decline in permeate flux, increase in solute rejection and affect the quality of permeate. It may increase the operation downtime and operating costs due to the need for intensive membrane cleaning or membrane replacement due to shorter life span.

Reversible and irreversible fouling can be a result of several mechanisms (Matsuura, 2004):

`

a) Pore blocking

b) Adsorption of solute on membrane surface

c) Concentration polarization

d) Cake or gel formation

2.3.2.1.1 Pore blocking

The motion of particles in crossflow filtration system is the result of tangential and transverse flow. Particles brought onto the membrane surface may not adsorb on the membrane surface, but the solutes may physically block the membrane pores due to sieving mechanism. The solutes may block the pores totally or may block the pores partially and caused pore restriction. It is irreversible and can be partly removed through backwashing. Pore blocking reduces the membrane porosity and thus decline in permeate flux as shown in Figure 2.10 (Costa et al., 2006).

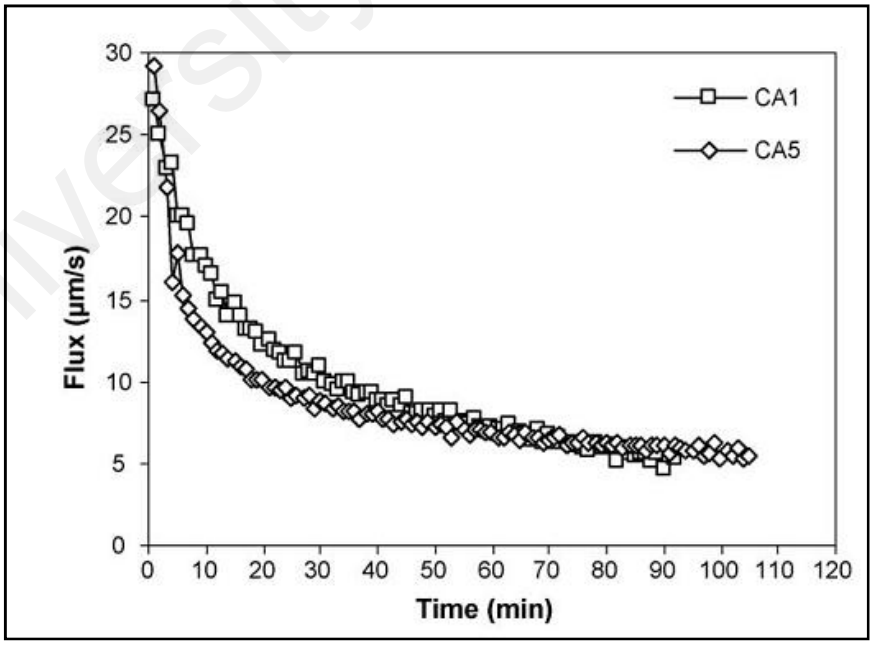

Figure 2.10: Change of permeate flux with filtration time of colloidal natural organic matter solution in a dead end filtration system (Costa et al., 2006)

The effect of pore blocking is more significant in microfiltration due to larger pore sizes which allow particles to penetrate and be deposited in the membrane pores. For ultrafiltration, fouling is mostly on the membrane surface (Marshall et al., 1997). The extent of pore blocking highly depends on the amount of particles arriving at the membrane surface, the amount of particle accumulation and filtration rate during filtration process (Hwang et al., 2007). However, filtration resistance due to pore blocking (R_{if}) is relatively small and can be negligible compared to filtration resistance due to cake (R_c) and concentration polarization (R_p) as shown in Figure 2.11 in the filtration of BSA (Hwang et al., 2006).

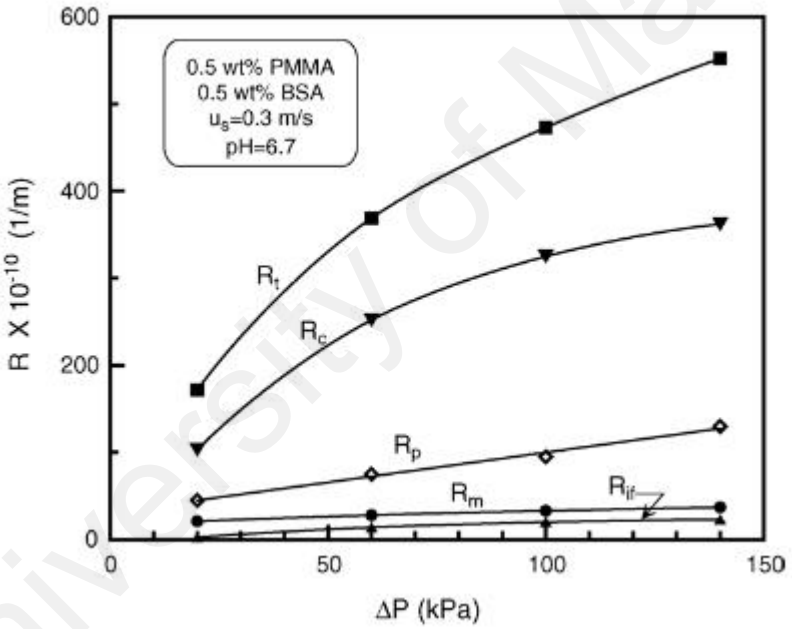

Figure 2.11: Effects of filtration pressure on the filtration resistances due to different sources (Hwang et al., 2006)

2.3.2.1.2 Adsorption of solute particles on membrane surface

Adsorption of particles on membrane surface may be the result of physical-chemical interactions due to electrostatic forces, hydrogen bonding, hydrophobic interactions and charge transfer. The interaction of particles-membrane is highly

affected by the particles properties and also membrane surface. Surface charges may affect the solution properties such as pH and ionic strength. Particles adsorption on membrane surface may be reversible, partially reversible or irreversible. As observed in the adsorption of albumin and γ-globulin on quartz, two stages were observed (Rodgers, 1999). Initially, proteins bound to the membrane surface are reversible. The particle can either diffuse back into the bulk solution or remain at membrane surface. As filtration prolonged, the applied pressure may cause the protein molecules to undergo conformation changes and lead to irreversible fouling. The extent of particles adsorption is also highly dependent on the operating conditions, such as solution concentration, transmembrane pressure and crossflow velocity.

2.3.2.1.3 Concentration polarization

Concentration polarization is reversible accumulation or deposition of retained particles on membrane surface during filtration. At the initial stage of filtration process, a fraction of solutes penetrates through the membrane while the others may be retained on the membrane surface or diffused back to the bulk solution. The retained particles result in a layer with a relatively high concentration at the membrane surface. This concentration polarization layer is usually more viscous and caused the increase in hydraulic resistance to permeate flow. The extent of the effect of concentration polarization layer is highly dependent on the extent of particles accumulation and its structure. The concentration polarization layer can either form a cake layer or increase the osmotic pressure at the membrane surface (Oers et al., 1992). The most important effects of concentration polarization is the reduction in permeate flux and increase in solutes retention and selectivity. Filtration of bentonite solution in previous study showed that still images captured during filtration showed that phenomenon of

concentration polarization featuring fluidized and stagnant layer was observed as shown in figure 2.11 (Marselina et al., 2009).

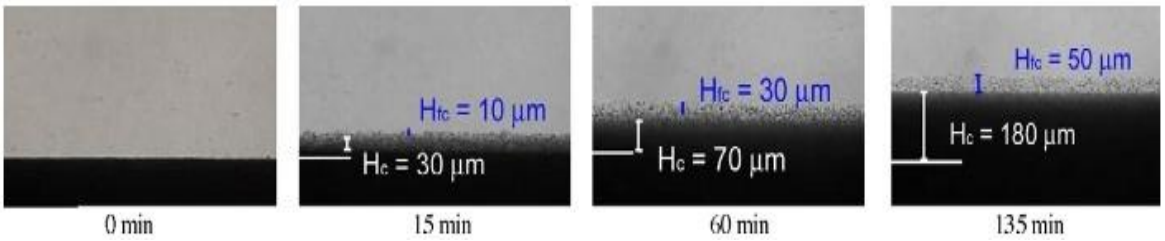

Figure 2.12: Still images captures for the changes in fouling deposition for bentonite filtration (Marselina et al., 2009)

However, flux decline due to concentration polarization is reversible and can be simply recovered by using water (Hwang et al., 2006; Singh, 2007). The extent of concentration polarization is highly dependent on operating conditions. As transmembrane pressure increases, more particles are brought to the membrane surface and encourage the formation of concentration polarization layer (Song & Elimelech, 1995). On the other hand the increase in crossflow velocity tends to reduce concentration polarization due to its scouring effect. In addition, the increase in solution concentration also caused the formation of concentration polarization layer.

2.3.2.1.4 Gel or cake layer formation

As filtration prolongs, particles deposition on membrane surface increases with time. As noted earlier particles concentration in concentration polarization layer also increasing with time. As solute concentration exceeds the critical limit, a cake or gel layer is formed. The particles interact between each other and caused a transition from concentration polarization to a cake layer with a compact structure. The cake layer acts as a secondary barrier and imposed hydrodynamic resistances on further particles through the membrane. Thus, permeate flux decreases and solute rejection increases.

Further increases in transmembrane pressure will increase the concentration of particles on membrane surface and the thickness of gel layer.

According to the compression model suggested by Hwang et al (2009), the typical cake compression mechanism of soft colloids can be divided into four stages. As filtration starts, particles were brought onto membrane surface and deposited randomly to form a concentration layer. At this stage, particles retained their original shape. As more and more particles are deposited on the membrane, the continued compressive pressure rearranged the particles into a more compact structure. The particles start to deform in shape as filtration continues, especially particles located next to membrane surface, to form a skin layer. This stage of particles compression is called localized deformation. As particles deformation continues and extend throughout the cake layer, homogeneous deformation occurs and a gel layer with high hydrodynamic resistance is formed. It was also found that the cake layer is more easily formed at high transmembrane pressure and low crossflow velocity (Vela et al., 2008).

`

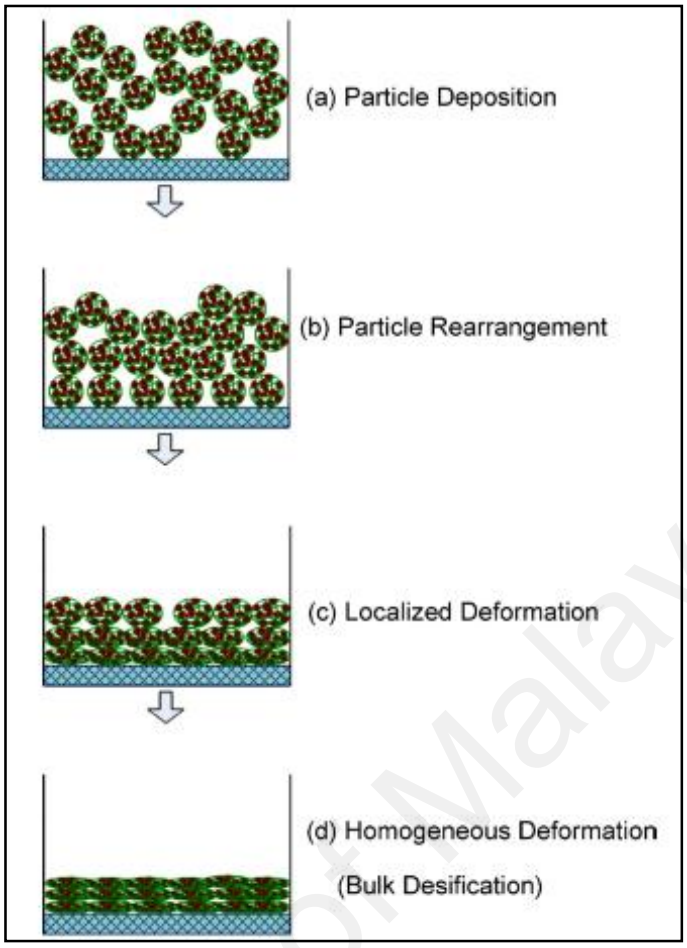

Figure 2.13: Four stages of cake compression during filtration of soft particles (Hwang et al., 2006)

The formation of gel or cake layer is affected by the operating conditions and the feed properties such as feed solution concentration and applied transmembrane pressure. As the feed solution concentration increases, more solute particles are brought to the membrane and reached the critical concentration. Increase of transmembrane pressure tends to compress the particles and encourage the particles to interact and caused phase transitions. It was also observed that new particles depositions are more likely to occur around the existing deposits spot (Li et al., 2000).

2.3.2.2 Limiting and critical flux

Previous studies and experiments had proved that there are a critical value and a liming flux in crossflow filtration process. Below this critical value, solute particles depositions are insignificant and above this value, the effect of fouling is severe and significant (Howell, 1995; Li et al., 1998).

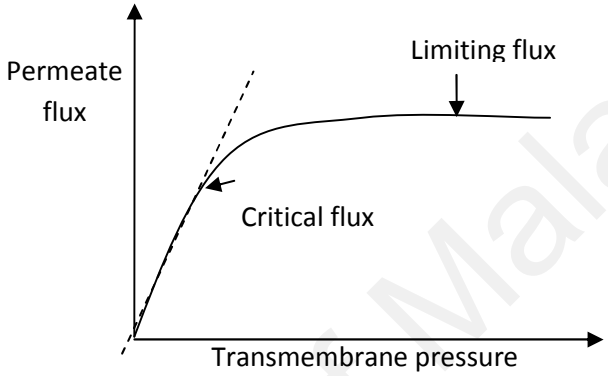

Figure 2.14: A plot of permeate flux as a function of transmembrane pressure

Critical flux can be observed in a plot of permeate flux versus transmembrane pressure. It is the flux when the plot starts to deviate from linearity (Figure 2.14). This deviation might be due to solutes adsorption, pore blocking and the formation of cake layer which increase the hydrodynamic resistance. Limiting flux is the maximum constant flux obtained as transmembrane pressure increases (Bacchina et al., 2002). Beyond limiting flux, increases in transmembrane pressure do not result in any further increase in permeate flux.

Critical flux can be defined as the transition point between concentration polarization and cake formation (Bacchina et al., 2002). The determination of critical flux is highly dependent on the balance of repulsive force and drag force acting on the particle (Tang et al., 2009). As pressure is applied in the system, particles are subjected

to transverse driving force in order to convey the particles towards the membrane surface. Repulsive force is due to the interaction between the particles and between the particles with the membrane surface. Below critical flux, repulsive force is higher than the driving force which lift the particles back to the bulk solution. Above critical flux, the transverse force becomes dominant to overcome the repulsive force and leads to particles deposition. Critical flux is reached when cake formation fouling occurs at a certain point on the membrane whereas limiting flux is reached when the whole membrane surface operates at the critical flux (Bacchina et al., 2002). Limiting flux also indicates a point where the rate of transport is independent of the driving force at high flux. Both the critical flux and limiting flux are highly dependent on membrane properties, feed solution properties (pH, ionic strength and feed solution concentration) and operating conditions. As in the study of Tang et al, limiting flux was reducing with the increase of ionic strength (Tang et al., 2009). It had been observed that critical flux decreased as protein concentration increased and it increased with increasing shear stress (Youravong et al., 2003). This is because the increase in shear stress tends to scour away the particles deposition and reduce fouling.

2.3.3 Factors Affecting Membrane Separation Process

Membrane separation process performance is highly dependent on operating condition such as membrane properties, feed solution properties, and operating parameters. The extent of fouling is determined by operating parameters such as crossflow velocity and transmembrane pressure. Factors such as particle sizes, surface reactivity and pore size also affect the interactions between particles and membrane surface (Singh, 2007).

2.3.3.1 Transmembrane pressure

Transmembrane pressure is the transverse driving force to drive the flow towards and through the membrane surface (Bacchina et al., 2002). As the applied pressure increases, particles deposition increases and leads to more severe fouling. Thus, an increase in filtration pressure results in a higher resistance and rejection coefficient. The initial pore blocking is more severe at higher pressure (Mourouzidis-Mourouzis & Karabelas, 2006). Particles concentration on membrane surface also reached gelling point faster. Therefore, for filtrations at constant pressure and crossflow velocity, the system operated at high transmembrane pressure reached the pseudo-steady state faster. Applied pressure increases the compressive force implied on the gel or cake layer. It leads to the formation of a denser and more compact cake layer with higher filtration resistance and eventually decrease in permeate flux (Hwang et al., 2006). However, it is important to optimize the permeate flux with transmembrane pressure because too low transmembrane pressure will result in low permeate flux. Meanwhile, increase of applied pressure does increase filtration permeate driving force but the severe fouling and increase of membrane resistance may offset the effect of flux enhancement. As observed in Figure 2.17, permeate flux is directly proportional to transmembrane pressure initially until the permeate flux exceeds critical value, it starts to deviate from the linearity and starts to level off. Permeate flux is independent from transmembrane pressure at this stage due to the increased fouling and compaction. In previous study of Veerasamy et al (2002), natural rubber latex was successfully concentrated from DRC 30% to 40%. In this study, it was found that permeate flux was increased with transmembrane pressure initially and then decreased after reached its maximum point as transmembrane pressure exceeds 2.9bar (Veerasamy, 2002).

2.3.3.2 Crossflow velocity

In filtration, solute particles are subjected to transverse drag force and tangential force in flow. Increase of feed flow velocity creates turbulence in the system and increases shear stress that scours away the accumulated particles (Akoum et al., 2005; Konieczny & Bodzek, 1996; Samuelsson et al., 1997; Springer et al., 2009). This will bring more particles to diffuse back to the bulk solution. Thus, the increase in crossflow velocity can reduce the concentration polarization and maintain the permeate flux performance. In a study of spent latex wastewaters ultrafiltration using polymeric membranes previously showed that increase of crossflow velocity had increased the permeate flux (Konieczny & Bodzek, 1996). This indicates that crossflow velocity can improve the mass transfer of solutes rejection (Akoum et al., 2005; Singh, 2007; Sulaiman & Aroua, 2002). This is because increases of wall shear stress leads to a decrease of the amount of deposited material. Limiting flux is also improved with crossflow velocity as wall shear stress is increased (Samuelsson et al., 1997).

In a study of crossflow microfiltration of skim milk using a ceramic membrane, increase of wall shear stress decreases deposit thickness and porosity by removal of larger particles away from the membrane (Berre & Daufin, 1996). The decrease in porosity is due to the fact that large particles are more likely to diffuse back to the bulk solution and leaving fine particles on membrane surface. Analysis of size distribution of the deposited particles at different crossflow velocity had proved that particle sizes in cake layer are smaller at higher crossflow velocities (Li et al., 1998; Singh, 2007). However, even if higher wall shear stress permits higher flux, an excessive increase of shear stress can cause a decrease of whey protein transmission(Berre & Daufin, 1996). An increase of crossflow velocity reduces the amount of fouling but the selective removal of larger sized particles results in a deposit where smaller size particles are

dominant leading to a thinner and less porous cake with a higher specific resistance and leads to lower whey protein transmission.

However, high crossflow velocity will also cause high pressure drops and inconsistent fouling along the membrane (Singh, 2007). In the study of Sulaiman & Aroua (2002), experiments were carried out using a tubular PVDF membrane in the ultrafiltration of skim latex serum. It was observed that permeate flux increases with feed flow velocity until a maximum limit, then permeate flux starts to decrease with the flow velocity. This might due to the fact that high feed flow may increase the internal pressure and increase fouling during filtration.

2.3.3.3 Feed solution concentration

Permeate flux is a function of feed concentration. In the study of Konieczny & Bodzek (1996) on ultrafiltration of spent latex wastewater, the influence of feed concentration is also studied. The permeate flux was found to decrease with the increase of the concentration. For solution of high concentration, permeate flux reaches steady state faster than solution of low concentration. This is because as the solution concentration increases, the amount of particles reaching the membrane surface per unit volume feed solution also increases. Increases in solution concentration can cause more severe concentration polarization effect and also faster formation of cake layer.

`

2.3.3.4 Particle size

In previous study, critical flux of a suspension tends to increase as particle size increases (Harmant & Aimar, 1998; Li et al., 1998). This may due to the fact that fine particles tend to form denser cake layer compared to larger particles. Therefore, fouling layer with higher resistance tends to form for small particles. Further, fine particles block the membrane pores easily and reduce the effective pores for filtration. Thus, it was found that permeate flux increase with the increase of particle diameter due to decrease in membrane pores blocking (Song & Elimelech, 1995).

Table 2.5 summarizes the effect of transmembrane pressure, crossflow velocity, feed concentration and particles size in filtration process. These parameters affect the particles motion during filtration and also the formation of fouled layer.

Table 2.5: Summary of effects of various parameters during filtration

Factors	Effects
Transmembrane pressure	➢ Increase in pressure increases particles convection force and increase fouling.
Crossflow velocity	➢ Increases in crossflow velocity increases shear stress and scour away depositions on membrane surface . ➢ However, in small surface area, increase of crossflow velocity also increases the internal pressure during filtration.
Feed solution concentration	➢ Amount of particle increase with concentration caused more severe fouling.
Particle size	➢ The effect of particle size depends on pore size of membrane used. ➢ Smaller particle can penetrate into membrane pores easily.

2.3.4 Membrane Transportation Model

2.3.4.1 Darcy equation

Darcy's Law is used to describe the flow of a fluid through a porous medium (Ebersold & Zydney, 2004). Darcy's Law is a simple equation which relates permeate volume through the medium with the fluid viscosity and the pressure gradient for a given distance.

$$Q = \frac{kA\Delta P}{\mu l} \quad \text{(Equation 2.2)}$$

Based on Darcy's Law (equation 2.2), the rate of permeate volume, Q (m^3/s), is the product of the permeability of the medium, k (m^2), the cross sectional area, A (m^2), and the pressure gradient, ΔP (Pa), divided by the product of dynamic viscosity, μ (Pa.s) and l (m) is the thickness of medium (Ghosh, 2006; Holdich, 2002). The equation is simplified by combining the medium permeability and thickness in terms of membrane resistance, R_m. Thus, equation 2.2 can be written as follows:

$$Q = \frac{dv}{dt} = \frac{A.\Delta P}{\mu R_m} \quad \text{(Equation 2.3)}$$

where v is the permeate volume collected (m^3). Membrane resistance can be obtained by a plot of filtrate volume (v) versus filtration time (t) for water filtration at constant pressure.

In cake layer filtration, particles formed a cake layer on the membrane surface and impose additional hydraulic resistance (R_c) to the permeate flow. Thus, the equation 2.3 can be written as:

$$Q = \frac{dv}{dt} = \frac{A.\Delta P}{\mu(R_m+R_c)} \quad \text{(Equation 2.4)}$$

Permeate flux rate (J) is then defined in the cake filtration equation as shown below:

$$J = \frac{dv}{dt}\frac{1}{A} = \frac{\Delta P}{\mu(R_m + R_c)} \quad \text{(Equation 2.5)}$$

2.3.4.2 Resistances model - Resistance in series model

Decline of permeate flux is the result of fouling. Fouling layer is considered as a physical barrier to permeate flow. Resistance in series model is derived from Darcy's Law for flow through cake filtration based on the concept that permeate flux is proportional to the driving force and inversely proportional to the total filtration resistances (Chang et al., 2009).

$$J = \frac{Dirivng\ force}{R_{total}} \quad \text{(Equation 2.6)}$$

Driving force in filtration is usually the result of pressure applied. According to resistance in series model, fouling is the combination of several mechanisms (Chang et al., 2009; Matsuura, 2004). Thus, the total filtration resistance (R_t) is contributed by the membrane resistance itself (R_m), irreversible internal fouling (R_f) and reversible surface fouling (R_c). Thus, filtration resistances can be written as below:

$$R_t = R_m + R_f + R_c \quad \text{(Equation 2.7)}$$

Thus, the basic filtration equation can be written as:

$$J = \frac{\Delta P}{\mu\,(R_m + R_f + R_c)} \quad \text{(Equation 2.8)}$$

Membrane initial resistance, R_m, can be obtained through water flux test for a new membrane before filtration starts. R_f and R_c are determined from the experimental data obtained after subtracting the R_m obtained previously. Resistance in series model is very useful in determining the resistance components which attributes to the deterioration of permeate flux. Irreversible internal fouling is insignificant compare to reversible fouling resistance. Reversible fouling is usually dominant and much greater in total filtration resistance compare to irreversible fouling resistance (Field, 2010). However, there are some limitations in resistances in series model. The results obtained might be affected by various factors such as the method used in the experiments (Chang et al., 2009; Yoon, 2011).

2.3.4.3 Fouling indices - Modified fouling index (MFI)

Modified fouling index (MFI) is used as an indicator of fouling potential in membrane filtration. MFI is developed based on cake filtration theory (Schippers et al., 1981). The theory assumed that cake filtration is the dominant mechanism in fouling. It is defined as the gradient of the linear region found in the plot of t/V versus V from the general cake filtration equation as follows:

$$\frac{t}{V} = \frac{\eta R_m}{A.\Delta P} + \frac{\eta I}{2\,\Delta P.A^2} v \qquad \text{(Equation 2.9)}$$

where v is permeate volume (m^3), t is filtration time (s), η is solution viscosity (Pa.s), ΔP is pressure gradient (Pa), A is membrane effective surface area (m^2), R_m is membrane resistance and I is the fouling potential, also known as resistivity (m^{-2}).

Modified fouling index is determined using the same equipments and method as for silt density index (SDI) in ASTM D4189 but permeate volume is recorded every 30s over a period of 15 minutes.

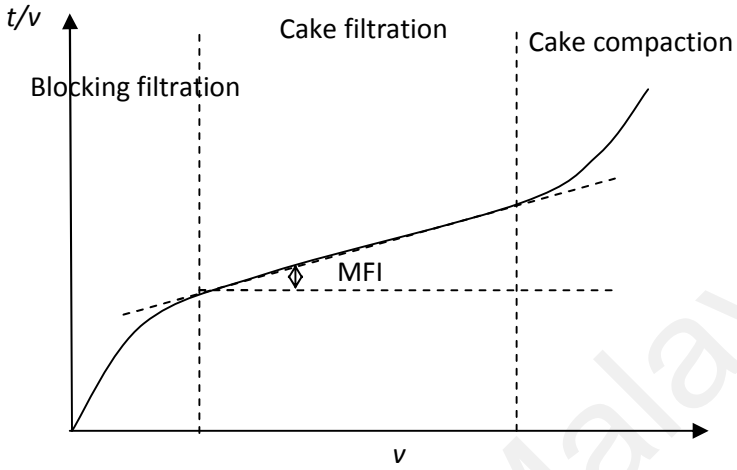

Figure 2.15: A typical plot of filtration time/permeate volume (*t/v*) as a function of permeate volume, *v*

A typical plot of *t/v* versus *v* curve is shown in Figure 2.15. For most of the case, linearity is observed except for the initial period. The linear relationship between *t/v* versus *v* at various operating conditions implies that cake layer filtration occurs. The slope of the curve seems to increase slowly with time. This may be because of the decrease in permeate flux due to the increase in filtration resistance. In previous study, MFI was investigated using polysulphone membrane in tap water experiments. The result showed that initial MFI measured was low and then increase with filtration time (Boerlage et al., 2002).

Fouling mechanism is usually dominated by pore blocking at the initial stage resulting in high slope (Hu et al., 2004; Kanani et al., 2008; Li et al.; Purkait et al., 2005). In the study of Blanpain-Avet et al (1999), it had been revealed that fouling starts from internal clogging to the buildup of an external fouling layer over the membrane surface. As filtration prolonged, fouling mechanism gradually switch to cake filtration

which is usually indicated by linear region of the curve (Boerlage et al., 2002). Thus, basically, the curve can be divided into three regions, i.e., pore blocking filtration, cake filtration and cake compaction (Hwang et al., 2007; Vela et al., 2008). The slope of the linear region is taken as MFI. As applied pressure is increased to critical level, further increases in pressure will cause cake layer compaction (Alhadidi et al., 2011). The studies of MFI over time previously showed that MFI is decreasing over time and then gradually approached a steady state (Boerlage et al., 2002).

Experimental results showed that MFI obtained in crossflow filtration is lower than in dead end filtration (Javeed et al., 2009). This is due to the fact that large particles tend to recirculate in the retentate in the flow because of shear flow along the membrane surface. In dead end filtration process, both large and small particles were transferred to membrane surface to form a fouled layer. Deposition of fine particles fill the voids of cake layer formed, resulting in cake layer with lower porosity. However, fouling in cross flow filtration is dominated by smaller particles. Large particles usually being scoured away by shear and inertial lift forces of the flow. The scouring effect is increased with cross flow velocity. Thus, MFI of cross flow filtration system is increased with smaller particles and high solution concentration (Park et al., 2006). The reduction in particles size caused more fine particles to form the fouled layer with higher hydraulic resistance and resulted in higher MFI. The fouling potential was also highly affected by membrane pore size (Sim et al., 2010). Smaller particles were retained as membrane pore size decreased. The retention of small particles in the solution caused the formation of highly compact fouled layer. Thus, MFI is increased with the reduction of membrane pore size. Higher MFI is also expected for solution with higher concentration. High concentration of particles causes the increase in the amount of fouling and the onset of cake compression (Boerlage et al., 2004).

`

MFI is also highly dependent on operating parameters. As transmembrane pressure increased, the particles drag force increased causing more particles to transport to membrane surface. Thus, more particles were deposited on membrane surface. Particles deposition contributed significantly to filtration resistance and hence leads to the increase in MFI as fouling increased (Sim et al., 2010). MFI is also affected by the flow velocity. In crossflow filtration, variation in crossflow velocity may alter the flow condition. According to the study by Sim et al (2010) of crossflow ultrafiltration of silica colloidal suspensions, it was found that at low crossflow velocity range, an increased in crossflow velocity leads to a reduction of MFI. This is because the additional shear force along the membrane had reduced particles deposition. While at high velocity range, the increases in crossflow velocity had caused the reduction in fouled layer average particles size. This had lead to a more compact cake layer and raised the values of specific cake resistance. Eventually, the increase in crossflow velocity can cause the increased in MFI values.

2.3.4.4 Rejection coefficient

Rejection coefficient is used to measure the membrane selectivity and membrane retention for solute. The difference between true rejection coefficient and the apparent rejection coefficient is shown below.

$$R_{rej} = \frac{C_m - C_p}{C_n} = 1 - \frac{C_p}{C_n} \qquad \text{(Equation 2.10)}$$

where C_b, C_p, C_m are the concentrations of solute in the bulk, in the permeate solution and at the membrane surface respectively, and R_{rej} is the rejection coefficient. Rejection coefficient of a membrane is not a constant and it is highly affected by the operating conditions. Apparent rejection coefficient is more commonly used for comparing to the

true rejection coefficient because the solute concentration on membrane surface is difficult to measure.

2.4 Application of membrane separation technology in natural rubber latex industry

Membrane separation technology can be used as an alternative to recover particles in skim latex. Previously, Veerasamy and coresearchers had run some studies on the application of membrane separation process to concentrate natural rubber latex (Veerasamy, 2002). The studies showed that natural rubber latex could be concentrated from 30% DRC to 46% DRC. However, the concentration and efficiency were considered inadequate to meet the market requirement. Further at that time, it was not cost effective to replace the typical latex processing industry with membrane separation technology. Thus, the attention was shifted and introduced membrane separation technology for skim latex processing. In this case, ultrafiltration of skim latex aims to concentrate skim latex from 6% dry rubber content to about 30% which is almost similar to the rubber content of field latex. As an option, concentrated skim latex then can be added into the new batch of field latex during centrifugation process. Ultrafiltration of skim latex also produces clear serum free of rubber as by-product.

Krusteva et al (1998) and Doneva et al (1999) had showed the possibility of using membrane separation technology for latex suspensions. In both studies, small scale laboratory crossflow microfiltration unit was used to study monodisperse latex suspensions. Studies of Krusteva (1998) showed that pseudoplastic behavior of dense suspension affected the tangential outflow of the cake in crossflow microfiltration (Krusteva et al., 1999). In the study of Doneva et al, monodisperse latex suspensions with different concentrations in crossflow microfiltration using polyacrylonitrile

membranes were studied. Latex suspensions were prepared by diluting latex from Acronal, Akzo, Netherlands with prefiltered distilled water. The experimental results showed that latex suspensions exhibit a pronounced pseudoplastic rheological behavior and its effect on crossflow microfiltration (Doneva et al., 1998).

2.5 Summary

As widely recognized, continued usage of membrane can lead to fouling problems entailing membrane replacement and increased operating costs. The presence of proteins in feed materials has been observed to be one of the causes of fouling to occur during processing. This phenomenon will have direct impact on process productivity and cleaning of membranes. Thus a scientific understanding of fouling behavior during ultrafiltration of skim latex is necessary to optimize its performance. However, there are only limited studies on application of membrane separation technology in rubber industry.

As mentioned in chapter 1, the objectives of this study are to study the skim latex ultrafiltration performance and to characterize fouling using different techniques so as to observe and explain fouling behavior and its corresponding mechanisms. The effect of operating parameters (transmembrane pressure and crossflow velocity) on filtration performance and protein concentration in permeate will also be studied. The experimental data obtained can be used to develop a protocol to clean fouled membrane and to assess the effectiveness of various membranes cleaning methods. The research also can suggest solutions to delay the onset of fouling phenomena thus prolonging life span of membranes and thus reduce operating cost in term of membrane replacement and productivity enhancement. Besides, the data can also be used to optimize the operation of process.

In this study, a bench scale crossflow ultrafiltration unit is used to study the fouling behavior of proteinaceous skim latex solution. Fouling in crossflow filtration is lower compared to dead end filtration system. Ultrafiltration is widely used in dairy industry. It is ideal process for fractionation, concentration and purification. Single channel tubular ceramic membranes are used as the medium. Ceramic membranes were chosen due to its high solvent resistance and thermal stability at extreme pH are suitable for food, biotechnology and pharmaceutical applications. However, ceramic membranes are mechanically weak.

Filtration performance and fouling behavior will be analyzed in terms of flux, resistance, MFI and rejection coefficient in order to determine the possible mechanisms (pore blocking, absorption, concentration polarization and gel layer formation).

`

CHAPTER 3

METHODOLOGY

3.1. Experimental methodology

The general experimental methodology is shown in Figure 3.1. The figure describes the initial and general process of experimental planning. Among man industries, skim latex processing in natural rubber industry was selected as the field of study. The purpose of the planning is to determine the flow and process during the study and also the materials used and the scope of experiments. Single channel ceramic membranes were selected as the medium in this study. Transmembrane pressure and crossflow velocity were choosen as the parameters to be studied in this experiment.

The actual experimental methodology is shown in Figure 3.2. Properties of skim latex such as total solids content (TSC), dry rubber content (DRC), acidity, viscosity and density were determined before filtration experiments. Ultrafiltration experiments were carried out in a range of different parameters (transmembrane pressure and crossflow velocity). The membranes and feed solution after filtration were then further analyzed using different technique. Experimental data observed was then being analyzed and studied. Analysis and interpretation of the data can provide some understandings on the fouling behavior on ultrafiltration of skim latex.

`

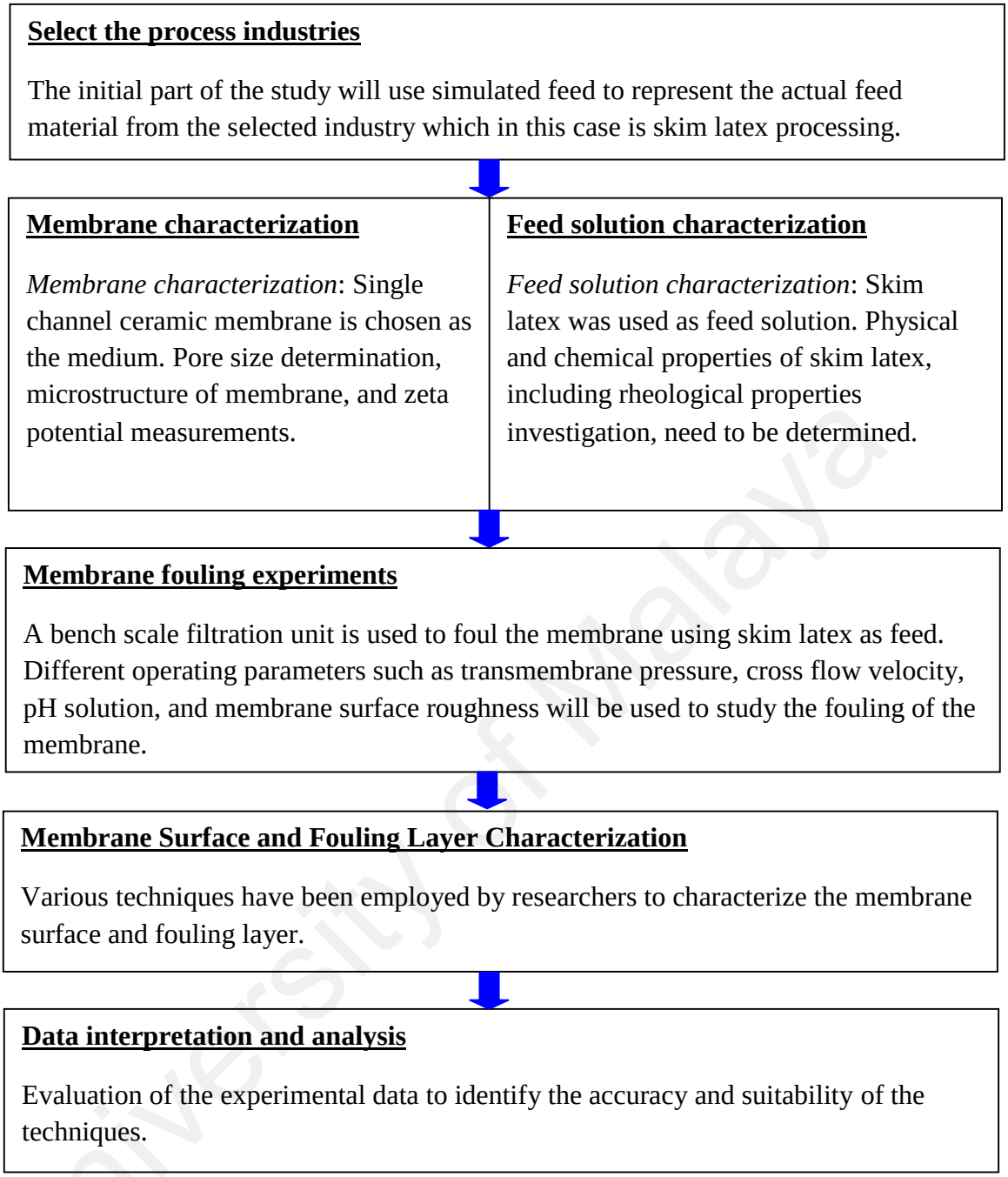

Figure 3.1: General experimental planning

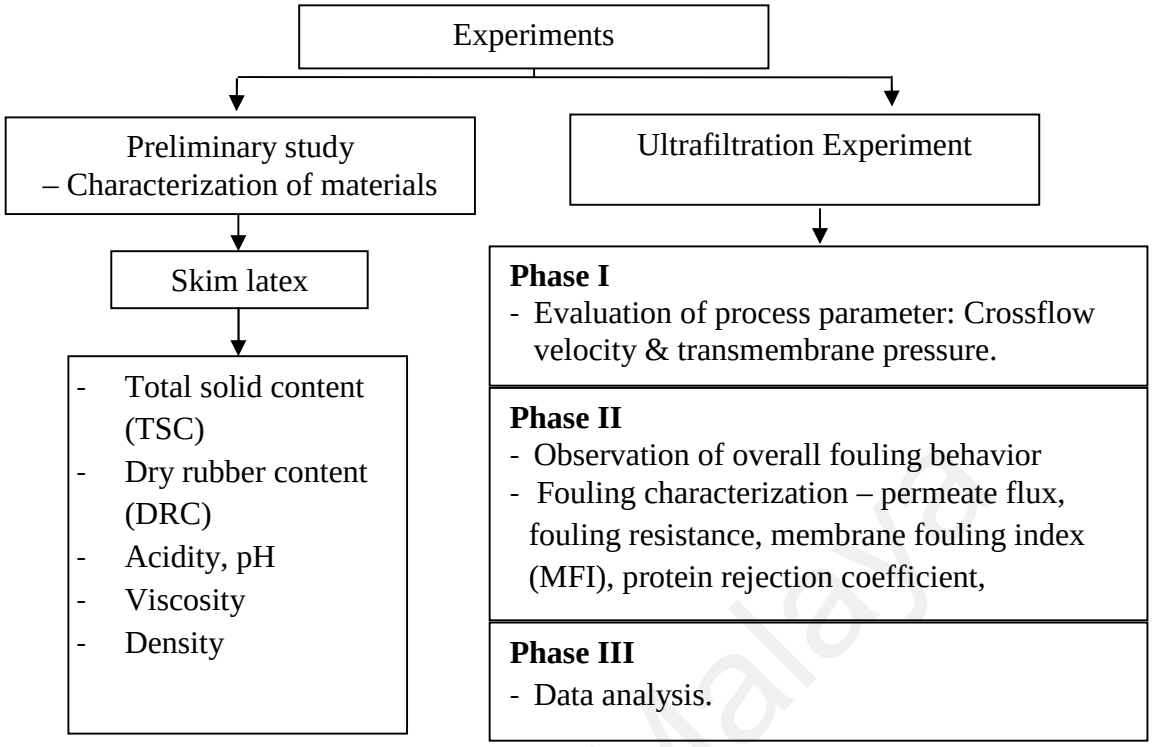

Figure 3.2: Experimental methodology

3.2. Materials

Single channel Al_2O_3 ceramic membranes were used with an inner diameter of 7mm, outer diameter 10mm, length 250mm and a mean pore size 0.05µm. The membranes used in the study were purchased from Gamma Scientific Research Sdn Bhd, Malaysia. Specifications of the membrane were provided as Appendix 1. Ceramic membranes were chosen due to its excellent selectivity, permeability, thermal and chemical stability (Li et al., 2006).

Skim latex used in this study was obtained from a local latex factory. The skim latex was stabilized with preservative solution to prevent premature coagulation during storage prior to ultrafiltration.

All chemicals used in this study including sodium hydroxide and total protein kit were purchased from Sigma-Aldrich, Malaysia.

3.3. Equipment setup

The schematic diagram of the bench scale crossflow membrane unit is illustrated in Figure 3.3. The unit includes a stainless steel membrane module, a peristaltic pump (Masterflex L/X, Cole-Parmer,USA), pressure gauges and a digital balance GF-400 (A&D Weighing, Milpitas, USA) which is connected to a computer. In this system, a 250mm single channel ceramic membrane was encased in a stainless steel module. Feed solution was circulated through the system using the peristaltic pump. The applied pressure was controlled by using a flow control valve. Two oil-filled type pressure gauges were fitted at the inlet and outlet of the module to measure the pressure. Transmembrane pressure was taken as the mean value of the inlet and outlet pressures measured.

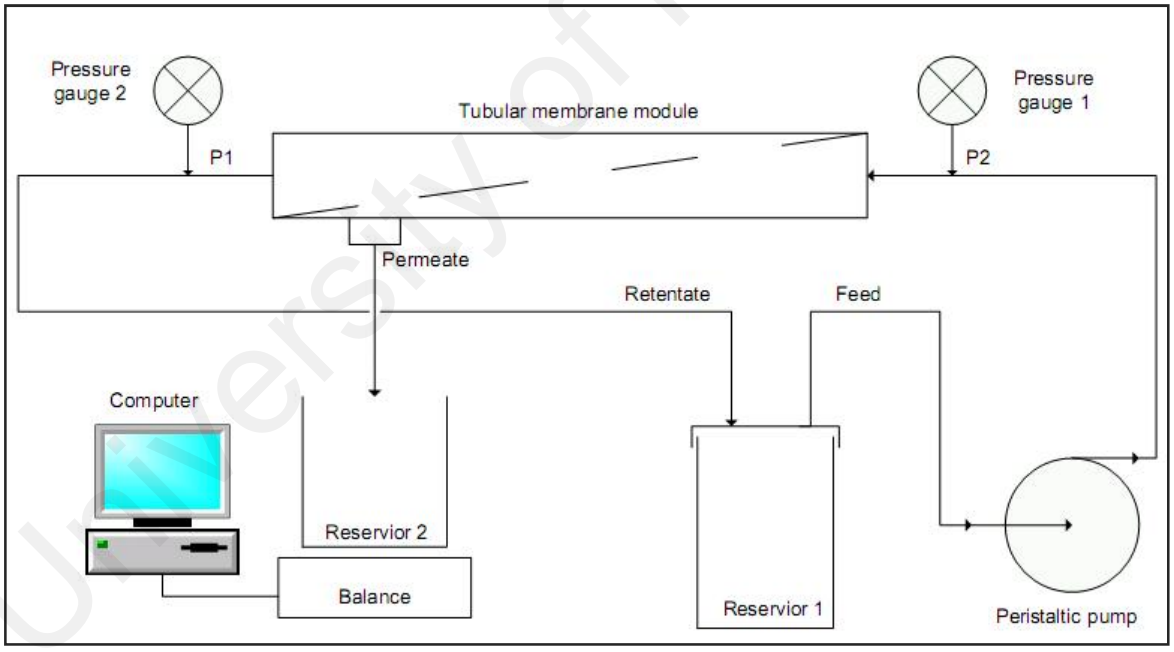

Figure 3.3: Schematic diagram of the bench scale crossflow ultrafiltration unit used in this study

3.4. Experimental procedure

3.4.1. Skim latex characterization

Total solid content, solution density, viscosity, dry rubber content, protein concentration and particle size distribution of skim latex were determined prior to the experiments. All characterizations were carried out using guideline as per ASTM D1076-88.

3.4.1.1. Total solid content (TSC)

Total solid content is defined as the percentage of non-volatile mass in the samples. An empty flat bottom dish was weighed using a digital balance GF-400 (A&D Weighing, Milpitas, USA) and a 2.5g ± 1g of skim latex samples (m_0) was added to the dish. The sample was dried in an oven at temperature of 100°C ± 2°C. After 2 hours of drying time, the sample was removed and cooled to room temperature in a desiccator. The dried latex was then weighed and placed into the oven again. The weighing and drying were repeated until a constant weight (m_1) was obtained. TSC was calculated as follow:

$$TSC = \frac{m_1}{m_0} x\ 100\% \qquad \text{(Equation 3.1)}$$

The experiments were repeated three times to calculate the average TSC of skim latex.

`

3.4.1.2. Dry rubber content (DRC)

Dry rubber content was defined as the percentage of coagulated rubber mass in a sample. A 10g ± 1g of skim latex sample (m_0) was weighed using a digital balance GF-400 (A&D Weighing, Milpitas, USA). 20% sulfuric acid (Sigma-Aldrich, Malaysia) was poured slowly at the edge of the dish which was then slowly rotated to coagulate the rubber. Then the dish was left undisturbed for 30mins. The coagulated latex was pressed by a spatula until a uniform sheet of rubber not exceeding 2mm in thickness was obtained. The coagulated rubber was soaked in water. The sample was dried in an oven (Memmert UFB 400, Germany) at 70°C ± 5°C. After 10 hours of drying, the sample was cooled to room temperature in a desiccator. The dried rubber was weighed and dried again. The weighing and drying were repeated every two hours until a constant weigh (m_1) was obtained. DRC was calculated as follow:

$$DRC = \frac{m_1}{m_0} x\ 100\% \qquad \text{(Equation 3.2)}$$

The experiments were repeated three times to calculate the average DRC of skim latex.

3.4.1.3. Density

Density of skim latex was determined using an indirect method as in ASTM D1076-88. A 100ml flask with stopper was weighed (m_0). The flask was filled with distilled water and marked. The mass of water and flask was determined (m_1). Volume (υ) of the flask up to the mark was determined based on the equation below:

$$\upsilon = \frac{m_1 - m_0}{\rho_{water}} \qquad \text{(Equation 3.3)}$$

where ρ_{water} is the density of water (0.9970479g/cm^3). The flask was cleaned and dried. Skim latex was filled into the flask until it was half full. Skim latex in the flask with stopper was weighed (m_2). Distilled water was added till the calibrated mark. The flask filled with skim latex and distilled water was weighed (m_3). Density (ρ) was determined using the following equation:

$$\rho = \frac{m_2 - m_0}{\left(v - \frac{m_3 - m_2}{\rho_{water}}\right)} \quad \text{(Equation 3.4)}$$

3.4.1.4. Viscosity

Skim latex viscosity was determined using the rotational viscometer (Haake VT-550, Germany). The picture of rotational viscometer is shown in Figure 3.4. Skim latex was placed in the sample cup. The motor was rotate predefined rotational speed. The sample tends to exert resistance force against the rotational movement due to its fluid viscosity. The resulting torque or resistant determines the sample viscosity. Five samples were measured and were repeated to calculate the average viscosity of skim latex.

Figure 3.4: Rotational viscometer, Haake VT-550 from Germany

3.4.1.5. Protein concentration

There are a number of ways to quantify protein in natural rubber latex. Modified Lowry method is used to determine total protein content according to ASTM D5712. Total protein kit used in this study as purchased from Sigma-Aldrich, Malaysia. The Lowry method procedure is based on Peterson's modification of the micro Lowry method. In this method, protein in skim latex is precipitated using DOC (deoxycholate) and TCA (trichloroacetic). The precipitated solution was then centrifuged using a centrifuge (Sigma 2-16, Germany) to remove the supernatant. The precipitated protein was then dissolved using the Lowry reagent solution, in which the peptide bonds of the protein will react with the alkaline cupric tartrate reagent. Folin & Ciocalteu's phenol reagent was then added to give a blue-purple solution. Absorbance of the colored solution was then measured at a wavelength between 500nm and 800nm using a spectrophotometer (Genesys 20, Thermo Scientific). The protein concentration is then determined from a calibration curve. Protein concentration in feed and permeate were determined using this modified Lowry method.

`

3.4.1.6. Particle size distribution

Skim latex particles size distribution was determined by using a Malvern Mastersizer 2000 (United Kingdom). Five measurements were carried out to obtain an average particle size distribution.

3.4.2. Membrane characterization

Before each experiment, the initial membrane resistance and permeability were determined by using water flux test. Distilled water was used as the feed solution. The initial membrane resistance was determined using the following equation:

$$R_m = \frac{\Delta P}{\mu_w J_w} \qquad \text{(Equation 3.5)}$$

where μ_w is the water viscosity, R_m is the membrane initial resistance and ΔP is the applied transmembrane pressure, and J_w is the water flux measured. The measurement was used as a baseline to assess the membrane performance throughout this study.

3.4.3. Ultrafiltration experiments

A schematic diagram of a bench scale crossflow ultrafiltration unit as shown in Figure 3.3 was used to conduct this study. The experiments were carried out at room temperature of 25°C. The transmembrane pressure used in this study was in the range of 0.6 to 1.3bar. The crossflow velocity ranged from 1.3cm/s to 4.6cm/s. A new membrane was used for each experiment. Before ultrafiltration, new membranes were immersed and rinsed with deionized water to remove the residues on membrane surface so that stable water permeate flux can be obtained (Chang et al., 2011).

Feed solution (skim latex) was pumped through the system by using a peristaltic pump. 500ml of skim latex was used in each experiment. The experiment was run in recycle mode, i.e. both retentate and permeate were recirculated through the feed reservoir by using a peristaltic pump to keep the concentration constant. The experiment at each set of operating conditions was run continuously for about 160 minutes until a pseudo steady state permeate flux was obtained. Permeate was collected into a reservoir placed on a digital balance which is connected to a computer before it was recirculated back to the feed tank. The measurements were collected 30 seconds after experimental run began in order to stabilize the transmembrane pressure. Permeate mass was collected at one minute interval and the results were stored in a computer. For analysis purpose, the pseudo steady state data were then averaged and plotted versus transmembrane pressure. The change in permeate flux was analyzed as a function of filtration time.

3.4.4. Membrane cleaning procedure

After completion of each ultrafiltration skim latex experiment, the system was drained. The system was flushed with deionized water and then cleaned by running 500ml of 2% NaOH aqueous solution for 30 minutes to remove any deposition on membrane surface (reversible cake fouling). The system was then drained and rinsed with 1L of deionized water.

`

3.4.5. Calculation

3.4.5.1. Determination of permeate flux at pseudo steady state

Permeate flux at pseudo steady state was determined from the obtained data. Permeate flux was plotted as a function of filtration time to obtain the relationship between permeate flux and filtration time. Permeate flux at pseudo steady state was determined using the equation based on the assumption that pseudo steady state was reached as permeate flux is about constant with time.

3.4.5.2. Determination of rejection coefficient

Protein concentration in feed, permeate and retentate were determined as mentioned in section 3.4.1.5. Rejection coefficient was then determined using the equation 2.10 (section 2.3.4.4).

3.4.5.3. Determination of filtration resistances

Filtration resistance is the contribution of membrane initial resistance (R_m) and fouling resistance (R_f and R_{if}) formed during filtration of skim latex. According to Darcy's Law, permeate flux can be expressed as in the equation 2.8 (section 2.3.4.3). The resistances can be calculated by using the equation 2.7 and experimental flux data obtained (Zhao et al., 2003).

The resistances were determined in a few stages. Firstly, membrane resistance (R_m) is determined before ultrafiltration process via water flux test. After each experiment, the membrane was rinsed with deionized water in order to remove the remaining feeds solutes on the membrane surface. Water flux test was then performed using deionized water. Membrane resistance (R'_m) was then calculated using the data obtained (Rai et al., 2006).

The membrane was then drained and cleaned thoroughly as mentioned in section 3.3.4. Water flux test was performed on this membrane. Membrane resistance (R''_m) was then calculated using permeate data obtained in equation 3.1.

Irreversible (R_{if}) and reversible fouling (R_f) resistances can be determined as follows:

$$R_{if} = R''_m - R_m \quad \text{(Equation 3.1)}$$

$$R_f = R''_m - R'_m \quad \text{(Equation 3.2)}$$

The determination of irreversible and reversible fouling are based on the assumption that reversible cake layer is effectively removed through the cleaning method as mentioned in 3.3.4. The difference of fouling resistance before and after cleaning is taken as reversible fouling resistance (R_f).

3.4.5.4. Scanning electron microscope analysis

Samples were carefully taken from the membrane after ultrafiltration and send to Combination Technology and Catalysis research Centre (COMBICAT), University Malaya for morphological analysis. The morphology of the fouled membrane surface was analyzed by using a field emission scanning electron microscope model FEI Quanta 200 (USA).

`

CHAPTER 4

RESULTS AND DISCUSSION

4. Results and discussion

The characteristics of skim latex were investigated to determine selected feed properties (skim latex) before ultrafiltration runs could proceed. The characteristics of skim latex are as followed:

4.1. Characteristics of skim latex

a. Particles size distribution

Particle size distribution of skim latex was investigated using particle size analyzer, Mastersizer 2000. The rubber particles in skim latex were in the range of 0.07 to 0.33± 0.012 µm. The particles size distribution was smaller than natural rubber latex which range from 0.2 µm to 3 µm (Cornish, 2001; Danwanichakul et al., 2011; Rippel et al., 2003; Thongmak et al., 2009). This is because larger particles were removed during centrifugation process.

b. pH

Skim latex was preserved with ammonia to avoid coagulation before processing. Thus, the pH value of skim latex is more alkaline, in the range of 9.62 ± 0.12. The value is similar to the pH values mentioned by Jayachandran & Chandrasekaran (1998) and Liang et al (2011).

c. Total solid content (TSC) and dry rubber content (DSC)

The percentage of total solid content (TSC) and dry rubber content (DRC) were analyzed to identify the amount of total solid and rubber in skim latex. The results show that TSC is in the range of 6.42 ± 0.02% and DRC is in the range of 4.24 ± 0.01%. TSC result is similar to the value obtained by Paiphansiri & Tangboriboonrat (2005). However, DRC obtained is slightly lower than the mentioned value, 6-8%.

d. Viscosity

The result obtained in Figure 4.1 indicates that skim latex is a pseudo plastic solution, i.e., apparent viscosity is decreasing with higher shear rate. Its behavior is similar to that of natural latex (Liang & Kai, 2011; Sridee, 2006). Similar to fresh tapped natural rubber latex, skim latex possesses shear thinning behavior (Liang & Kai, 2011). Hence, viscosity of skim latex decreases with increasing shear rate. However, viscosity of skim latex is lower than natural rubber latex as rubber content in skim latex is lower than in natural rubber latex (30% DRC).

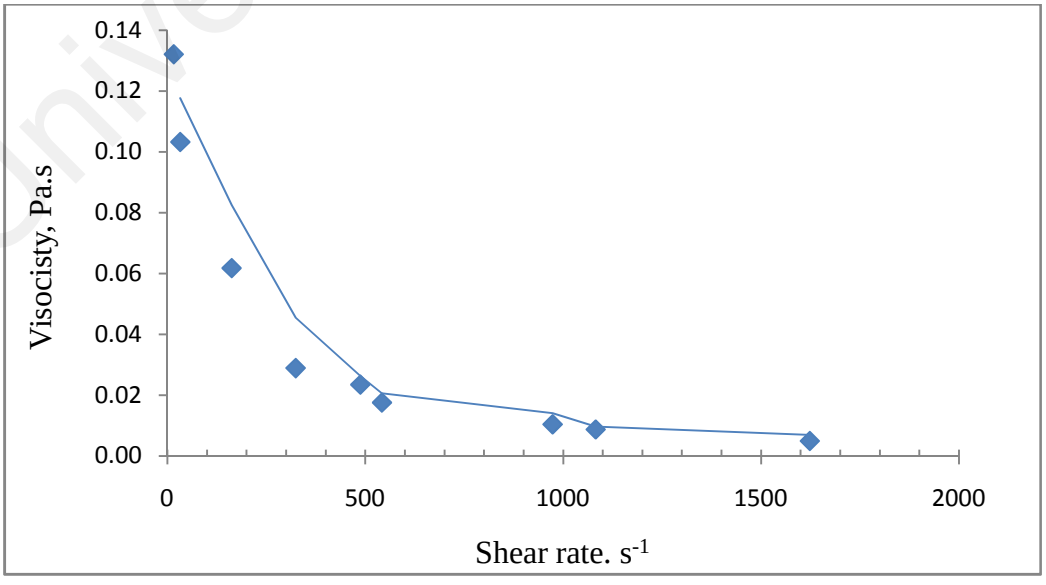

Figure 4.1: Rheological behavior of skim

The characteristics of skim latex were summarized in table 4.1 as shown below:

Table 4.1: Characteristics of skim latex

Charateristics	Result	Std dev	Unit
Particles size distribution	0.07 – 0.33	± 0.012	µm
pH	9.62	± 0.12	-
Density	0.9957	± 0.0072	g/cm^3
Total solid content	6.42	± 0.02	%
Dry rubber content	4.24	± 0.01	%

4.2. Ultrafiltration of skim latex

4.2.1. Effect of transmembrane pressure at crossflow velocity 1.3cm/s

a. Initial permeate flux

Figure 4.2 shows the change of permeate flux with filtration time for skim latex at fixed crossflow velocity 1.3 cm/s and transmembrane pressure ranging from 0.6 bar to 1.3 bar. The experimental results show that at constant crossflow velocity 1.3 cm/s, initial permeate flux increased for about 5.6% as transmembrane pressure increased from 0.6 bar to 1.0 bar. The initial permeate flux increased 57% as transmembrane pressure increased further to 1.3 bar. This is because the increase in transmembrane pressure had increased the feed solution particles convection force and pushed more particles to pass through the membrane (Hu et al., 2004; Hwang & Huang, 2009). As in previous study of skim milk ultrafiltration using modified polysulfone membranes, initial permeate flux drop rapidly immediately after the filtration started (Rinaldoni et al., 2009). The results in their study are in parallel with the experimental results showed that the initial permeate flux increased with the increase of transmembrane pressure.

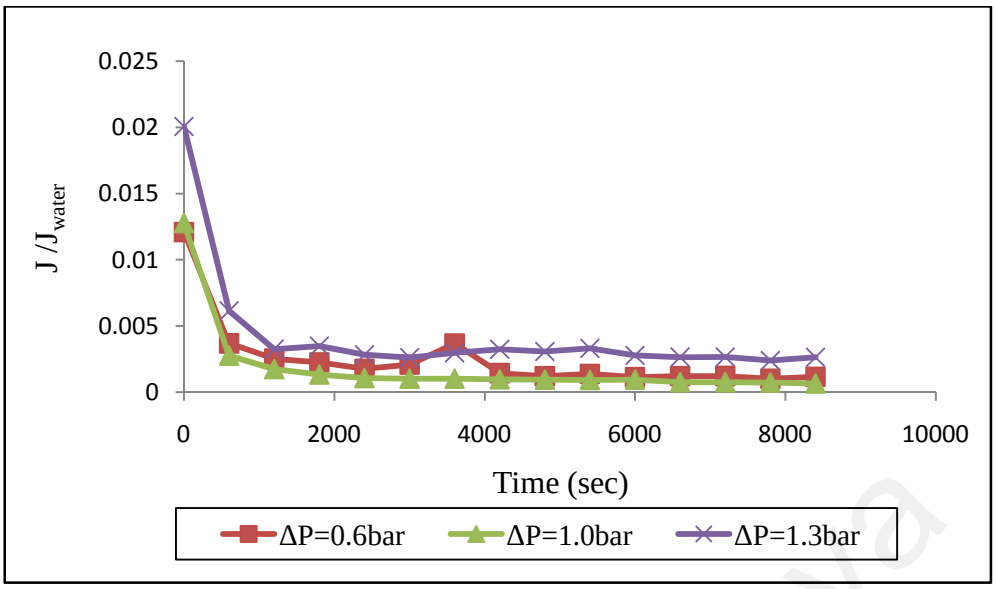

Figure 4.2: Permeate flux was plotted as a function to filtration time for ultrafiltration of skim latex at crossflow velocity 1.3 cm/s and transmembrane pressure 0.6, 1.0 and 1.3bar

b. Permeate flux at pseudo steady state

As ultrafiltration time approached 2000s, permeate flux tends to reach pseudo steady state where permeate flux is almost constant. As shown in Figure 4.3, permeate flux at pseudo steady state decreased slightly for about 38% as transmembrane pressure increased from 0.6 bar to 1.0 bar due to the increases in filtration resistance as more particles were foul on membrane surface as transmembrane pressure increased. Permeate flux at pseudo steady state is highest at transmembrane pressure 1.3 bar due to the decrease of filtration resistance.

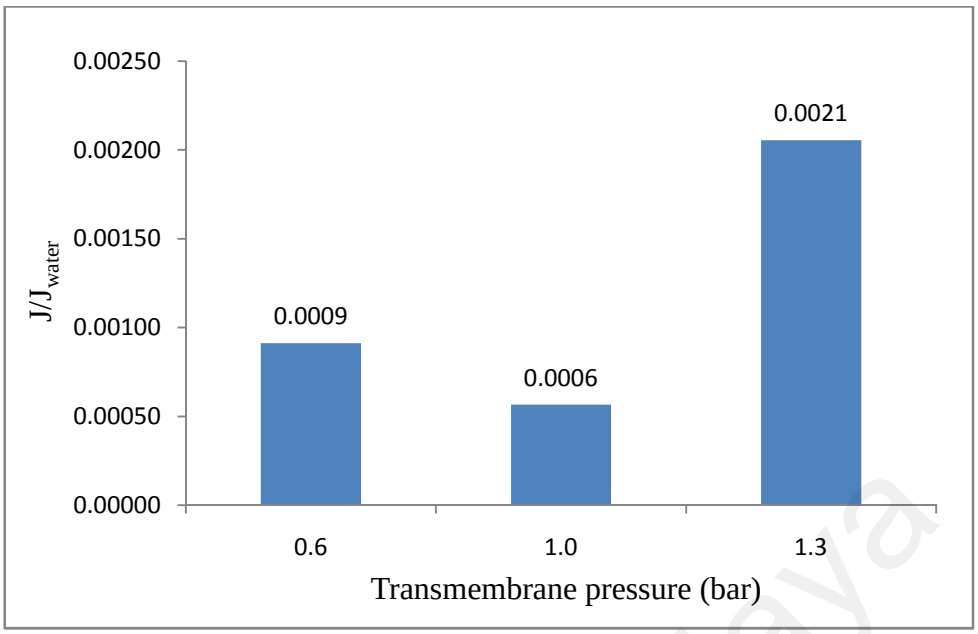

Figure 4.3: Permeate flux at pseudo steady state is plotted as a function of transmembrane pressure at fixed crossflow velocity 1.3 cm/s

c. Filtration resistance

As shown in Figure 4.4, in general, filtration resistance is increased rapidly initially due to fouling and then reached pseudo steady state. The change in filtration resistance is similar to that in previous study (Blanpain-Avet et al., 1999; Purkait et al., 2005). In Figure 4.4, the trend of the filtration resistance with time showed that filtration resistance is higher at transmembrane pressure 1.0 bar compared to 0.6 bar.This is because the increase in transmembrane pressure had increased the particles convection force and lead to more severe fouling. As applied pressure increases further to 1.3 bar, filtration resistance tends to be lower than 1.0 bar (Figure 4.4). This is the main reason for the increase of permeate flux at pseudo steady state (263%) as transmembrane pressure increased to 1.3 bar as permeate flux is inversely proportional to filtration resistance. The reduction in filtration resistance is due to the increase in transmembrane pressure had caused large particles to deposit on membrane surface to form cake layer with lower porosity and hydraulic resistance.

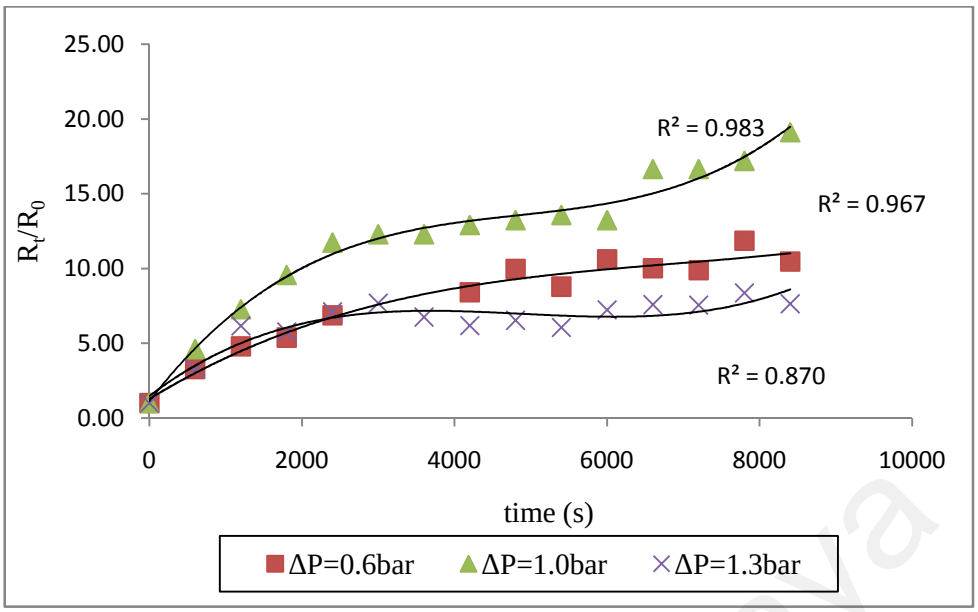

Figure 4.4: Filtration resistance is plotted as a function of time for ultrafiltration of skim latex at fixed crossflow velocity 1.3 cm/s and variant transmembrane pressure

The analysis of filtration resistance shows that reversible fouling resistant (R_f) dominating (99.9%) compare to irreversible fouling resistance (R_{if}) which is only 0.1-0.5% (Table 4.2) (Zhao et al., 2003). Thus, the change in filtration resistance is mainly due to the reversible fouling resistance. Reversible fouling resistance is increased as transmembrane pressure increased from 0.6 bar to 1.0 bar due to more severe fouling. As applied pressure exceeds 1.0 bar, reversible fouling resistance is decreased as fouled layer porosity increased. SEM images of membrane surface after filtration are shown in Figure 4.5.

Table 4.2: Analysis of reversible resistance (R_f) and irreversible resistance (R_{ir}) during the ultrafiltration of skim latex at crossflow velocity 1.3 cm/s

Crossflow velocity (cm/s)	Transmembrane pressure (bar)	R_r/R_m	%	R_{ir}/R_m	%
1.3 cm/s	0.6 bar	430.34	99.7	1.25	0.5
1.3 cm/s	1.0 bar	1756.39	99.9	1.59	0.1
1.3 cm/s	1.3 bar	1071.25	99.8	1.90	0.2

(a) (b)

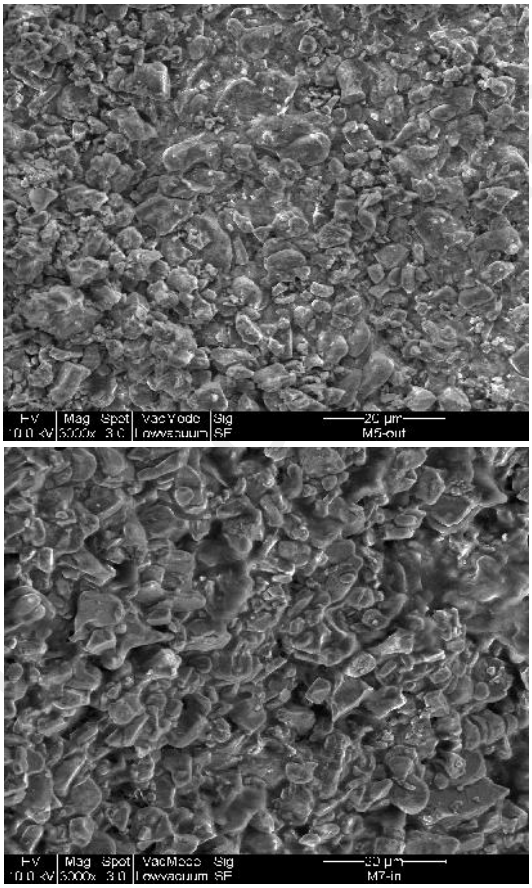

Figure 4.5: SEM images of fouled membrane surface under crossflow velocity 3.3 cm/s and transmembrane pressure (a) 0.9 bar and (b) 1.3 bar

The images show that fouled layer porosity is more obvious at transmembrane pressure 1.3 bar. Low porosity cake layer has lower filtration resistance. Meanwhile, irreversible fouling resistance increased with applied pressure. R_{if} increased 27.2% as pressure increased from 0.6 bar to 1.0 bar and increased 19.5% when increased further

to 1.3 bar. The increases in applied pressure had increased the particle convection force and pushed more fine particles towards the membrane and block the pores (Purkait et al., 2004).

d. Modified fouling index and resistivity

Figure 4.6 showed the plot of *t/v* as s function of permeate volume, *v*. The curves increases rapidly initially and then slow down and tends to level off at high transmembrane pressure. The slope of the regression line of the linear region is taken as the value of modified fouling index (MFI). Resistivity, *I*, can be calculated from the obtained modified fouling index values. The curves show similar trend, i.e. the slope increase rapidly initially and tends to decrease as filtration prolonged. The estimated initial slope at transmembrane pressure 0.6 bar was 633.3 s/cm^6, and then reduced around 5.2% to 600 s/cm^6, reduced further for about 74.4% to 154 s/cm^6. Fouling mechanism at initial stage is usually dominated by pore blocking, this resulting in high slope. The decrease in initial slope with transmembrane pressure at crossflow velocity 1.3 cm/s implied that pore blocking is reduced with the increase in transmembrane pressure. This may be because as transmembrane pressure increased, larger particles were brought to the membrane surface. Large particles are difficult to penetrate into membrane pores and may block the pores.

MFI is used as an indicator of fouling potential. As shown in Table 4.3, MFI results show that fouling potential is decreasing with transmembrane pressure at crossflow velocity 1.3 cm/s. The result implies that at low crossflow velocity, cake layer formation is decreasing with transmembrane pressure. However, the fouled layer resistivity is increased to 50.4% as applied pressure increased from 0.6 bar to 1.0 bar. As applied pressure increased further to 1.3 bar, the resistivity is reduced to 98%. This

is because the increase of applied pressure had increased the cake layer fouling potential. However, fouled layer resistivity is decreasing due to the change in cake layer microstructure.

A typical *t/v* versus *v* plot is given in Figure 4.6 previously shows fouling started with pore blocking, followed by cake filtration and cake compaction. The curve at transmembrane pressure 0.6 bar does not show obvious trends of cake compaction compare to the curves for transmembrane pressure 1.0 bar and 1.3 bar. Thus, cake compaction occurred at higher transmembrane pressure (Alhadidi et al., 2011). As a result, reversible fouling resistance is also increased with transmembrane pressure as shown previously in Table 4.2.

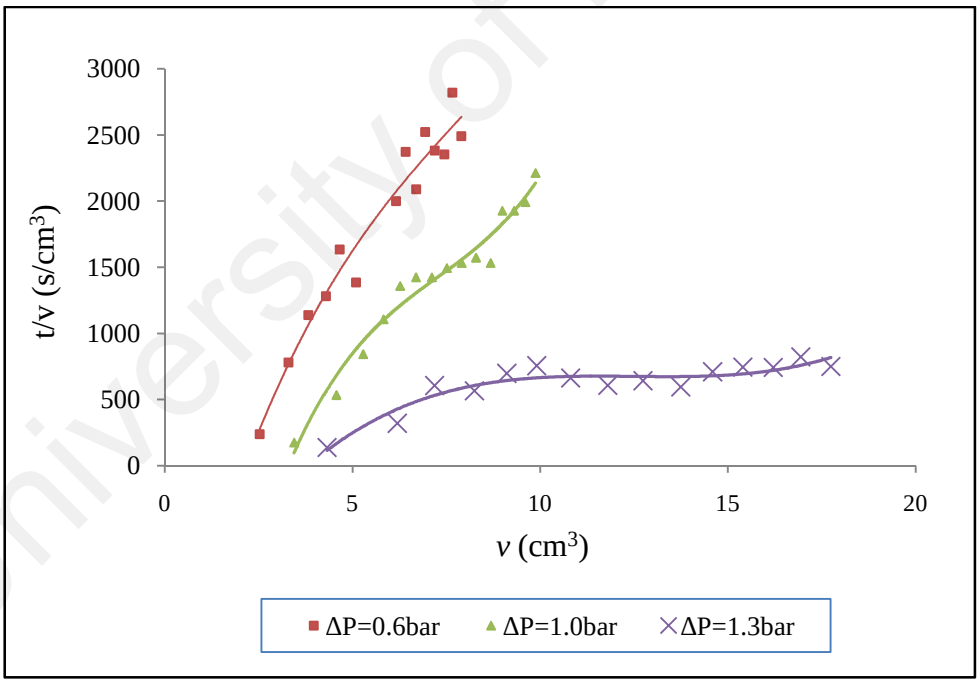

Figure 4.6: Plot of *t/v* as a function of permeate volume, *v*, for skim latex ultrafiltration at fixed crossflow velocity 1.3cm/s and transmembrane pressure 0.6 bar, 1.0 bar and 1.3 bar

Table 4.3: Modified fouling index, MFI, and resistivity, I, at various operating parameter

CFV (cm/s)	TMP (bar)	MFI ($s.cm^{-6}$)	Resistivity, I x 10^{11} (cm^{-2})
1.3	0.6	550.0	8.14
1.3	1.0	480.0	12.24
1.3	1.3	7.1	0.24

4.2.2. Effect of transmembrane pressure at crossflow velocity 4.6cm/s

a. Initial permeate flux

Figure 4.7 shows the filtration flux time course during crossflow filtration of skim latex at crossflow velocity fixed at 4.6 cm/s with increasing transmembrane pressure ranging from 0.6 bar to 1.3 bar. The results showed that the initial permeate flux decreased slightly about 3.62% as transmembrane pressure increased from 0.6 bar to 1.0 bar. As transmembrane pressure increased further to 1.3 bar, the initial permeate flux increased about 12.4%. This is because the increase in pressure had increased the amount of particles arriving at the membrane surface during the initial stage and accelerated fouling process. Thus, the effective membrane area for particles permeation is decreased as transmembrane pressure increased. This can be observed from the analysis of filtration resistance in later discussion.

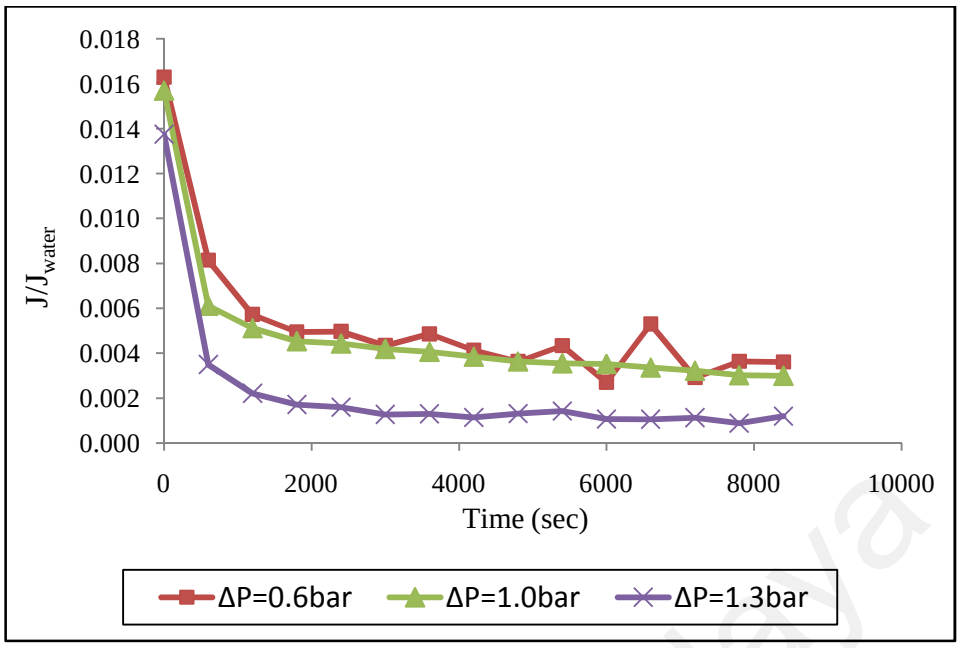

Figure 4.7: Permeate flux was plotted as a function to filtration time for ultrafiltration of skim latex at crossflow velocity 4.6 cm/s and transmembrane pressure 0.6, 1.0 and 1.3 bar

b. Permeate flux at pseudo steady state

Permeate flux reach pseudo steady state as filtration time approached 2000s. The analysis showed that permeate flux at pseudo steady state is decreasing with transmembrane pressure (Figure 4.8). Permeate flux at pseudo steady state was reduced about 7.8% as transmembrane pressure increased from 0.6 bar to 1.0 bar and decreased for about 70% as transmembrane pressure reached 1.3 bar. The experimental result is similar to the results obtained by Shah et al (Shah & Sulaiman, 2009). This is because the increases in transmembrane pressure caused severe fouling by bring more particles to membrane surface during filtration process. Thus filtration resistance is also increased as shown in Figure 4.9 (Hu et al., 2004; Zhao et al., 2003).

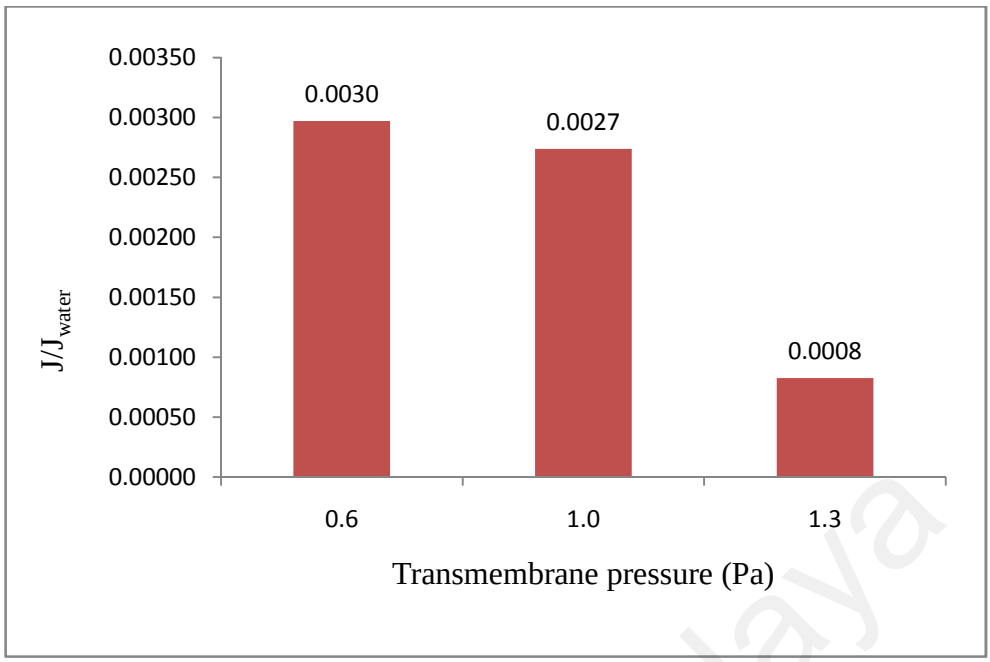

Figure 4.8: Permeate flux at pseudo steady state is plotted as a function of transmembrane pressure at fixed crossflow velocity 4.6 cm/s

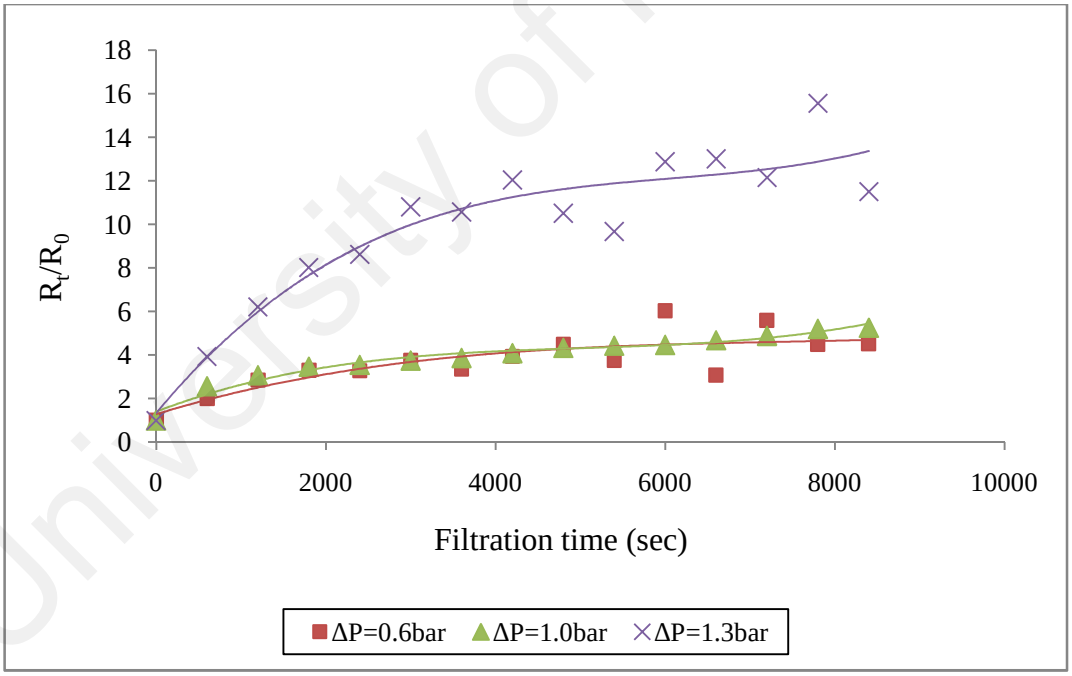

Figure 4.9: Filtration resistance is plotted as a function of time for ultrafiltration of skim latex at fixed crossflow velocity 4.6 cm/s

c. Filtration resistance

Figure 4.9 shows that the trend of filtration resistance with filtration time is higher at 1.3 bar. As shown in Table 4.4, the change in filtration resistance is mainly due to the reversible fouling instead of irreversible fouling. This is because irreversible fouling is less significant as mentioned previously. Reversible fouling is increased to 78.5% upon the increase of transmembrane pressure from 0.6 bar to 1.0 bar. Reversible fouling increased for 171% as transmembrane pressure increased further to 1.3 bar. However, experimental results also showed that irreversible fouling resistance decreased with transmembrane pressure due to more severe surface fouling covering the surface and reduce pore blocking.

Table 4.4: Analysis of reversible resistance (R_f) and irreversible resistance (R_{ir}) during the ultrafiltration of skim latex at crossflow velocity 4.6 cm/s

Crossflow velocity (cm/s)	Transmembrane pressure (bar)	R_r/R_m	%	R_{ir}/R_m	%
4.6cm/s	0.6bar	207.49	99.1	1.81	0.9
4.6cm/s	1.0bar	370.41	99.7	1.29	0.4
4.6cm/s	1.3bar	1003.75	99.9	1.35	0.1

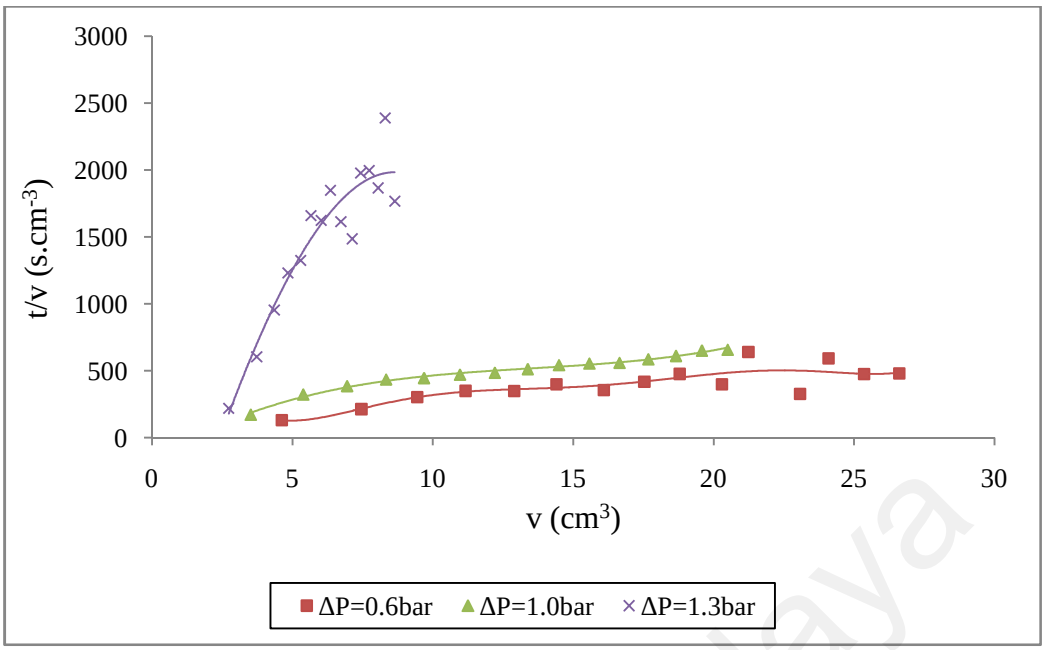

Figure 4.10: A plot of *t/v* versus as a function of filtration volume for ultrafiltration of skim latex at fixed crossflow velocity 4.6cm/s

d. Modified fouling index and resistivity

A plot of the *t/v* versus *v* for crossflow velocity 4.6 cm/s, is shown in Figure 4.10. Table 4.5 showed that, at crossflow velocity 4.6 cm/s, MFI and *I* increased with transmembrane pressure. As transmembrane pressure increased from 0.6 bar to 1.0 bar, MFI increased slightly for about 9%. It implies that fouling potential only increased slightly as transmembrane pressure increased from 0.6 bar to 1.0 bar. As transmembrane pressure increased to 1.3 bar, fouling potential increased tremendously as shown in Table 4.5. High pressure leads to higher concentration on membrane surface and caused the increase of fouling (Boerlage et al., 2004). The result shows similar trend with the analysis of permeates flux performance and fouling resistance results obtained. Particles drag force increased as transmembrane pressure increased. This had caused more particles to be deposited on membrane surface. Particles deposition leads to the increase in MFI as fouling increased (Sim et al., 2010). Due to more severe fouling, resistivity, I,

increased for 86.4% as transmembrane pressure increased from 0.6 bar to 1.0 bar and increased about 2766% at 1.3 bar.

Table 4.5: Modified fouling index, MFI, and resistivity, I, at crossflow velocity 4.6 cm/s and transmembrane pressure 0.6 bar, 1.0 bar and 1.3 bar

CFV (cm/s)	TMP (bar)	MFI ($s.cm^{-6}$)	Resistivity, I x 10^{11} (cm^{-2})
4.6	0.6	16.7	0.59
4.6	1.0	18.2	1.10
4.6	1.3	400.0	31.53

Skim latex ultrafiltration performances with transmembrane pressure observed were different at constant crossflow velocity 1.3 cm/s and 4.6 cm/s. The main reason is due to the increase in crossflow velocity can increase the particles tangential shear force along the membrane surface. The increase in shear stress can cause more particles to diffuse back to the bulk solution and reduced fouling (Hwang & Huang, 2009). This may also because the increase of crossflow velocity can also increase internal pressure.

4.2.3. Effect of crossflow velocity at transmembrane pressure 0.3 bar

a. Initial permeate flux

Ultrafiltration of skim latex at fixed transmembrane pressure 0.3 bar and 1.0 bar across the crossflow velocity range from 1.3 cm/s to 4.6 cm/s were also studied. At transmembrane pressure 0.3 bar, initial permeate flux decreased for 59.3% as crossflow velocity increased from 1.3 cm/s to 3.6 cm/s. However, as crossflow velocity increased further to 4.6 cm/s, initial crossflow velocity had improved for 117.3% (Figure 4.11). This may be because as crossflow velocity increased from 1.3 cm/s to 3.6 cm/s, larger particles are more likely to diffuse back into the bulk solution (Berre & Daufin, 1996).

Smaller particles were brought to the membrane and caused more severe pore blocking effect. However, as crossflow velocity increase further to 4.6 cm/s, in a limited space, increase of crossflow velocity can cause the increase of internal pressure and caused cake layer formed faster (Chen & Hsiau, 2009).

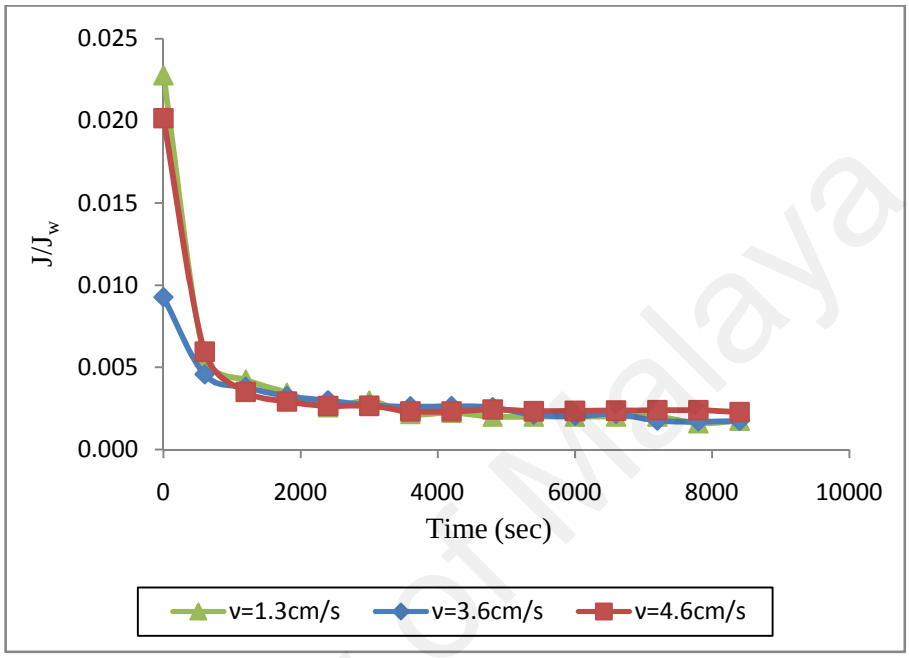

Figure 4.11: Permeate flux was plotted as a function of filtration time for ultrafiltration of skim latex at fixed transmembrane pressure 0.3 bar across the range of crossflow velocity

b. Permeate flux at pseudo steady state

Permeate flux reached pseudo steady state as filtration time approached 1600s. At pseudo steady state, permeate flux is almost constant. At pseudo steady state, permeate flux is improved as crossflow velocity increased (Figure 4.12). As crossflow velocity increased from 1.3 cm/s to 3.6 cm/s, permeate flux at pseudo steady state had improved 15.5%. As crossflow velocity increased to 4.6 cm/s, permeate flux at pseudo steady state increased 8.8%. Permeate flux at pseudo steady state can be improved by reducing fouling. The increase of crossflow velocity can increase flow shear stress and scoured away fouled particles.

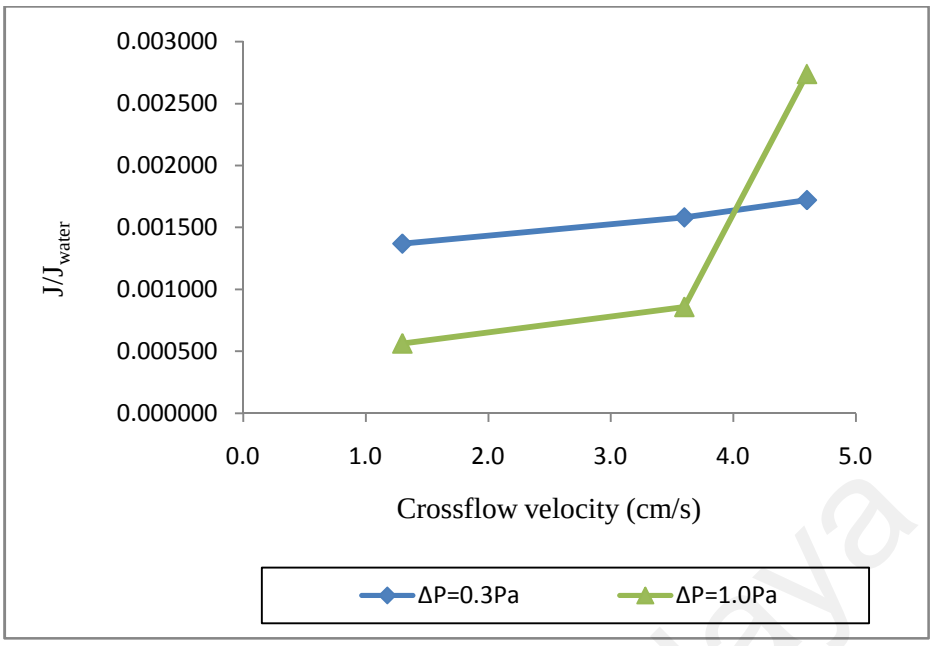

Figure 4.12: Permeate flux at pseudo steady state is plotted as a function of crossflow velocity at fixed transmembrane pressure 0.3 bar

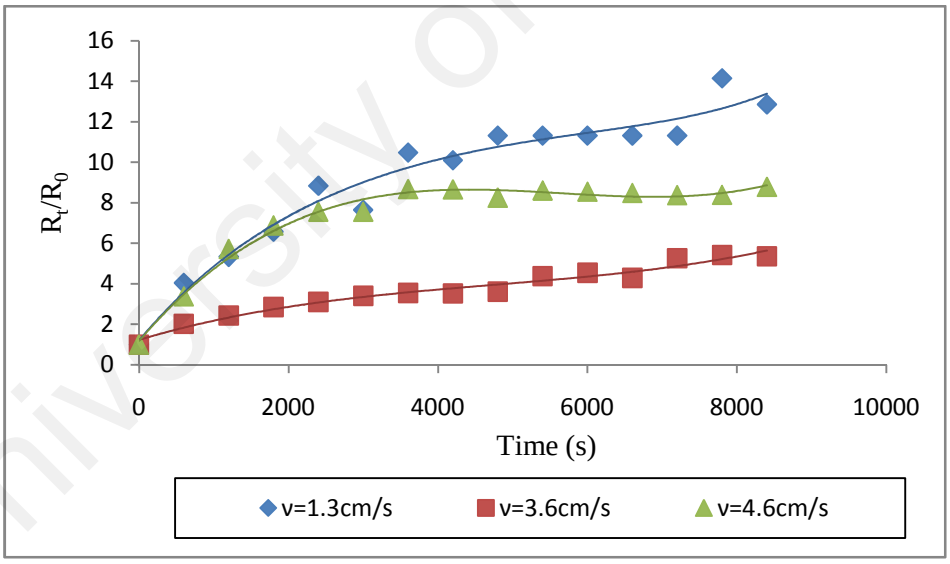

Figure 4.13: Filtration resistance is plotted as a function of time for ultrafiltration of skim latex at transmembrane pressure 0.3 bar across ranges of crossflow velocity

c. Filtration resistance

The analysis of filtration resistance ratio (R_t/R_0) also indicates that at transmembrane pressure 0.3 bar, filtration resistance trend is decreased as crossflow velocity increased from 1.3 cm/s to 3.6 cm/s (Figure 4.13). The reduction in filtration resistance ratio is due to the scouring effect which had reduced fouling. However, as crossflow velocity increased further to 4.6cm/s, the trend of filtration resistance ratio is increased instead of decreased. This may be because the increase of crossflow velocity can also lead to the formation of compact cake layer with lower average particles size and higher filtration resistance as mentioned previously. (Mikulasek et al., 1998; Zhao et al., 2003). The combination of these two effects is the main reason of the increase in filtration resistance as crossflow velocity increases further to 4.6 cm/s.

d. Modified fouling index and resistivity

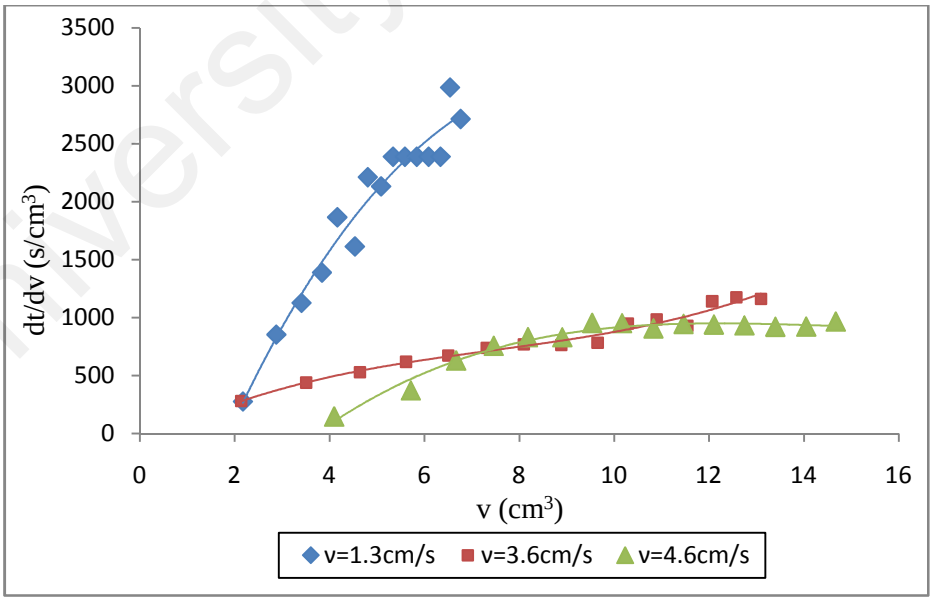

Figure 4.14: Plot of *t/v* as a function of permeate volume, *v*, for skim latex ultrafiltration at transmembrane pressure 0.3 bar and crossflow velocity 1.3 cm/s, 3.6 cm/s and 4.6 cm/s

Table 4.6: Modified fouling index, MFI, and resistivity, I, at transmembrane pressure and crossflow velocity 1.3 cm/s, 3.6 cm/s and 4.6 cm/s

CFV (cm/s)	TMP (bar)	MFI ($s.cm^{-6}$)	Resistivity, I x 10^{11} (cm^{-2})
1.3	0.3	708.3	5.42
3.6	0.3	62.5	0.96
4.6	0.3	229.2	4.17

Figure 4.14 is the regression of *t/v* as a function of permeates volume, *v*, the slope of the initial linearity is highest at crossflow velocity 1.3 cm/s. As mentioned previously in literature review, fouling mechanism is usually dominated by pore blocking at the initial stage resulting in high slope (Hu et al., 2004; Kanani et al., 2008; Li et al.; Purkait et al., 2005). Thus, pore blocking is more severe at crossflow velocity 1.3 cm/s. Previous study also showed that fouling usually starts from internal clogging to the buildup of an external fouling layer over the membrane surface. As filtration prolonged, fouling mechanism gradually switch to cake filtration which is usually indicated by linear region of the curve (Boerlage et al., 2002). The MFI results imply that cake layer fouling potential is the highest at crossflow velocity 1.3 cm/s (Table 4.6). The result implies that cake layer formation is the most drastic at crossflow velocity 1.3 cm/s. As crossflow velocity increased to 3.6 cm/s, the scouring effect had reduced the cake layer formation potential for 91.2% and the fouled layer resistivity, I, for 4.46 x 10^{11} cm^{-2}. At low transmembrane pressure (0.3 bar), as crossflow velocity increased further to 4.6 cm/s, fouling potential (MFI) and cake layer resistivity (*I*) is increased for 266.7% and 334.4%, respectively. This is due to the fact that the increase of crossflow velocity tends to induce more fine particles to be deposited and form compact fouled layer. The result is consistent with the analysis of filtration resistance and permeates flux.

4.2.4. Effect of crossflow velocity at transmembrane pressure 1.0 bar

a. Initial permeate flux

As shown previously in Figure 4.12, at transmembrane pressure 1.0 bar, the initial permeate fluxes increased as cross flow velocity increased. Figure 4.15 also implies that permeates fluxes at pseudo steady state are also increased as cross flow velocity increased. As crossflow velocity increased from 1.3 cm/s to 3.6 cm/s, the normalized initial permeate flux had increased for 263.5% from 0.0028 to 0.0101. As crossflow velocity increases further to 4.6 cm/s, initial permeate flux had increased for 55.7%. The increment of permeate flux with crossflow velocity is similar to the experimental results of Mikulasek on crossflow microfiltration experiments of aqueous dispersion of titanium dioxide through a ceramic membrane (Mikulasek et al., 1998). In the study of Mikulasek, it showed that steady state fluxes increased with crossflow velocity. This is because increase in crossflow velocity tends to increase shear stress along the membrane surface. Shear stress can scour away the particles deposition or accumulation on membrane surface and reduce fouling (Faibish & Cohen, 2001; Hwang & Huang, 2009; Thomassen et al., 2005).

`

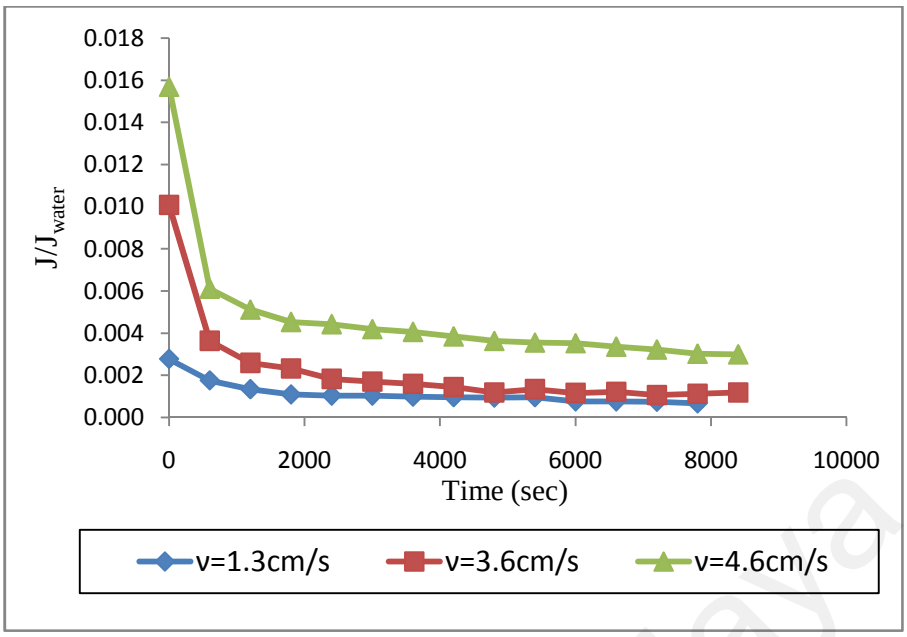

Figure 4.15: Permeate flux was plotted as a function of filtration time for ultrafiltration of skim latex at fixed transmembrane pressure 1.0 bar across the range of crossflow velocity

b. Filtration resistance

The analysis of filtration resistance with filtration time in Figure 4.16 showed that the trend of filtration resistance is lower at higher crossflow velocity. This is because as shear stress increased, fouled layer was scoured away causing reduction in hydraulic filtration resistance.

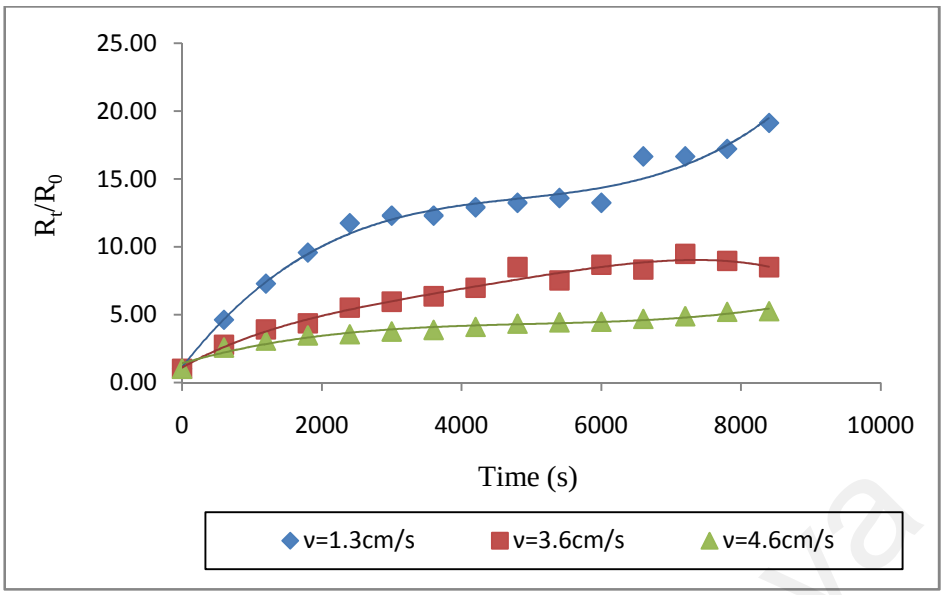

Figure 4.16: The changes of filtration resistance are plotted as a function of filtration time at transmembrane pressure 1.0 bar and variant crossflow velocity

c. Modified fouling index and resistivity

As can be seen in the regression analysis of *t/v* versus *v*, the slope of the curve is decreased as crossflow velocity is increased from 1.3 cm/s to 4.6 cm/s (Figure 4.17). The result implies that the slope linearity is decreasing as crossflow velocity increased. The slope of linearity was taken as MFI. In Table 4.7, MFI had reduced by 41.9% as crossflow velocity increased from 1.3 cm/s to 3.6 cm/s. As crossflow velocity increased further to 4.6 cm/s, MFI has reduced for 93.5% from 278.9 $s.cm^{-6}$ to 18.2 $s.cm^{-6}$.

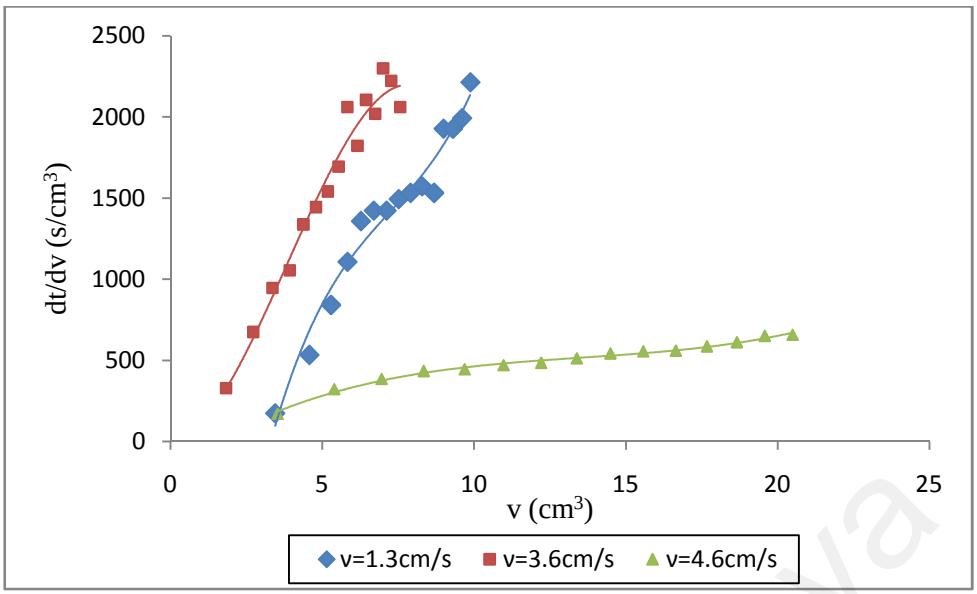

Figure 4.17: Plot of *t/v* as a function of permeate volume, *v*, for skim latex ultrafiltration at transmembrane pressure 1.0 bar and crossflow velocity 1.3 cm/s, 3.6 cm/s and 4.6 cm/s

Table 4.7: Modified fouling index, MFI, and resistivity, I, at transmembrane pressure and various crossflow velocities

CFV (cm/s)	TMP (bar)	MFI ($s.cm^{-6}$)	Resistivity, I x 10^{11} (cm^{-2})
1.3	1.0	480.0	12.24
3.6	1.0	278.9	14.33
4.6	1.0	18.2	1.10

Decrease of MFI with crossflow velocity is most likely due to the reduction in cake layer formation potential as shear stress increased. However, as crossflow velocity increased from 1.3cm/s to 3.6cm/s, fouled layer resistivity slightly increased by 17.1%. This is because the increase of crossflow velocity has also caused the decrease of cake layer average particles size (Sim et al., 2010). Increases in crossflow velocity cause fine particles to deposit on membrane surface instead of large particles. Most of the large particles were lifted back into the bulk solution. It will lead to the formation of compact cake layer and higher filtration resistance (Mikulasek et al., 1998; Zhao et al., 2003).

Zhao et al showed that the hydraulic resistance is decreased with crossflow velocity in a study on the effect of operational parameters on fouling of ceramic membranes during microfiltration titanium white acid (Zhao et al., 2003). As crossflow velocity increased further to 4.6cm/s, fouled layer resistivity had reduced for 92.3% due to scouring effect as crossflow velocity increased had reduced fouling.

The filtration performance at transmembrane pressure 0.3 bar and 1.0 bar with crossflow velocity have different trends. This is because as transmembrane pressure increases from 0.3 bar to 1.0 bar, particles convection force is increased. Convection force on the particles plays an important role in determining the movement of particles in the flow as shown in the experimental result.

`

4.3. Protein rejection coefficient

4.3.1. Effect of transmembrane pressure on rejection coefficient

Rejection coefficient is used to measure the membrane selectivity and membrane retention for solute. Rejection coefficient of protein during ultrafiltration of skim latex at crossflow velocity 1.3 cm/s and 4.6 cm/s were shown in Figure 4.18 and Figure 4.19. The results show that protein rejection coefficient is decreasing with transmembrane pressure at crossflow velocity 1.3 cm/s and 4.6 cm/s.

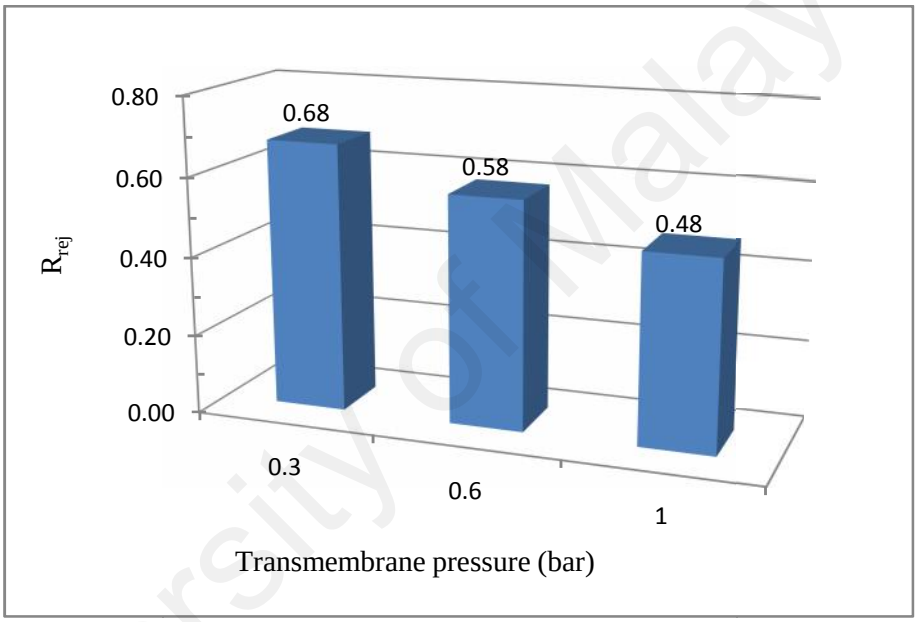

Figure 4.18: Coefficient rejection of protein in skim latex during ultrafiltration of skim latex at crossflow velocity 1.3 cm/s

At crossflow velocity 1.3cm/s, as transmembrane pressure increased from 0.3 bar to 0.6 bar, protein rejection coefficient had decreased for 14.7%. As transmembrane pressure increased to 1.0 bar, protein rejection coefficient had reduced 17.2%.

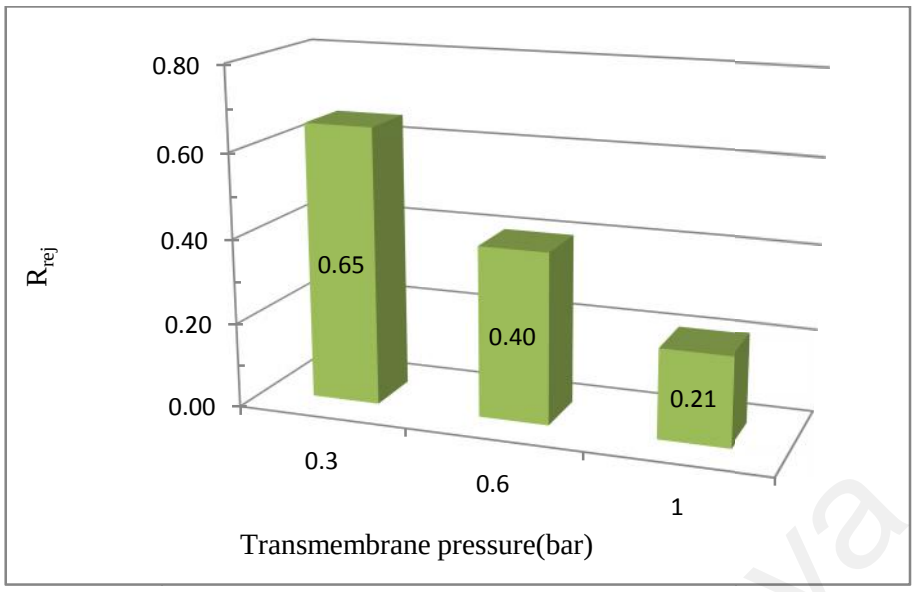

Figure 4.19: Coefficient rejection of protein in skim latex during ultrafiltration of skim latex at crossflow velocity 4.6 cm/s

Protein rejection coefficient had decreased 38.5% and 47.5% when transmembrane pressure increased from 0.3 bar to 0.6 bar and then further to 1.0 bar. The results showed that protein permeation through the membrane increased with the increase of transmembrane pressure. This may be because the increase of transmembrane pressure had increased the particles convection force and more protein molecules are pushed through the membrane. Protein rejection coefficient is also highly dependent on resistance of the medium to the permeation of proteins through the medium. The rate of reduction of protein rejection coefficient is higher at crossflow velocity 4.6 cm/s compare to at 1.3 cm/s. This had proved that the effect of transmembrane pressure is more significant at higher crossflow velocity.

4.3.2. Effect of crossflow velocity on rejection coefficient

Rejection coefficient increased with crossflow velocity at transmembrane pressure 0.3 bar (Figure 4.20). The increment is 13.9% as crossflow velocity increased from 1.3 cm/s to 3.6 cm/s and 73.2% as crossflow velocity increased to 4.6 cm/s. The results imply that protein permeation through the membrane is reduced with the increase of crossflow velocity at transmembrane pressure 0.3 bar. This is because at low transmembrane pressure range, the increase of crossflow velocity shear increase the particles inertial lift force and reduce the particle convection through the membrane.

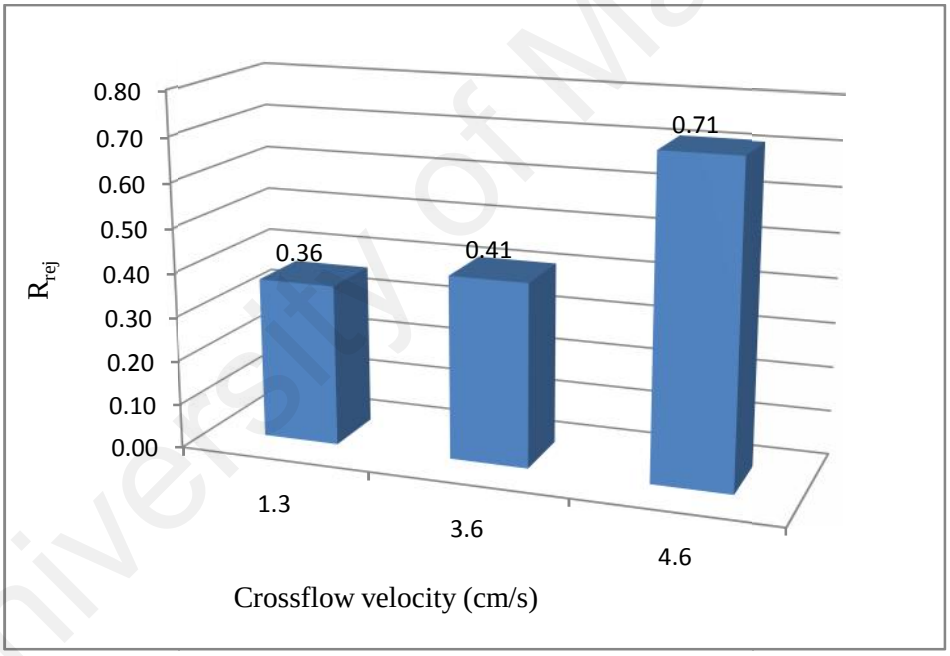

Figure 4.20: Coefficient rejection of protein in skim latex during ultrafiltration of skim latex at transmembrane pressure 0.3 bar

However, at transmembrane pressure 1.0 bar, rejection coefficient is slightly increased for 3.4% as crossflow velocity increased from 1.3 cm/s to 3.6 cm/s (Figure 4.21). Protein permeation is reduced as crossflow velocity increased from 1.3 cm/s to 3.6 cm/s due to particles inertial lift back to bulk solution instead of permeate through

the membrane. As crossflow velocity increase further to 4.6 cm/s, rejection coefficient reduced rapidly for 33.3%. This may due to the increase of crossflow velocity which increased the internal pressure and more proteins were pushed through the membrane.

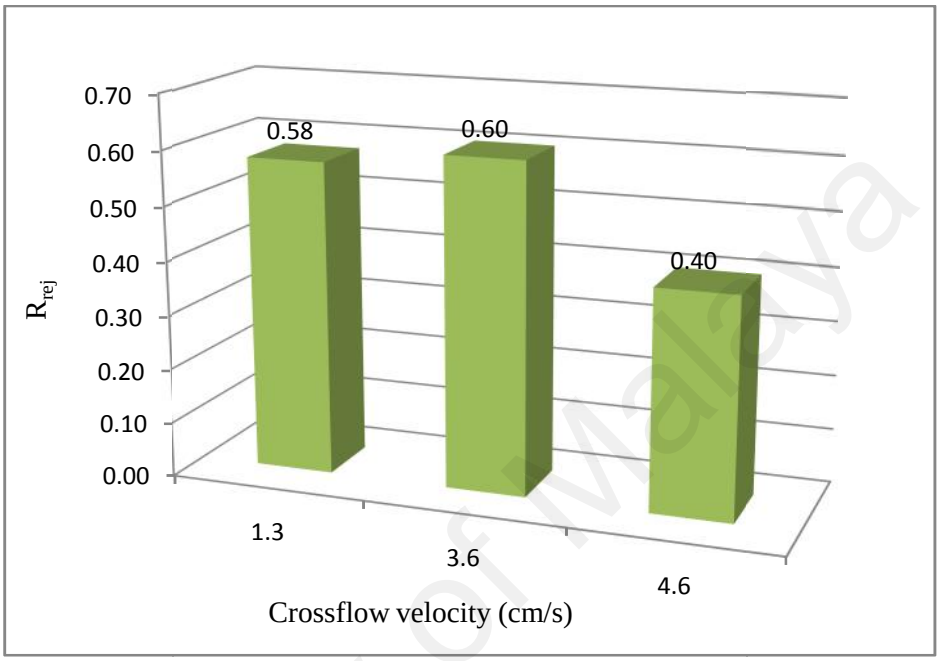

Figure 4.21: Coefficient rejection of protein in skim latex during ultrafiltration of skim latex at transmembrane pressure 1.0 bar

CHAPTER 5

CONCLUSION AND FUTURE WORK

5.1 Conclusion

The experimental results in this study showed that filtration performance and fouling in the ultrafiltration of skim latex is highly dependent on transmembrane pressure and crossflow velocities do affect the filtration performances. The effect of transmembrane pressure on fouling has different trends at a range of crossflow velocity and transmembrane pressure. This study allows us to gain a better understanding in the effect of transmembrane pressure and crossflow velocity on fouling and filtration performance in ultrafiltration of skim latex.

The skim latex used in this study was alkaline (pH 9.62 ± 0.12) with a particle size distribution range of 0.07 to 0.33 ± 0.012 µm and density 0.9957 ± 0.0072 g/cm^3. The feed solution used has TSC of 6.42 ± 0.02% and 4.24 ± 0.01%. Ultrafiltration of skim latex was studied using single tubular ceramic membrane of 0.05µ in a bench scale ultrafiltration unit.

The experimental results showed that, in general, permeate flux decreases with filtration time. Permeate flux decreased drastically at the initial period and then gradually reached pseudo steady state as filtration time approached 1600 s. The reduction in permeate flux with filtration time is basically caused by the buildup of fouling layer on membrane surface. The initial rapid reduction in permeate flux is because severe fouling is occurred at the initial stage (Hwang & Sz, 2010). As filtration prolonged, particles start to block the pores and reduce the available membrane area for filtration. Thus, particles start to accumulate and deposit on surface to form polarization

layer. Permeate flux had reduced for about rapidly for 79-92% as permeate flux reached pseudo steady state. At this point, the particle deposition rate is equal to the particles back diffusion rate. Thus, no further fouling occurred at this point and permeates flux and resistance had reached an almost constant state. At pseudo steady state, further growth of fouling layer is restricted by the flow shear stress across the fouled layer. Thus, the trend of filtration resistance is increasing with filtration time. Filtration resistance is increased rapidly initially due to fouling and then reached pseudo steady state. The rapid increased in filtration resistance is the main reason leads to the drastic reduction in permeate flux.

5.1.1 Effects of crossflow velocity

The effect of transmembrane pressure on permeate flux performance is different from that of crossflow velocity 1.3 cm/s and 4.6 cm/s. At low crossflow velocity range 1.3 cm/s, the increase in transmembrane pressure can cause the increase of initial permeate flux. However, permeate flux at pseudo steady state decreased 38% due to more severe fouling. As transmembrane pressure 1.0bar, the increase in particles convection force can cause large particles to deposit and formed fouled layer with higher porosity and lower resistance. Thus, permeate flux at pseudo steady state had improved. At crossflow velocity 4.6 cm/s, the increase of transmembrane pressure tends to increase the particles convection force to membrane surface and cause more severe fouling. As a consequence, initial permeate flux and flux at pseudo steady state tend to decrease as transmembrane pressure increased. Filtration resistance is increased (78-171%) with transmembrane pressure due to more severe fouling.

The studies also reveal that reversible fouling is predominant (99%) compared to irreversible fouling resistance (<1%) in the fouling of skim latex. The increase of

transmembrane pressure caused the increase in cake layer formation which contributed to reversible fouling resistance. MFI and fouled layer resistivity (I) are also increased with transmembrane pressure. The increment is higher as transmembrane pressure increased from 1.0 bar to 1.3 bar. MFI had increased 2097.8% and *I* had increased 2766.4%.

5.1.2 Effects of transmembrane pressure

This experimental results showed that permeate fluxes are increased upon the increase of crossflow velocity at transmembrane pressure 1.0 bar. Initial permeate flux and permeate flux at pseudo steady state had increased as transmembrane pressure increased at constant crossflow velocity. The filtration resistance trend is lower at higher crossflow velocity. However, at transmembrane pressure 0.3 bar, where convection force is lower, the increase of crossflow velocity reduced the average particles size of fouled layer by lifted large particles in fouled layer as crossflow velocity increased from 1.3 cm/s to 3.6 cm/s. As the result, filtration resistance trend is increased as crossflow velocity increased from 3.6 cm/s to 4.6 cm/s at 0.3 bar transmembrane pressure. Modified fouling index (MFI) and resistivity (*I*) also increased as crossflow velocity increased to 4.6 cm/s a transmembrane pressure 0.3 bar.

`

5.1.3 Protein rejection coefficient

Protein rejection coefficient is decreased with transmembrane pressure at crossflow velocity 1.3 cm/s and 4.6 cm/s due to the increase in particles convection force. At constant crossflow velocity 1.3 cm/s, protein rejection coefficient had reduced as transmembrane pressure increased. At crossflow velocity 4.6 cm/s, protein rejection coefficient is reduced for about 38-48%. The reduction rate is more obvious at higher crossflow velocity (4.6 cm/s).

At constant transmembrane pressure 0.3 bar, the increase of crossflow velocity caused the increase of protein rejection coefficient. This is because the increase of shear stress had reduced the protein particles convection force. Less protein was pushed through the membrane. At higher transmembrane pressure, 1.0 bar, the increase of crossflow velocity caused the increased of protein rejection coefficient. The different behavior might due to the increase in applied pressure have affected the particles convection force. Protein permeation is reduced because particles tend to lift back to bulk solution instead of permeate through the membrane. As crossflow velocity increased further to 4.6 cm/s, rejection coefficient reduced rapidly for 33.3% due to the increase internal pressure and more proteins were pushed through the membrane.

`

5.2 Future work

This study is limited to operating parameters transmembrane pressure and crossflow velocity. It is recommended to perform studies on the effect of feeds properties such as pH, feeds concentration, and feeds temperature and viscosity. Effects of other parameters such as membrane dimension, membrane types, and pore size should also be investigated.

Another key element to understand the fouling behavior is to conduct characterization of fouled membrane. Besides scanning electron microscope (SEM), different techniques such as X-ray photoelectron spectroscopy (XPS), UV spectroscopy and atomic force microscopy (AFM) can also be used to characterize the fouled membrane surface. Particles size analysis on the retentate should be carried out to studied the size of particles deposited on membrane during the ultrafiltration of skim latex. As skim latex is polydispersed biopolymer, compression of fouled layer during the ultrafiltration of skim latex are also should be considered for future study. Such studies would allow us to gain further understanding on skim latex fouling and develop a method to clean the used membranes and assess the effectiveness of various membrane cleaning methods. The data obtained can also be used to develop a model of fouling and filtration behavior. An optimum operating parameter can be obtained using the model developed in order to optimize the filtration performance.

`

CHAPTER 6

REFERENCES

Akoum, O., Jaffrin, M. Y., & L.H., D. (2005). Concentration of Total Milk Proteins by Shear Ultrafiltration in a Vibrating Membrane Module. *Journal of Membrane Science, 247*, 211-220.

Alhadidi, A., Kemperman, A. J. B., Blankert, B., Schippers, J. C., Wessling, M., & Meer, W. G. J. v. d. (2011). Silt denisty index and modified fouling index relation, and effect of pressure, temperature and membrane resistance. *Desalination, 273*, 48-55.

. All About Natural Rubber Latex. (2009) Retrieved March 01, 2011, from http://rubberasia.com/

. *Annual Rubber Statistics Malaysia 2010*. Retrieved from http://www.statistics.gov.my/portal/.

Bacchina, P., Si-Hassena, D., Starovb, V., Cliftona, M. J., & Aimar, P. (2002). A Unifying Model for Concentration Polarization, Gel Layer Formation and Particles Deposition in Cross-flow Membrane FIltration of Colloidal Suspensions. *Chemical Engineering Science 57*, 77-91.

Beilen, J. B. v., & Poirier, Y. (2007). Establishment of new crops for the production of natural rubber. *Trends in Biotechnology, 25*(11), 522-529. doi: 10.1016/j.tibtech.2007.08.009

Belfer, S., Gilron, J., & Kedem, O. (1999). Characterization of Commercial RO & UF Modified and Fouled Membranes by Means of ATR/FTIR. *Desalination, 124*, 175-180.

Berre, O. L., & Daufin, G. (1996). Skimmilk crossflow microfiltration performance versus permeation flux to wall shear stress ratio. *Journal of Membrane Science, 117*, 261-270.

Blanpain-Avet, P., Doubrovine, N., Lafforgue, C., & Lalande, M. (1999). The effect of oscillatory flow on crossflow microfiltration of beer in a tubular mineral membrane system - Membrane fouling resistance decrease and energetic considerations. *Journal of Membrane Science, 152*(2), 151-174.

Boerlage, S. F. E., Kennedy, M., Tarawneh, Z., Faber, R. D., & Schippers, J. C. (2004). Developement of the MFI-UF in constant flux filtration. *Desalination, 161*, 103-113.

Boerlage, S. F. E., Kennedy, M. D., Dickson, M. R., El-Hodali, D. E. Y., & Schippers, J. C. (2002). The modified fouling index using ultrafiltration membranes (MFI-UF): characterisation, filtration mechanisms and proposed reference membrane. *Journal of Membrane Science, 197*(1-2), 1-21.

Cecil, J., & Mitchell, P. (2005). Processing of Natural Rubber, 2011, from http://ecoport.org/ep?SearchType=earticleView&earticleId=644&page=-2

Chang, E. E., Yang, S. Y., Huang, C. P., Liang, C. H., & Chiang, P. C. (2011). Assessing the fouling mechanisms of high-pressure nanofiltration membrane using the modified Hermia model and the resistance-in-series model. *Separation and Purification Technology, 79*(3), 329-336.

Chang, I. S., Field, R., & Cui, Z. (2009). Limitations of resistance-in-series model for fouling analysis in membrane bioreactors: A cautionary note. *Desalination and Water Treatment, 8*, 31-36.

Chen, Y. S., & Hsiau, S. S. (2009). Influence of filtration superficial velocity on cake compression and cake formation. *Chemical Engineering and Processing: Process Intensification, 48*(5), 988-996.

Cho, J., Amy, G., & Pellegrino, J. (2000). Membrane filtration of natural organic matter: factors and mechanisms affecting rejection and flux decline with charged ultrafiltration (UF) membrane. *Journal of Membrane Science, 164*, 89-110.

Cornish, K. (2001). Similarities and differences in rubber biochemistry among plant species. *Phytochemistry, 57*(7), 1123-1134. doi: 10.1016/s0031-9422(01)00097-8

Costa, A. R., Pinho, M. N. d., & Elimelech, M. (2006). Mechanisms of Colloidal Natural Organic Matter Fouling in Ultrafiltration. *Journal of Membrane Science, 281*, 716-725.

Cotterill, L. (1996). Ultrafiltration Basics. *Water & Wastes Digest*.

. Crossflow Microfiltration (2002) Retrieved March 07, 2011, from http://www.treatmentproducts.com/micro.pdf

Danwanichakul, P., Werathirachot, R., Kongkaew, C., & Loykulnant, S. (2011). Coagulation of skim natural rubber latex using chitosan or polyacrylamide as an alternative to sulfuric acid. *European Journal of Scientific Research, 62*(4), 537-547.

Deng, Y., & Deng, D. (2000). Study on extraction of quebrachitol from natural rubber. *Natural Product Research and Development, 12*(6), 61-65.

Doneva, T. A., Vassilieff, C. S., & Krusteva, E. D. (1998). Cross-flow microfiltration of latex suspensions: test of different models. *Colloids and Surfaces A: Physicochemical and Engineering Aspects, 138*(2–3), 245-254. doi: 10.1016/s0927-7757(96)03955-6

Ebersold, M. F., & Zydney, A. L. (2004). The effect of membrane properties on the separation of protein charge variants using ultrafiltration. *Journal of Membrane Science, 243*(1-2), 379-388.

Ernst, M., Bismarck, A., Bismarck, J., & Jekel, M. (2000). Zeta-potential and rejection rates of a polyethersulfone nanofiltration membrane in single salt solutions. *Journal of Membrane Science, 165*(2), 251-259.

Faibish, R. S., & Cohen, Y. (2001). Fouling and rejection behavior of ceramic and polymer-modified ceramic membranes for ultrafiltration of oil-in-water emulsions and microemulsions. *Colloids and Surfaces A: Physicochemical and Engineering Aspects, 191*(1-2), 27-40.

Field, R. (2010). Fundamentals of Fouling *Membrane Technology* (pp. 1-23): Wiley-VCH Verlag GmbH & Co. KGaA.

Ghosh, R. (2006). Chapter 10 Filtration *Principles of Bioseparations Engineering*. Singapore: World Scientific Publishing Co. Pte. Ltd.

Haris, U., Prastanto, H., Alfa, A. A., & Maspanger, D. R. (2010). The Economic Potential of Skim Latex Processing on the Latex Concentrate Industry: Indonesian Case: Indonesian Rubber Research Institute.

Harmant, P., & Aimar, P. (1998). Coagulation of colloids in a boundary layer during cross-flow filtration. *Colloids and Surfaces A: Physicochemical and Engineering Aspects, 138*(2-3), 217-230.

Heinisch, K. F. (1974). *Dictionary of Rubber*: Applied Science Publisher.

Holdich, R. G. (2002). Filtration of Liquids *Fundamentals of Particle Technology*. United Kingdom: Midland Information Technoloby and Publishing.

Hong, S., & Elimelech, M. (1997). Chemical and physical aspects of natural organic matter (NOM) fouling of nanofiltration membranes. *Journal of Membrane Science, 132*, 159-181.

. How Products Are Made. (2006-2011). *Volume 3 Latex* Retrieved Jan 30, 2010, from http://www.madehow.com/Volume-3/Latex.html

Howell, J. A. (1995). Sub-critical flux operation of microfiltration. *Journal of Membrane Science, 107*(1-2), 165-171.

Howell, J. A., Sanchez, V., & Field, R. W. (1993). *Membrane in Bioprocesing: Theory and Applications*. Cambridge: Chapman & Hall.

Hu, X., Bekassy-Molnar, E., & Koris, A. (2004). Study of modelling transmembrane pressure and gel resistance in ultrafiltration of oily emulsion. *Desalination, 163*(1-3), 355-360.

Hwang, K.-J., Chou, F.-Y., & Tung, K.-L. (2006). Effects of operating conditions on the performance of cross-flow microfiltration of fine particle/protein binary suspension. *Journal of Membrane Science, 274*(1-2), 183-191.

Hwang, K. J., & Huang, P. S. (2009). Cross-flow microfiltration of dilute macromolecular suspension. *Separation and Purification Technology, 68*, 328-334.

Hwang, K. J., Liao, C. Y., & Tung, K. L. (2007). Analysis of Particle Fouling during MIcrofiltration by Use of Blocking Models. *Journal of Membrane Science, 287*, 287-293.

Hwang, K. J., & Sz, P. Y. (2010). Filtration characteristics and membrane fouling in cross-flow microfiltration of BSA/dextran binary suspension. *Journal of Membrane Science, 347*, 75 - 82.

. The Industry. (2003-2011) Retrieved January 30, 2011 from http://www.mrepc.com/img/panel/panelIndustry.gif

Javeed, M. A., Chinu, K., Shon, H. K., & Vigneswaran, S. (2009). Effect of pre-treatment on fouling propensity of feed as depicted by the modified fouling index (MFI) and cross-flow samplerâ€“modified fouling index (CFSâ€“MFI). *Desalination, 238*(1-3), 98-108.

Jayachandran, K., & Chandrasekaran, M. (1998). Biological Coagulation of Skim Latex using Acinetpbacter sp. Isolated from Natural Rubber Latex Centrifugation Effluent. *Biotechnology Letters, Vol 20*(No 2), 161-164.

Jebamani, I. S., Gopalakrishnan, V., & Senthilkumar, G. (2009). Brine solution recovery using nanofiltration. Retrieved from Green Pages website: http://www.eco-web.com/edi/090714.html

Kanani, D. M., Sun, X., & Ghosh, R. (2008). Reversible and irreversible membrane fouling during in-line microfiltration of concentrated protein solutions. *Journal of Membrane Science, 315*(1-2), 1-10.

Kennedy, M. D., Kamanya, J., Rodrigue, S. G. S., Lee, N. H., Schippers, J. C., & Amy, G. (2008). Water Treatment by Microfiltration and Ultrafiltration. In N. N. Li, A. G. Fane, W. S. Winston & T. Matsura (Eds.), *Advanced Membrane Technology and Applications*. New Jersey: John Wiley & Sons, Inc.

Konieczny, K., & Bodzek, M. (1996). Ultrafiltration of Latex Wastewaters. *Desalination, 104*, 75-82.

Krusteva, E. D., Doneva, T. A., & Vassilieff, C. S. (1999). Pseudoplasticity of filter cakes explains cross-flow microfiltration. *Colloids and Surfaces A: Physicochemical and Engineering Aspects, 149*(1–3), 499-506. doi: 10.1016/s0927-7757(98)00603-7

Kumar, A. K. (2012). Expanding the supply base for Indian rubber industry: IL& FS Cluster Development Initiative Limited.

`

Li, H., Fane, A. G., Coster, H. G. L., & Vigneswaran, S. (1998). Direct Observation of Particles Deposition on the Membrane Surface during Crossflow Microfiltration. *Journal of Membrane Science, 149*, 83-97.

Li, H., Fane, A. G., Coster, H. G. L., & Vigneswaran, S. (2000). An Assessment of Depolarisation Models of Crossflow Microfiltration by Direct Observation Through the Membrane. *Journal of Membrane Science, 172*, 135-147.

Li, M., Zhao, Y., Zhou, S., & Xing, W. Clarification of raw rice wine by ceramic microfiltration membranes and membrane fouling analysis. *Desalination, 256*(1-3), 166-173.

Li, W., Xing, W., Jin, W., & Xu, N. (2006). Effect of pH on microfiltration of Chinese herb aqueous extract by zirconia membrane. *Separation and Purification Technology, 50*(1), 92-96.

Liang, C. C., & Kai, H. Z. (2011). *Rheological properties of natural rubber and its variants.* Degree of Chemical Engineering, University Malaya.

. Market Information in the Commodities Area. (2011). *Rubber-Characeristics* Retrieved Jan 30, 2011, from http://www.unctad.org/infocomm/anglais/rubber/characteristics.htm

Marselina, Y., Lifia, Le-Clech, P., Stuetz, R. M., & Chen, V. (2009). Characterisation of membrane fouling deposition and removal by direct observation technique. *Journal of Membrane Science, 341*(1-2), 163-171.

Marshall, A. D., Munro, P. A., & Trägårdh, G. (1997). Influence of permeate flux on fouling during the microfiltration of [beta]-lactoglobulin solutions under cross-flow conditions. *Journal of Membrane Science, 130*(1-2), 23-30.

Mart, A., Martinez, F., Malfeito, J., Palacio, L., Pradanos, P., & Hernandez, A. (2003). Zeta potential of membranes as a function of pH: Optimization of isoelectric point evaluation. *Journal of Membrane Science, 213*(1-2), 225-230.

Matsuura, T. (2004). Membrane separation technologies *Membrane separation processes where the driving force is pressure* Retrieved from http://www.eolss.net/EolssSampleChapters/C07/E2-14-01-02/E2-14-01-02-TXT-03.aspx#5._Membrane_separation_processes_where_the_driving_force_is_partial_pressure_

Mikulasek, P., Wakeman, R. J., & Marchant, J. Q. (1998). Crossflow microfiltration of shear-thinning aqueous titanium dioxide dispersions. *Chemical Engineering Journal, 69*, 53-61.

Mondor, M., & Moresolib, C. (2002). Shear Induced HYdrodynamic Diffusion Model for Cross-flow Microfiltration: Role of the Particle Volume Fraction. *Desalination, 145*, 123-128.

Mourouzidis-Mourouzis, S. A., & Karabelas, A. J. (2006). Whey Protein Fouling of Microfiltration Ceramic Membranes - Pressure Effects. *Journal of Membrane Science, 282*(124-132), 124.

Nawamawat, K., Sakdapipanich, J. T., Ho, C. C., Ma, Y., Song, J., & Vancso, J. G. Surface nanostructure of Hevea brasiliensis natural rubber latex particles. *Colloids and Surfaces A: Physicochemical and Engineering Aspects, 390*(1鈥?), 157-166.

Nawamawat, K., Sakdapipanich, J. T., Ho, C. C., Ma, Y., Song, J., & Vancso, J. G. (2011). Surface nanostructure of Hevea brasiliensis natural rubber latex particles. *Colloids and Surfaces A: Physicochemical and Engineering Aspects, 390*(1–3), 157-166. doi: http://dx.doi.org/10.1016/j.colsurfa.2011.09.021

Oers, C. W. v., Vorstman, M. A. G., Muijselaar, W. G. H. M., & Kerkhof, P. J. A. M. (1992). Unsteady-state flux behaviour in relation to the presence of a gel layer. *Journal of Membraen Science, 73*, 231-246.

Paiphansiri, U., & Tangboriboonrat, P. (2005). Prevulcanisation of skim latex: morphology and its use in natural rubber based composite material. *Colloid and Polymer Science, 284*, 251-257.

Park, C., Kim, H., Hong, S., & Choi, S.-I. (2006). Variation and prediction of membrane fouling index under various feed water characteristics. *Journal of Membrane Science, 284*(1-2), 248-254.

Perrellaa, F. W., & Gaspari, A. A. (2002). Natural Rubber Latex Protein Reduction with an Emphasis on Enzyme Treatment. *Methods, 27*, 77-86.

. Pollution Control Implementation Division - III. (2011). *Natural Rubber Processing Industry*, from http://www.cpcb.nic.in/oldwebsite/about%20us/Division%20at%20Head%20office/PCI-III/pciiiidivrubber.html

Porter, M. C. (1990). Ultrafiltration *Handbook of Industrial Membrane Technology* (pp. 132). United States: Noyes Publications.

Purkait, M. K., Bhattacharya, P. K., & S.De. (2005). Membrane filtration of leather plant effluent: Flux decline mechanism. *Journal of Membrane Science, 258*(1-2), 85-96.

Purkait, M. K., DasGupta, S., & De, S. (2004). Resistance in series model for micellar enhanced ultrafiltration of eosin dye. *Journal of Colloid and Interface Science, 270*(2), 496-506.

Rai, P., Rai, C., Majumdar, G. C., DasGupta, S., & De, S. (2006). Resistance in series model for ultrafiltration of mosambi (Citrus sinensis (L.) Osbeck) juice in a stirred continuous mode. *Journal of Membrane Science, 283*(1-2), 116-122.

Rinaldoni, A. N., Campderros, M., Menendez, C. J., & Padilla, A. P. (2009). Fractionation of skim milk by an integrated membrane process for yoghurt elaboration and lactose recuperation. *International Journal of Food Engineering, 5*(3), 1-17.

Rippel, M. M., Lee, L. T., Leite, Carlos, A. P., & Galembeck, F. (2003). Skim and Cream Natural Rubber Particles: Colloidal Properties, Coalescence and Film Formation. *Journal of Colloid and Interface Science 268*, 330-340.

Rodgers, V. G. J. (1999). Protein Adsorption on Ultrafiltration Membrane Surfaces and Effect on Transport. In T. S. Sorensen (Ed.), *Surface Chemistry and Electrochemistry of Membranes*. United States of Americe: Marcel Dekker Inc. .

Samuelsson, G., Dejmek, P., Trägårdh, G., & Paulsson, M. (1997). Minimizing whey protein retention in cross-flow microfiltration of skim milk. *International Dairy Journal, 7*(4), 237-242.

Schippers, J. C., Hanemaayer, J. H., Smolders, C. A., & Kostense, A. (1981). Predicting flux decline of reverse osmosis membranes. *Desalination, 38*, 339-348.

Seidel, A., & Elimelech, M. (2002). Coupling between chemical and physical interactions in natural organic matter (NOM) fouling of nanofiltration membranes: implications for fouling control. *Journal of Membrane Science, 203*, 245-255.

Shah, R. S., & Sulaiman, N. M. N. (2009). *Ultrafiltration for Zero Waste: Natural Rubber Skim Latex Concentration*. Paper presented at the 2nd International Congress on Green Process Engineering & 2nd European Process Intensification Conference (GPE-EPIC), Venice, Italy.

`

Sim, L. N., Ye, Y., Chen, V., & Fane, A. G. (2010). Comparison of MFI-UF constant pressure, MFI-UF constant flux and Crossflow Sampler-Modified Fouling Index Ultrafiltration (CFS-MFIUF). *Water Research, 45*(4), 1639-1650.

Singh, M. (2007). *Analyzing The Effect of Cross Flow Velocity, Uniform Transmembrane Pressure and pH on Permeate Flux, Retentate Composition and Energy Consumption During Cross Flow Microfiltartion of Skim Milk.* Master of Science, Cornell University

Song, L., & Elimelech, M. (1995). Theory of Concentration Polarization in Crossflow Filtration. *J. Chem. Soc. Faraday Trans. , 91(19)*, 3389-3398.

Springer, F., Ghidossi, R., Carretier, E., Veyret, D., Dhaler, D., & Moulin, P. (2009). Determination of the Wall Shear Stress by Numerical Simulation: Membrane Process. *Chemical Product & Process Modeling, Vol.4*(Iss.4), Art.5, 1-11.

Sridee, J. (2006). *Rheological Properties of Natural Rubber Latex.* Degree of Master of Engineering in Polymer Engineering, Suranaree University of Technology.

Sulaiman, H. N., & Aroua, M. K. (2002). Cake Layer Reduction by Gas Sparging Cross Flow Ultrafiltration of Skim Latex Serum. *Songklanakarin J. Sci. Technol., 24*(Membrane Sci. & Tech), 947-953.

Tang, C. Y., Kwon, Y. N., & Leckie, J. O. (2009). The Role of Foulant-foulant Electrostatic Interaction on Limiting Flux for RO and NF Membranes during Humic Acid Fouling-Theoretical Basis, Experimental Evidence, and AFM Interaction Force Measurement. *Journal of Membrane Science, 326*, 526-532.

Tekasakul, P., & Tekasakul, S. (2006). Environmental problem related to natural rubber production in Thailand. *Journal of Aerosol, 21*(2), 122-129.

Thomassen, J. K., Faraday, D. B. F., Underwood, B. O., & Cleaver, J. A. S. (2005). The effect of varying transmembrane pressure and crossflow velocity on the microfiltration fouling of a model beer. *Separation and Purification Technology, 41*(1), 91-100.

Thongmak, N., Sridang, P., Dantheravanich, S., Thaveepreeda, W., Wanichapichart, P., & Annop, S. (2009, 12-15 May 2009). *Filterability of latex serum and skim latex using lab scale plane organic membrane filtration: Application to recovery valued compound and to concentrate latex particle.* Paper presented at the 7th International Conference on Membrane Science and Technology (MST2009), Kuala Lumpur Malaysia

Van, H. N. T., Duong, D. T. T., Thanh, N. T. M., Trang, T. H. T. T., Dinuriah, I., Sharmin, S., . . . Huy, T. N. Q. (2007). Waste Abatement and Management in Natural Rubber Processing Sector: Asian Institute of Technology.

Veerasamy, D., Sulaiman, N. M., Nambiar, J., & Aziz, Y. (2003). Environment Friendly Natural Rubber Latex Concentration by Membrane Separation Technology. *Proceedings of The 5th International Membrane Science and Technology Conference*. Sdyney, Australia: University of New South Wales.

Veerasamy, D., Sulaiman, N.M., Nambiar, J., and Aziz, Y. (2002). *Environment Friendly Natural Rubber Latex Concentration by Membrane Separation Technology.* . Paper presented at the Proceedings of Regional Symposium on Chemical Engineering 2002.

Veerasamy, V., Supurmaniam, A., & Nor, Z. M. (2009). Evaluating the Use of In-situ Ultrafiltration to Reduce Fouling during Natural Rubber Skim Latex (waste latex) Recovery by Ultrafiltration *Desalination, 236*, 202-207.

Vela, M. C. V., Blanco, S. A., Garcia, J. L., & Rodriguez, E. B. (2008). Analysis of membrane pore blocking models applied to the ultrafiltration of PEG. *Separation and Purification Technology, 62*(3), 489-498.

`

Vyas, H. K., Bennett, R. J., & Marshall, A. D. (2002). Performance of crossflow microfiltration during constant transmembrane pressure and constant flux operations. *International Dairy Journal*, *12*(5), 473-479.

Yoon, S. H. (2011). Online MBR Information Retrieved Dec 20, 2011, from http://onlinembr.info/index.htm

Youravong, W., Lewis, M. J., & Grandison, A. S. (2003). Critical Flux in Ultrafiltration of Skimmed Milk. *Trans IChemE,, Vol 81, Part C*, 303-308.

. Zetasizer Nano series technical notes. 2012, from http://www.malvern.com/labeng/products/zetasizer/zetasizer.htm

Zhao, Y., Xing, W., Xu, N., & Shi, J. (2003). Hydraulic resistance in microfiltration of titanium white waste acid through ceramic membranes. *Separation and Purification Technology*, *32*(1-3), 99-104.

`

APPENDIXES

2010 Aug 04 - MSDS membrane 0.05µm

FCRI IMPORT & EXPORT CO., LTD.

Tel : 0086-757-82780713
Fax: 0086-757-82705122
Add: NO. 18, Liu Yuan Road, Shiwan, Foshan, Guangdong Province, P. R. China, 528031

TEST REPORT OF CERAMIC MEMBRANCE FILTER

To:Global Science Resources Sdn.Bhd.
Delivery time: 2010-07-29
Invoice No: IN-E-10-0601A

Type	1. Model no.	0206010702
	2.Number of Channels	1
	3. Pore size	0.05um
Dimension	4. Out dia	10mm (-0, +0.5)
	5. Inside Dia	7mm (-/+0.5)
	6.Thickness	3mm
	7. Length	250mm
Parameters	8. Breaking strength	54.21MPa
	9.Porosity of support	43.04%
	10.Flux of purified water	>500L/m^{2}h

Approved by:Testing Centre

Operating: Yonghui Wu

IMPORT & EXPORT CO. LTD. 佛山市金刚进出口贸易有限公司

MASTERSIZER 2000

Result Analysis Report

Sample Name:
Latex - Average

Sample Source & type:

Sample bulk lot ref:

SOP Name:

Measured by:
Malvern Mastersizer

Result Source:
Averaged

Measured:
Monday, December 07, 2009 2:29:11 PM

Analysed:
Monday, December 07, 2009 2:29:12 PM

Particle Name:
Rubber Latex 0.001

Particle RI:
1.435

Dispersant Name:
Water

Accessory Name:
Hydro 2000MU (A)

Absorption:
0.001

Dispersant RI:
1.330

Analysis model:
General purpose

Size range:
0.020 to 2000.000 um

Weighted Residual:
40.545 %

Sensitivity:
Enhanced

Obscuration:
0.00 %

Result Emulation:
Off

Concentration:
0.0000 %Vol

Specific Surface Area:
53.6 m²/g

Span :
1.354

Surface Weighted Mean D[3,2]:
0.112 um

Uniformity:
0.421

Vol. Weighted Mean D[4,3]:
0.141 um

Result units:
Volume

d(0.1): 0.068 um **d(0.5):** 0.125 um **d(0.9):** 0.238 um

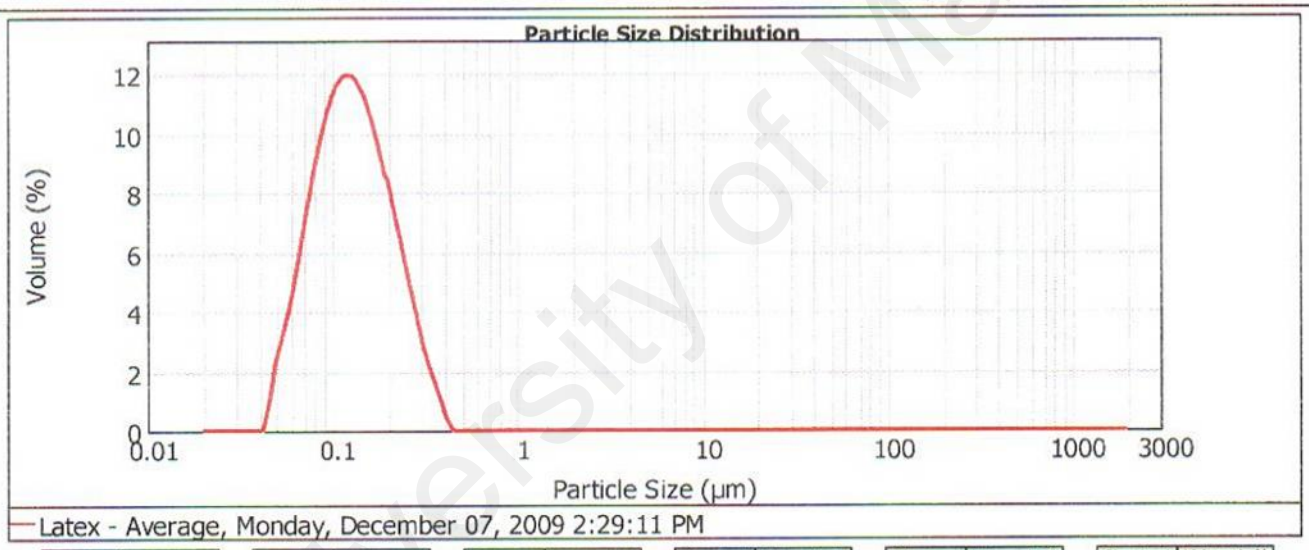

Size (µm)	Volume In %
0.010	0.00
0.011	0.00
0.013	0.00
0.015	0.00
0.017	0.00
0.020	0.00
0.023	0.00
0.026	0.00
0.030	0.00
0.035	0.00
0.040	0.13
0.046	2.08
0.052	3.35
0.060	4.94
0.069	6.97
0.079	8.73
0.091	10.00
0.105	

Size (µm)	Volume In %
0.105	10.68
0.120	10.72
0.138	10.14
0.158	9.05
0.182	7.59
0.209	5.96
0.240	4.34
0.275	2.88
0.316	1.70
0.363	0.74
0.417	0.00
0.479	0.00
0.550	0.00
0.631	0.00
0.724	0.00
0.832	0.00
0.955	0.00
1.096	

Size (µm)	Volume In %
1.096	0.00
1.259	0.00
1.445	0.00
1.660	0.00
1.905	0.00
2.188	0.00
2.512	0.00
2.884	0.00
3.311	0.00
3.802	0.00
4.365	0.00
5.012	0.00
5.754	0.00
6.607	0.00
7.586	0.00
8.710	0.00
10.000	0.00
11.482	

Size (µm)	Volume In %
11.482	0.00
13.183	0.00
15.136	0.00
17.378	0.00
20.000	0.00
22.909	0.00
26.303	0.00
30.200	0.00
34.674	0.00
39.811	0.00
45.000	0.00
52.481	0.00
60.256	0.00
69.183	0.00
79.433	0.00
91.201	0.00
104.713	0.00
120.226	

Size (µm)	Volume In %
120.226	0.00
138.038	0.00
158.489	0.00
181.970	0.00
208.930	0.00
239.883	0.00
275.423	0.00
316.228	0.00
363.078	0.00
416.869	0.00
478.630	0.00
549.541	0.00
630.957	0.00
724.436	0.00
831.764	0.00
954.993	0.00
1096.478	0.00
1258.925	

Size (µm)	Volume In %
1258.925	0.00
1445.440	0.00
1659.587	0.00
1905.461	0.00
2187.762	0.00
2511.886	0.00
2884.032	0.00
3311.311	0.00
3801.894	0.00
4365.158	0.00
5011.872	0.00
5754.399	0.00
6606.934	0.00
7585.776	0.00
8709.636	0.00
10000.000	

Operator notes:

Malvern Instruments Ltd.
Malvern, UK
Tel := +[44] (0) 1684-892456 Fax +[44] (0) 1684-892789

Mastersizer 2000 Ver. 5.60
Serial Number : MAL1027744

File name: LATEX
Record Number: 8
12/8/2009 12:40:29 PM

MASTERSIZER 2000

Result Analysis Report

Sample Name:
Latex5 - Average

SOP Name:

Measured:
Tuesday, December 08, 2009 11:55:10 AM

Sample Source & type:

Measured by:
Malvern Mastersizer

Analysed:
Tuesday, December 08, 2009 11:55:12 AM

Sample bulk lot ref:

Result Source:
Averaged

Particle Name:
Rubber Latex 0.001

Accessory Name:
Hydro 2000MU (A)

Analysis model:
General purpose

Sensitivity:
Enhanced

Particle RI:
1.435

Absorption:
0.001

Size range:
0.020 to 2000.000 um

Obscuration:
0.00 %

Dispersant Name:
Water

Dispersant RI:
1.330

Weighted Residual:
40.706 %

Result Emulation:
Off

Concentration:
0.0000 %Vol

Span :
1.353

Uniformity:
0.423

Result units:
Volume

Specific Surface Area:
53.7 m²/g

Surface Weighted Mean D[3,2]:
0.112 um

Vol. Weighted Mean D[4,3]:
0.140 um

---

d(0.1): 0.069 um **d(0.5):** 0.124 um **d(0.9):** 0.236 um

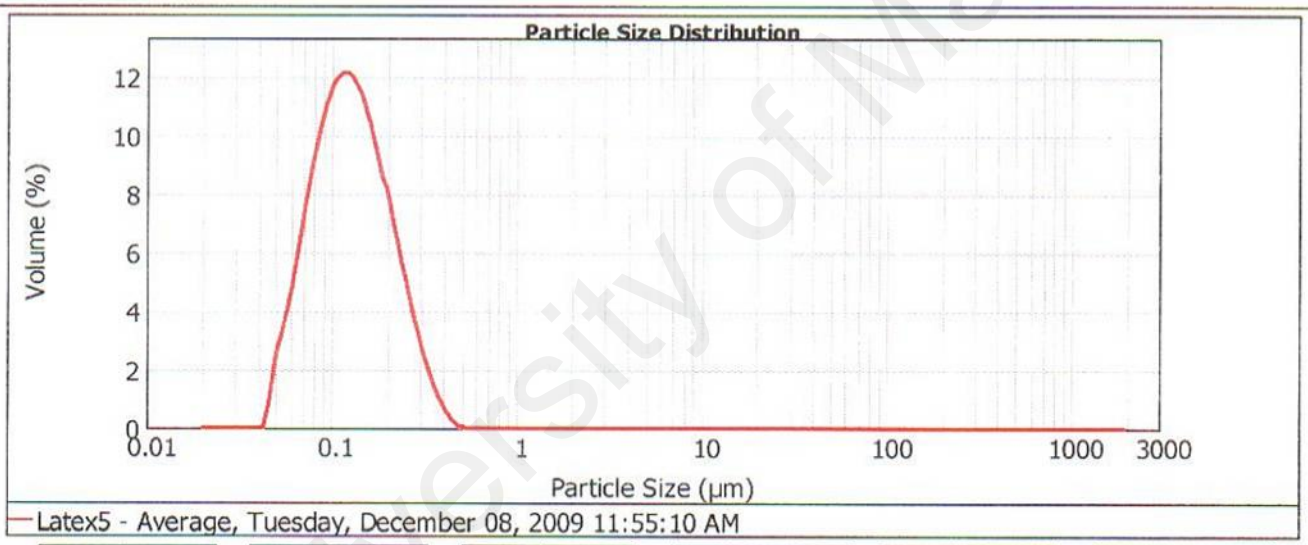

Size (µm)	Volume In %
0.010	0.00
0.011	0.00
0.013	0.00
0.015	0.00
0.017	0.00
0.020	0.00
0.023	0.00
0.026	0.00
0.030	0.00
0.035	0.00
0.040	0.02
0.046	1.95
0.052	3.39
0.060	5.04
0.069	7.17
0.079	8.98
0.091	10.26
0.105	

Size (µm)	Volume In %
0.105	10.88
0.120	10.82
0.138	10.12
0.158	8.90
0.182	7.36
0.209	5.70
0.240	4.10
0.275	2.72
0.316	1.59
0.363	0.77
0.417	0.22
0.479	0.00
0.550	0.00
0.631	0.00
0.724	0.00
0.832	0.00
0.955	0.00
1.096	

Size (µm)	Volume In %
1.096	0.00
1.259	0.00
1.445	0.00
1.660	0.00
1.905	0.00
2.188	0.00
2.512	0.00
2.884	0.00
3.311	0.00
3.802	0.00
4.365	0.00
5.012	0.00
5.754	0.00
6.607	0.00
7.586	0.00
8.710	0.00
10.000	0.00
11.482	

Size (µm)	Volume In %
11.482	0.00
13.183	0.00
15.136	0.00
17.378	0.00
20.000	0.00
22.909	0.00
26.303	0.00
30.200	0.00
34.674	0.00
39.811	0.00
45.000	0.00
52.481	0.00
60.256	0.00
69.183	0.00
79.433	0.00
91.201	0.00
104.713	0.00
120.226	

Size (µm)	Volume In %
120.226	0.00
138.038	0.00
158.489	0.00
181.970	0.00
208.930	0.00
239.883	0.00
275.423	0.00
316.228	0.00
363.078	0.00
416.869	0.00
478.630	0.00
549.541	0.00
630.957	0.00
724.436	0.00
831.764	0.00
954.993	0.00
1096.478	0.00
1258.925	

Size (µm)	Volume In %
1258.925	0.00
1445.440	0.00
1659.587	0.00
1905.461	0.00
2187.762	0.00
2511.886	0.00
2884.032	0.00
3311.311	0.00
3801.894	0.00
4365.158	0.00
5011.872	0.00
5754.399	0.00
6606.934	0.00
7585.776	0.00
8709.636	0.00
10000.000	

Operator notes:

Malvern Instruments Ltd.
Malvern, UK
Tel := +[44] (0) 1684-892456 Fax +[44] (0) 1684-892789

MASTERSIZER 2000

Result Analysis Report

Sample Name:
Latex6 - Average

SOP Name:

Measured:
Tuesday, December 08, 2009 12:32:28 PM

Sample Source & type:

Measured by:
Malvern Mastersizer

Analysed:
Tuesday, December 08, 2009 12:32:31 PM

Sample bulk lot ref:

Result Source:
Averaged

Particle Name:
Rubber Latex 0.001

Accessory Name:
Hydro 2000MU (A)

Analysis model:
General purpose

Sensitivity:
Enhanced

Particle RI:
1.435

Absorption:
0.001

Size range:
0.020 to 2000.000 um

Obscuration:
0.00 %

Dispersant Name:
Water

Dispersant RI:
1.330

Weighted Residual:
41.243 %

Result Emulation:
Off

Concentration:
0.0000 %Vol

Span :
1.264

Uniformity:
0.394

Result units:
Volume

Specific Surface Area:
51.3 m²/g

Surface Weighted Mean D[3,2]:
0.117 um

Vol. Weighted Mean D[4,3]:
0.142 um

---

d(0.1): 0.072 um **d(0.5):** 0.127 um **d(0.9):** 0.233 um

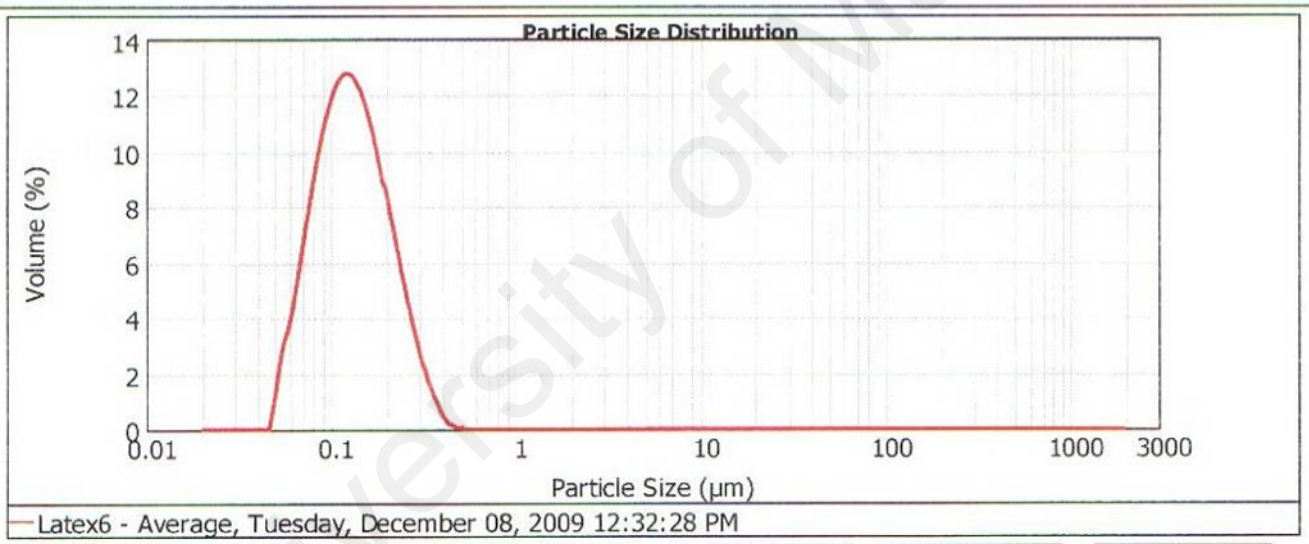

Size (µm)	Volume In %
0.010	0.00
0.011	0.00
0.013	0.00
0.015	0.00
0.017	0.00
0.020	0.00
0.023	0.00
0.026	0.00
0.030	0.00
0.035	0.00
0.040	0.00
0.046	0.74
0.052	2.86
0.060	4.45
0.069	6.75
0.079	8.87
0.091	10.48
0.105	

Size (µm)	Volume In %
0.105	11.38
0.120	11.50
0.138	10.83
0.158	9.53
0.182	7.81
0.209	5.93
0.240	4.14
0.275	2.61
0.316	1.42
0.363	0.59
0.417	0.10
0.479	0.00
0.550	0.00
0.631	0.00
0.724	0.00
0.832	0.00
0.955	0.00
1.096	

Size (µm)	Volume In %
1.096	0.00
1.259	0.00
1.445	0.00
1.660	0.00
1.905	0.00
2.188	0.00
2.512	0.00
2.884	0.00
3.311	0.00
3.802	0.00
4.365	0.00
5.012	0.00
5.754	0.00
6.607	0.00
7.586	0.00
8.710	0.00
10.000	0.00
11.482	

Size (µm)	Volume In %
11.482	0.00
13.183	0.00
15.136	0.00
17.378	0.00
20.000	0.00
22.909	0.00
26.303	0.00
30.200	0.00
34.674	0.00
39.811	0.00
45.000	0.00
52.481	0.00
60.256	0.00
69.183	0.00
79.433	0.00
91.201	0.00
104.713	0.00
120.226	

Size (µm)	Volume In %
120.226	0.00
138.038	0.00
158.489	0.00
181.970	0.00
208.930	0.00
239.883	0.00
275.423	0.00
316.228	0.00
363.078	0.00
416.869	0.00
478.630	0.00
549.541	0.00
630.957	0.00
724.436	0.00
831.764	0.00
954.993	0.00
1096.478	0.00
1258.925	

Size (µm)	Volume In %
1258.925	0.00
1445.440	0.00
1659.587	0.00
1905.461	0.00
2187.762	0.00
2511.886	0.00
2884.032	0.00
3311.311	0.00
3801.894	0.00
4365.158	0.00
5011.872	0.00
5754.399	0.00
6606.934	0.00
7585.776	0.00
8709.636	0.00
10000.000	

Operator notes:

Malvern Instruments Ltd.
Malvern, UK
Tel := +[44] (0) 1684-892456 Fax +[44] (0) 1684-892789

PUBLICATIONS

Effects of Crossflow Velocity and Transmembrane Pressure on Ultrafiltration of Naturally-Occurring Proteins in Skim Latex Serum

Nik Meriam Sulaiman, Ho Kar Wei, Mohamed Kheireddine Aroua

Department of Chemical Engineering, University of Malaya, 50603 Kuala Lumpur, Malaysia: vione_kw@live.com

Abstract

The concentration on natural rubber latex via centrifugation results in a skim latex by-product stream. Membrane separation process offers an attractive alternative separation method to recover the remaining 6-8% of rubber particles as well as the by-product serum from the skim latex stream, thus avoiding the need for a wastewater treatment plant. However, it is recognized that continuous membrane filtration suffers from fouling phenomenon. This study investigates the behavior of skim latex during ultrafiltration in particular pertaining to the protein fractions in the feed solution. The effects of crossflow velocity and transmembrane pressure during ultrafiltration were also investigated. A bench scale crossflow ultrafiltration unit using tubular ceramic membranes, with pore size 0.05µm, was used in this study. Fouled membranes were examined using scanning electron microscope. The results showed that, increasing the feed flow velocity or filtration pressure led to higher filtration permeate fluxes. Increasing the crossflow velocity resulted in higher filtration permeate flux but decreases in protein rejection coefficient. The increment in filtration flux was due to tangential flow sweeping effect and reduced fouling. The scanning electron microscopy results showed that increase of crossflow velocity leads to an increase in cake layer porosity and decrease in cake layer thickness. Increase in transmembrane pressure causes reduction in filtration permeate while increase in protein rejection coefficient. This might due to the fact that increase of applied pressure increase the filtration driving force causing more serious fouling and increase of fouling resistance. Scanning electron microscope results also showed that increase in transmembrane pressure resulted in a decrease in cake layer porosity and thickness due to high compaction.

Keywords: Ultrafiltration; skim latex, fouling, ceramic membrane

PAPER ID: 138

FOULING OF SKIM LATEX SERUM NATURALLY-OCCURRING PROTEINS: EFFECTS OF TRANSMEMBRANE PRESSURE AND CROSSFLOW VELOCITY

NIK MERIAM SULAIMAN, HO KARWEI, MOHAMED KHEIREDDINE AROUA

- *Department of Chemical Engeering,*
  University of Malaya,
  50603 Kuala Lumpur, Malaysia
  e-mail : vione_kw@live.com

Abstract. During concentration of natural rubber latex, large volume of skim latex (consists of 6-8% DRC) is produced as by-product. Membrane separation process can be used to recover the skim rubber particles as well as the by-product serum from the skim latex stream, thus avoiding the need for the wastewater treatment plant. However, it is recognized that continuous membrane filtration suffers from fouling phenomenon. As such a study has been initiated to gain an understanding of the fouling behavior of skim latex, in particular pertaining to the protein fractions in the feed solution. A bench scale crossflow ultrafiltration unit using single channel tubular ceramic membrane with pores size 0.05µm was used in this study. The effect of operating conditions, i.e. crossflow velocity and transmembrane pressure were investigated. As overall, filtration performance has a similar trend, i.e. filtration starts with high initial permeate flux, permeate flux and then decreases rapidly. Finally, permeate flux attained pseudo steady state where permeate flux is almost constant at this stage. An increase in crossflow velocity or transmembrane pressure resulted in higher filtration flux. Based on the analysis of dt/dV versus permeate volume, V, the filtration can be divided into two regions. The changes in operating parameters affect the fouling mechanism. Fouling due to pore blocking becomes less significant as transmembrane pressure or crossflow velocity increase. In this study, transmembrane pressure and crossflow velocity need to be optimized in order to improve the skim latex filtration performance.

Key-words. Ultrafiltration; skim latex; protein fouling; ceramic membrane

INTRODUCTION

Natural rubber latex contains of about 30% dry rubber content needs to be concentrated to about 60% dry rubber content for further downstream processing into a variety of rubber products. In this process, a large volume of skim latex, which consists of 6 to 8% dry rubber content, is produced as a by-product. Thus, it is environmental and economically desires to recover the remained skim rubber in skim latex. Conventionally, rubber particles in the skim are recovered using cheap grade sulphuric acid. In this process, highly acidic polluting effluent which can lead to malodour problems upon degradation is produced. It will be economically and environmentally to apply membrane separation process to recover the remaining 4-6% dry rubber content. Compare to conventional method, membrane separation allows the recovery of potential by-product in skim latex which contains valuable nutraceutical and other value-added components without chemicals contamination. Further, rubber waste stream needs not further treatment before it can be discharged into the waterways.

In rubber industry, membrane separation process has provides an alternative to concentrate rubber content in skim latex (Sulaiman & Arous, 2002; D. Veerasamy, Sulaiman, Nambiar, & Aziz). Natural field latex consists of about 30% dry rubber content (DRC). However, it is recognized that continuous membrane filtration suffers from fouling phenomenon (Datta, Bhattacharjee, & Datta, 2008; Lamminen, Walker, & Weavers, 2004). Prolonged usage of membrane in filtration process can leads to fouling problems entailing membrane replacement and increased operating costs. However, a scientific understanding of fouling behavior during ultrafiltration of skim latex is necessary to optimize its performance (Holdich & Zhang, 1995; Konieczny & Bodzek, 1996; Lamminen et al., 2004; Novalic, Heisler, & Lahnsteiner, 1997; D. Veerasamy, Sulaiman, Nambiar, & Aziz, 2003). Previous studies had shown that air sparging (Sulaiman & Arous, 2002) and ultrasound (V. Veerasamy, Supurmaniam, & Nor, 2009) can be used to reduce fouling in the filtration of skim latex. In the case of natural rubber skim latex, fouling behavior can be attributed to the presence of naturally-occuring proteins.

In this study, a bench scale crossflow filtration unit using single channel tubular ceramic membranes was used to study the effect of crossflow velocity and transmembrane pressure on skim latex ultrafiltration. The obtained data is tried to fit into the Hermia's equation in order to estimate the fouling mechanism.

MATERIALS AND METHODS

Ultrafiltration experiments of skim latex in this study were carried out in the crossflow velocity range of 1.3cm/s to 4.6cm/s and transmembrane pressure in the range of 0.3bar to 1.3bar. A bench scale filtration unit was used in this study. Single channel ceramic membrane, posses a inner diameter 6mm, outer diameter 10mm and length 250mm, was used uncased in a stainless steel module in the unit. Skim latex, obtained from the Rubber Research Institute Experiment Station, Sungai Buloh, Malaysia, was circulated in the system using a peristaltic pump. Permeate was collected directly onto a digital balance which connected to a computer to obtained the permeate flux. Each ultrafiltration experiment was carried out at a temperature of 25°C for 160 minutes until a pseudo steady state is obtained.

RESULTS AND DISCUSSION

Effect of transmembrane pressure

The filtration flux time course results showed that permeate flux decays rapidly initially and reached pseudo steady state gradually. The rapid decreases in permeate flux indicates that most fouling occurred at the initial stage of filtration as indicates in figure 2 (K. J. Hwang & Sz, 2010). The initial fouling is contributed to pore blocking. The filtration curve of dt/dV versus V showed that pore blocking is more significant upon the increases of transmembrane pressure (figure 4). The filtration curve of dt/dV versus V analysis depicts a concave curve followed by a straight line (figure 4). It proved that ultrafiltration of skim latex is the combination of a few fouling mechanisms. The concave trend at the initial stage is mainly due to pore blocking. The curve slopes decrease upon the increase of transmembrane pressure indicates that pore blocking is more significant as transmembrane pressure decreases (figure 4). This can be explained by the fact that as transmembrane pressure increases, large amount of particles were brought to the membrane surface and form cake layer. The formation of cake layer had reduces pore blocking as most of the pores were blocked by the cake layer. Thus, permeate flux decay more rapidly as transmembrane pressure increases (figure 1).

Constant n in Hermia's equation can be obtained by regression analysis of dt/dV versus V. The regression analysis shown that at low transmembrane pressure fouling mechanism is slowly shifts to cake layer formation as the constant n is change from $n\approx2$ to $n\approx0$ (table 1). As transmembrane pressure reached 1.3bar, as large amount of particles accumulated at membrane surface, cake fouling is dominating (table 1).

It was found that permeate fluxes at steady state tends to increases as transmembrane pressure increases (figure 3). This is because the increase in transmembrane pressure had increased the particles driving forces towards the membrane surface. Thus, more particles were transfer towards the membrane (K.-J. Hwang & Huang, 2009; Thomassen, Faraday, Underwood, & Cleaver, 2005).

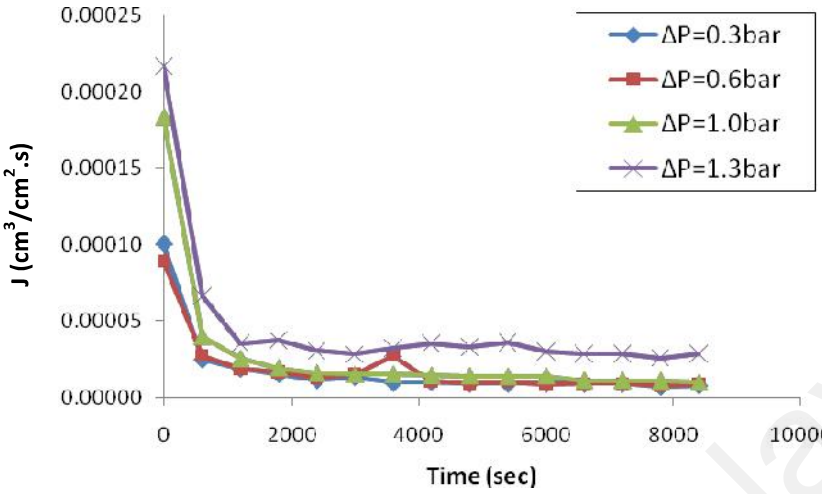

Figure 1: Filtration permeate flux time course during filtration of skim latex at constant crossflow velocity 1.3cm/s.

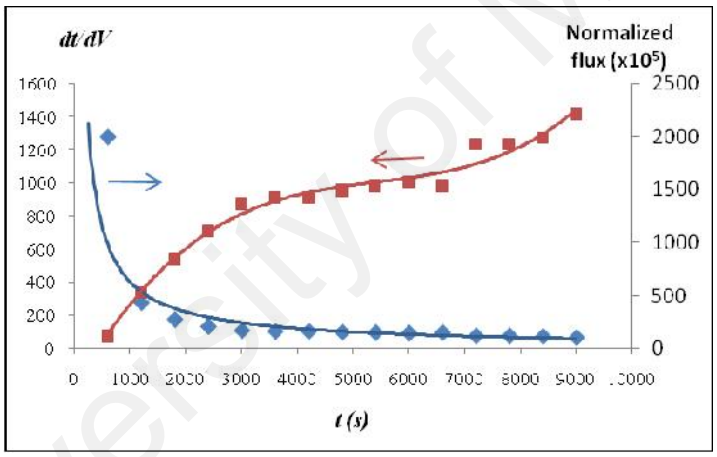

Figure 2: Filtration curve *dt/dV* (left scale) and normalized permeate flux (right scale) versus t for skim latex filtration at crossflow velocity of 1.3cm/s and transmembrane pressure 1.0Pa.

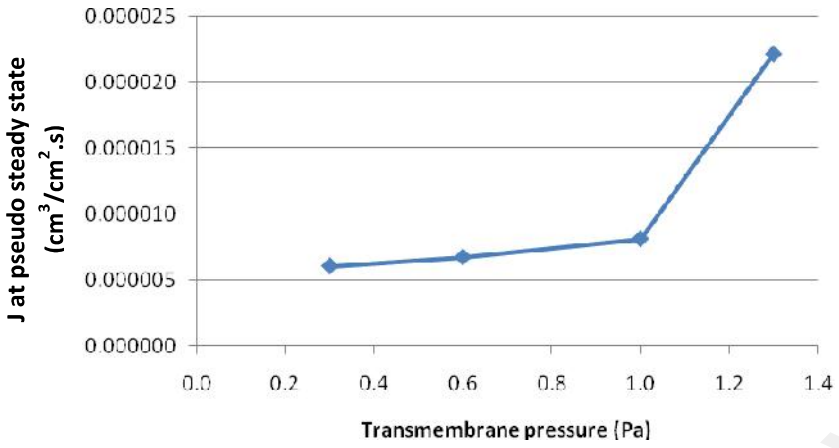

Figure 3: Variation of permeate flux at pseudo steady state during filtration of skim latex at constant crossflow velocity 1.3cm/s.

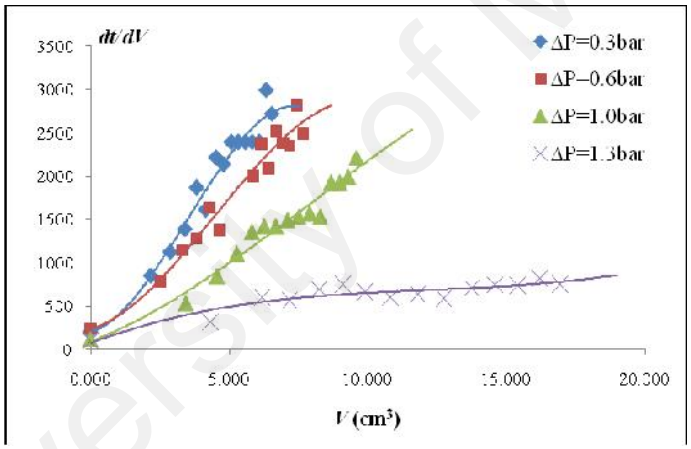

Figure 4: Filtration curve of *dt/dV* versus *V* of skim latex at crossflow velocity 1.3cm/s using ceramic membranes.

Table 1: Summary analysis results of the filtration data based on Hermia's model.

TMP (bar)	Estimation of constant *n*	
	t < 20000s	t > 20000s

0.3	2.10	0
0.6	1.97	0
1.0	1.90	0
1.3	0.22	0

Effect of crossflow velocity

Increase in crossflow velocity induces shear stress along the membrane surface and scoured away particles that deposited on membrane surface. Thus, particles back diffusion into the bulk solution tends to increase with crossflow velocity. Figure 5 and figure 6 show that at constant transmembrane pressure, initial permeate flux and permeate flux at pseudo steady state tend to increase with crossflow velocity. The filtration curve of dt/dV versus V for skim latex at transmembrane pressure 1.0bar and various crossflow velocities is shown in figure 7. It was observed that the filtration curvature increases as crossflow velocity increases from 1.3cm/s to 3.6cm/s had implies that pore blocking is more significant at crossflow velocity 3.6cm/s. However, from the constant n obtained in table 2, the effect is not as significant. This may because as crossflow velocity increases, it also increases the internal pressure that increases the rate of particles convection towards membrane surface. The increase in particles convections may offset the scouring effect. As crossflow velocity increases further to 4.6cm/s, pore blocking is least significant (figure 7 and table 2).

From the regression data obtained in table 2, pore blocking is predominated at the initial stage of filtration process as $n \approx 2$ (K.-J. Hwang et al., 2007). As filtration prolonged, constant n is approaching 0, implies that cake formation is dominated at the later stage. At initial stage of low crossflow velocity filtration, no significant differences were observed. However, at high crossflow velocity, constant n is reducing, indicates that fouling due to pore blocking is less severe. From the results obtained, we can observed that crossflow velocity does affect the filtration performance by alter the fouling mechanisms. However, an optimization of crossflow velocity needs to be carried out in order to optimize the filtration performance.

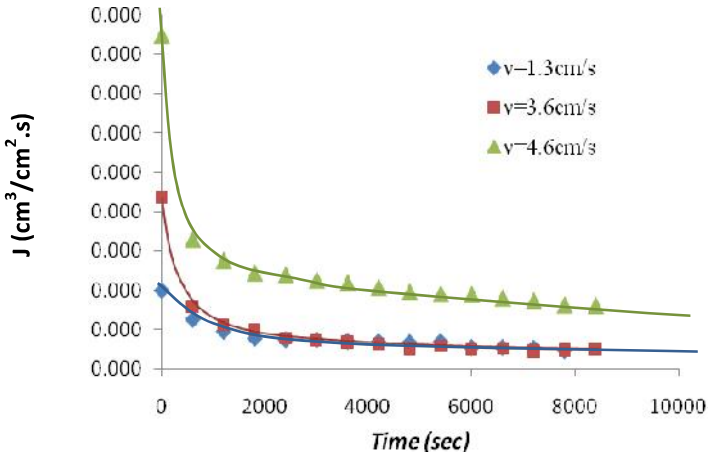

Figure 5: Filtration curve time course of ultrafiltration of skim latex at constant transmembrane pressure 1.0Pa and various feed flow velocity, *v*.

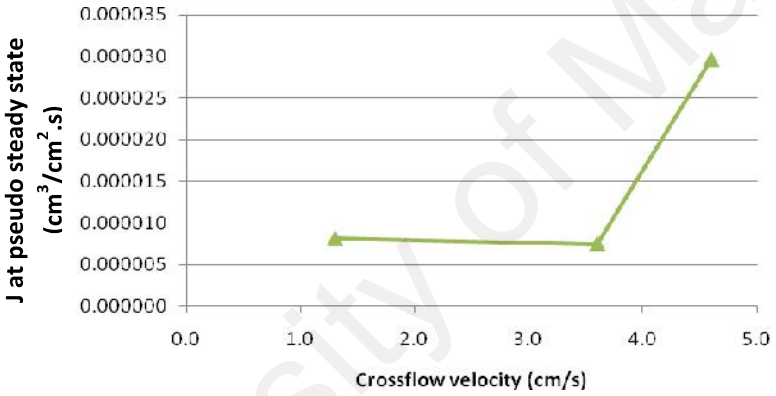

Figure 6: Variation of permeate flux at pseudo steady state during filtration of skim latex at constant transmembrane pressure 1.0bar.

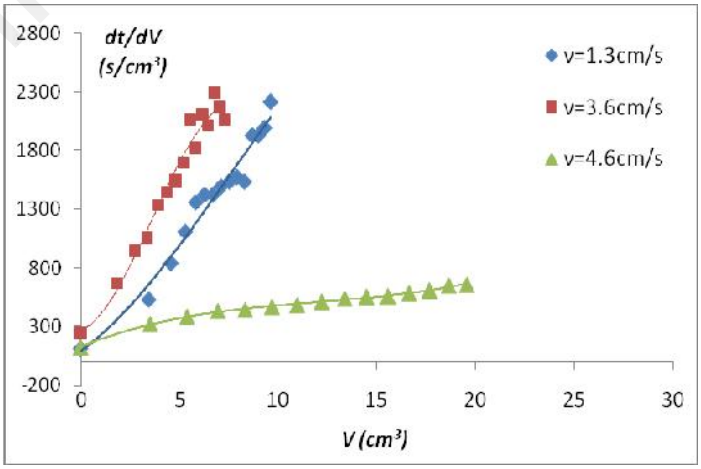

Figure 7: Filtration curve of *dt/dV* versus *V* of skim latex at transmembrane pressure 1.0bar using ceramic membranes.

Table 2: Summary analysis results of the filtration data based on Hermia's model.

Crossflow velocity (cm/s)	Estimation of constant *n*	
	t < 20000s	t > 20000s
1.3	1.81	0
3.6	1.82	0
4.6	1.66	0

CONCLUSION

The effect of transmembrane pressure and crossflow velocity in ultrafiltration performance of skim latex were studied. It had been shown that transmembrane pressure and crossflow velocity do affects the ultrafiltration process in terms of initial permeate flux, decay rate and filtration at pseudo steady state. It was showed that the increase in transmembrane pressure and crossflow velocity had lead to higher initial permeate flux and pseudo steady state fluxes. This is because the increased in transmembrane pressure and crossflow velocity had increased the particles driving force and scouring effect. The regression analysis showed that in an ultrafiltration process, combination of different fouling mechanisms is observed (Chase, Li, & Ho, 2006). In overall, at the initial stage of skim latex filtration was dominated by pore blocking as constant $n \approx 2$ and followed by cake layer formation as $n \approx 0$ at later stage. At low transmembrane pressure, it was observed that pore blocking is the dominating mechanism. As transmembrane pressure increases, fouling mechanism had slowly shifted to cake formation as constant *n* approaching. At low crossflow velocity, the effect of crossflow velocity was not as significant as the effect of transmembrane pressure. At high crossflow velocity, the increases in driving force had overcome the scouring effect. Thus, initial permeate flux and permeate flux at pseudo steady state increased as crossflow velocity increased to 4.6cm/s. Thus, optimum parameters need to be determined in order to optimize the filtration performance.

REFERENCES

Casa, E. J. d. l., Guadix, A., Ibanez, R., Camacho, F., & Guadiz, E. M. (2008). A combined fouling model to decsribe the influence of the electrostatic environment on the cross-flow microfiltration of BSA. *Journal of Membrane Science, 318*, 247-254.

Chase, D.-O., Li, W., & Ho, C.-C. (2006). A three mechanism model to describe fouling of microfiltration membranes. *Journal of Membrane Science, 280*, 856-866.

Datta, D., Bhattacharjee, C., & Datta, S. (2008). Whey Protein Fractionation using Membrane Filtration – A Review. *IE(I) Journal-CH, Vol 89*(September 2008), 45 - 50.

Holdich, R. G., & Zhang, G. M. (1995). Internal Fouling of Microporous Cross-Flow Filtration Membranes with Dilute Latex Suspensions. *The Chemical Engineering Journal, 60*, 31-37.

Hwang, K.-J., Chou, F.-Y., & Tung, K.-L. (2006). Effects of operating conditions on the performance of cross-flow microfiltration of fine particle/protein binary suspension. *Journal of Membrane Science, 274*(1-2), 183-191.

Hwang, K.-J., & Huang, P. S. (2009). Cross-flow microfiltration of dilute macromolecular suspension. *Separation and Purification Technology, 68*, 328-334.

Hwang, K.-J., Liao, C. Y., & Tung, K. L. (2007). Analysis of Particle Fouling during MIcrofiltration by Use of Blocking Models. *Journal of Membrane Science, 287*, 287-293.

Hwang, K. J., & Sz, P. Y. (2010). Filtration characteristics and membrane fouling in cross-flow microfiltration of BSA/dextran binary suspension. *Journal of Membrane Science, 347*, 75 - 82.

Konieczny, K., & Bodzek, M. (1996). Ultrafiltration of Latex Wastewaters. *Desalination, 104*, 75-82.

Lamminen, M. O., Walker, H. W., & Weavers, L. K. (2004). Mechanisms and Factors Influencing the Ultrasonic Cleaning of Particle-fouled Ceramic Membranes. *Journal of Membrane Science, 237*(213-233), 213.

Novalic, S., Heisler, G., & Lahnsteiner, J. (1997). Cross-flow Filtration of Latex Emulsion on a Pilot Scale using Organic and Inorganic Membranes with Different Cut-off Values. *Journal of Membrane Science 130*, 1-5.

Sulaiman, H. N., & Arous, M. K. (2002). Cake Layer Reduction by Gas Sparging Cross Flow Ultrafiltration of Skim Latex Serum. *Songklanakarin J. Sci. Technol., 24*(Membrane Sci. & Tech), 947-953.

Thomassen, J. K., Faraday, D. B. F., Underwood, B. O., & Cleaver, J. A. S. (2005). The effect of varying transmembrane pressure and crossflow velocity on the

microfiltration fouling of a model beer. *Separation and Purification Technology, 41*(1), 91-100.

Veerasamy, D., Sulaiman, N. M., Nambiar, J., & Aziz, Y. Environment Friendly Natural Rubber Latex Concentration by Membrane Separation Technology. . pp.1 - 7.

Veerasamy, D., Sulaiman, N. M., Nambiar, J., & Aziz, Y. (2003). Environment Friendly Natural Rubber Latex Concentration by Membrane Separation Technology. . pp.1 - 7.

Veerasamy, V., Supurmaniam, A., & Nor, Z. M. (2009). Evaluating the Use of In-situ Ultrafiltration to Reduce Fouling during Natural Rubber Skim Latex (waste latex) Recovery by Ultrafiltration *Desalination, 236*, 202-207.

Vela, M. C. V., Blanco, S. A., Garcia, J. L., & Rodriguez, E. B. (2008). Analysis of membrane pore blocking models applied to the ultrafiltration of PEG. *Separation and Purification Technology, 62*(3), 489-498.

Effects of Transmembrane Pressure and Crossflow Velocity in the Ultrafiltration of Skim Latex Serum

Nik Meriam Sulaiman, Ho Kar Wei, Mohamed Kheireddine Aroua

Department of Chemical Engineering, University of Malaya, 50603 Kuala Lumpur, Malaysia: karwei0808@hotmail.com

ABSTRACT

Natural field latex with about 30% dry rubber content (DRC) needs to be further concentrated to about 60% DRC for further downstream processing into a variety of products. In this process, a large volume of skim latex (consists of 6-8% DRC) is produced as by-product. Membrane separation process can be used to recover the skim rubber particles as well as the by-product serum from the skim latex stream, thus avoiding the need for the wastewater treatment plant. However, it is recognized that continuous membrane filtration suffers from fouling phenomenon. As such a study has been initiated to gain an understanding of the fouling behavior of skim latex, in particular pertaining to the protein fractions in the feed solution. A bench scale crossflow ultrafiltration unit using single channel tubular ceramic membrane with pores size 0.05µm was used in this study. The effect of operating conditions, i.e. crossflow velocity and transmembrane pressure were investigated. In overall, filtration performance has a similar trend, i.e. initial permeate fluxes of filtrations start up high and then decreases rapidly. Finally, permeate flux attained pseudo steady state where permeate flux is almost constant at this stage. At crossflow velocity 4.6cm/s, initial permeate flux and permeate flux at pseudo steady state are decreasing with the increase in transmembrane pressure. However, at crossflow velocity 1.3cm/s, the trends of initial permeate flux and fluxes at pseudo steady state are different. Initial permeate flux is increasing with cross flow velocity. While, permeate flux at pseudo steady state is slightly reduced as transmembrane pressure increased from 0.6bar to 1.0bar. Permeate flux at pseudo steady state is increased drastically as transmembrane pressure increased further to 1.3bar. This is mainly due to the change in the microstructure of fouled.

Keywords: Ultrafiltration; skim latex

1. Introduction

Membrane separation technology is gaining wider acceptance nowadays in various process industries such as dairy, food and beverage, pharmaceutical and wastewater treatment. Membrane separation is commonly used in dairy industry to fractionate milk fat and separation of whey protein cheese brine purification [1]. In rubber industry, membrane separation process has provides an alternative to concentrate rubber content in skim latex [2, 3]. Natural field latex consists of about 30% dry rubber content (DRC). It needs to be concentrated to about 60% DRC for further downstream processing into a variety of products. In Malaysia, about 85 to 90% of latex concentrate is obtained by through centrifugation process. In this process, besides of cream with 60% DRC and a large volume of skim latex (6-8% DRC) is produced. Conventionally, rubber particles in the skim are recovered using cheap grade sulphuric acid. In this process, highly acidic polluting effluent which can lead to malodour problems upon degradation is produced. It will be economically and environmentally to apply membrane separation process to recover the remaining 4-6% dry rubber content. Compare to conventional method, membrane separation allows the recovery of potential by-product in skim latex which contains valuable nutraceutical and other value-added components without chemicals contamination. Further, rubber waste stream needs not further treatment before it can be discharged into the waterways.

However, it is recognized that continuous membrane filtration suffers from fouling phenomenon [4, 5]. Prolonged usage of membrane in filtration process can leads to fouling problems entailing membrane replacement and increased operating costs. It will also affect the process productivity. As such a study has been initiated to gain an understanding of the fouling behavior of skim latex, in particular pertaining to the protein fractions in the feed solution. In order to overcome this problem, efforts had been carried out to study the fouling mechanism and also cleaning methods to restore the membrane performance. Ultrasound [6] and gas sparging [3] have been used as a cleaning method for fouling during natural rubber skim latex. However, a scientific understanding of fouling behavior during ultrafiltration of skim latex is necessary to optimize its performance [5, 7-10]. In the case of natural rubber skim latex, fouling behavior can be attributed to the presence of naturally-occurring proteins. The extent of fouling mechanisms on flux decline are depend on various factors such as pore size, particle size distribution, membrane material and operating parameters (cross-flow velocity, transmembrane pressure, solution ionic strength, etc.).

Earlier studies have shown the possibility of using membrane separation technology in processing skim latex. In this study, a bench scale crossflow filtration unit using single channel tubular ceramic membranes was used to study the effect of crossflow velocity and transmembrane pressure on skim latex ultrafiltration. The effects of crossflow velocity and transmembrane pressure on filtration performance and filtration resistance are analyzed. Membrane fouling index and fouled layer resistivity are also calculated in order to study fouling mechanism.

2. Materials and Methods

2.1. Materials

Skim latex was used as feed solution. The skim latex obtained was stabilized with suitable preservative solution to prevent premature coagulation during storage time before filtration process. Single channel ceramic tubular membranes with pore size 0.05µm, inner diameter 7mm, outer diameter 10mm and length 250mm were used in this study. The ceramic membrane were made up of aluminium oxide (Al_2O_3).The ceramic membrane was encased in the stainless steel module in the filtration rig as shown in fig. 1 below. The bench scale filtration unit is included a membrane housing, a peristaltic pump, an analytical balance and two oil-filled type pressure gauges were fitted at inlet and outlet of the module to measure the feed flow pressures. The flow pressure was adjusted by using a flow control valve and indicated on the pressure gauge at the inlet and outlet of the module.

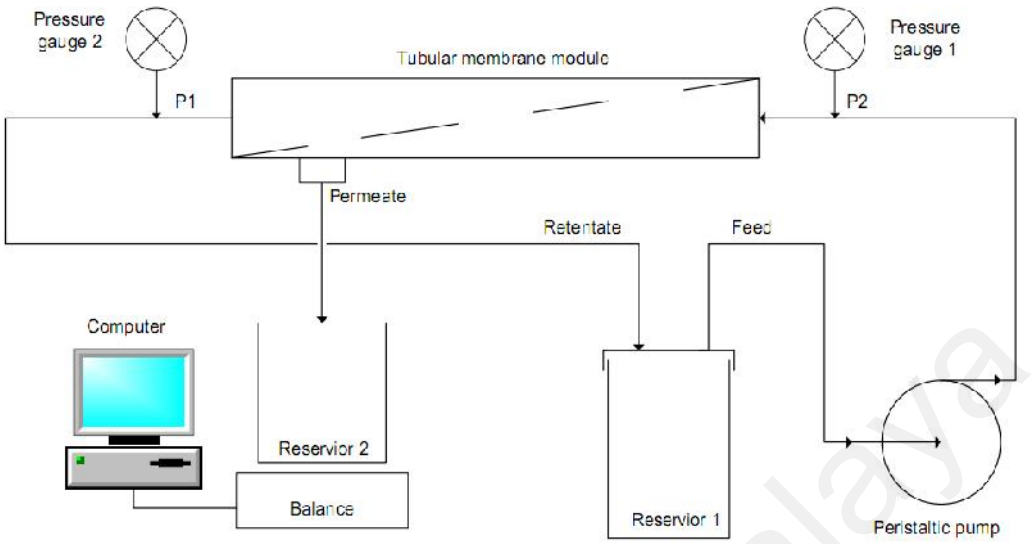

Fig. 1. Schematic diagram of the bench scale crossflow ultrafiltration unit.

2.2. Filtration of experiments

For each new membrane, before experiment, pure water flux tests were carried out over a range of transmembrane pressures in order to determine its water permeability. The crossflow velocity was set at 3.3cm/s.

For filtration of skim latex, each experiment was carried out using 500ml skim latex at temperature 25°C. Skim latex was circulated in the system using a peristaltic pump with variable speed which allowing study of a range of crossflow velocity can be carried out. Applied pressure was adjusted by using a flow control valve. The crossflow velocity is between 1.3cm/s to 4.6cm/s and the transmembrane pressure was in the ranged of 0.3bar to 1.3bar.

Retentate was recycled back to the feed solution in order to reticulate in the system. Permeate was collected directly onto a digital balance which connected to a computer. Flux was measured by monitoring the mass of collected permeate before recirculate back to the feed tank in order to maintain the feed solution concentration. The experiments were performed at various crossflow velocity and transmembrane pressure. The experiments were carried out for 160

minute each until a pseudo steady state reached. Filtration resistances were determined from the pseudo steady state permeates flux using Darcy's Law.

2.3. Determination of membrane resistance before and after ultrafiltration of skim latex

Membrane resistance and filtration resistance is determined using Darcy's Law:

$$J = \frac{\Delta P}{\mu R}$$

where R is the filtration resistance, ΔP is the pressure gradient, μ is the viscosity of the solution and J is the permeate flux obtained.

Membrane resistance, R_m, is determined by using the initial water flux test. The membranes were subjected to water filtration at transmembrane pressure 0.5bar and crossflow velocity 3.3 cm/s. Membrane resistance was calculated through Darcy's Law. The membranes resistances are constant and not affected by fouling during ultrafiltration.

After filtration process, membrane is rinsed with pure water flux to remove all traces of skim latex. The membrane total resistance, R_t, was determined by subjected the membrane to water filtration test. Total resistance obtained the results of the membrane initial resistance (R_m), reversible cake fouling resistances (R_c) and irreversible fouling resistance (R_f) as shown in equation below.

$$R_t = R_m + R_c + R_f$$

The membrane was then cleaned by rinsing it with 2% sodium hydroxide solution and deionized water thoroughly in order to remove any deposition on membrane surface (reversible cake fouling). The cleaning procedure was repeated until no further increases in water permeate flux. Membrane resistance after cleaning is determined. Internal fouling resistance can be determined based on the assumption that cake layer is effectively removed through cleaning. The difference of filtration resistance before and after cleaning is taken as reversible cake fouling resistance (R_c).

3. Results and Discussion

3.1. Typical filtration performance

Based on the results obtained, at both 1.3cm/s and 4.6cm/s, permeate flux decreases drastically at the initial period of time and then gradually reached pseudo steady state as filtration time exceeding 2000s (fig. 2). The initial rapid reduction in permeate flux implies that the most severe fouling is occurred at the initial stage [11]. The reduction in permeate flux with filtration time is basically caused by the buildup of fouling layer on membrane surface which increases the filtration resistance as shown in fig. 2 (resistance ratio versus filtration time). According to Waniek et al, the dependency of permeate flux on time at the initial stage is related to irreversible fouling developed [12]. As filtration prolonged, particles larger than the membrane pores start to block the pores and reduce the available membrane area for filtration. Thus, particles start to accumulate and deposit on surface to form polarization layer [13]. More particles were retained as the hydraulic resistance increases.

As fouling increased with filtration time, resistance analysis showed that filtration resistance increases rapidly initially and then reached a pseudo steady state as in fig. 3. The change in filtration resistance is similar to that in the study of Blanpain-Avet et al and Purkait et al [14, 15]. The rapid increased in filtration resistance resulted in the drastic reduction in permeate flux. As filtration continued, the concentration of accumulated or deposited particles on membrane surface increased reached a critical point. At this point, the particle deposition rate is equal to the particles back diffusion rate. Thus, no further fouling occurred at this point and permeates flux and resistance had reached an almost constant state. At this point, further growth of fouling layer is restricted by the solution axial shear stress applied upon the fouled layer [16].

3.2. Effects of transmembrane pressure on filtration performance at crossflow velocity 4.6cm/s

Fig. 2 is the plot of permeate flux versus filtration time at constant crossflow velocity 4.6cm/s. The plot shows that the initial permeate flux is decreased upon the increased of transmembrane pressure. High convection force as applied pressure increased had caused large amount of particles brought to the membrane surface simultaneously and caused particles to accumulate and deposit to form cake layer [17]. Formation of cake layer had reduced the tendency of particles to penetrate into the membrane pores and also the effective membrane. This had caused increases the filtration resistance (fig. 4) and reduction of the volume of permeate pass through the membrane. As the particle convection force is increased upon the increases of transmembrane pressure, the rate of cake layer formation is also speed up. Consequently, the rates of attenuation of permeate fluxes also increased with transmembrane pressure. Due to more severe fouling, permeate fluxes at pseudo steady state is also decreasing with the increases of transmembrane pressure (fig. 3). The obtained results are similar to the results in the previous studies [18-21].

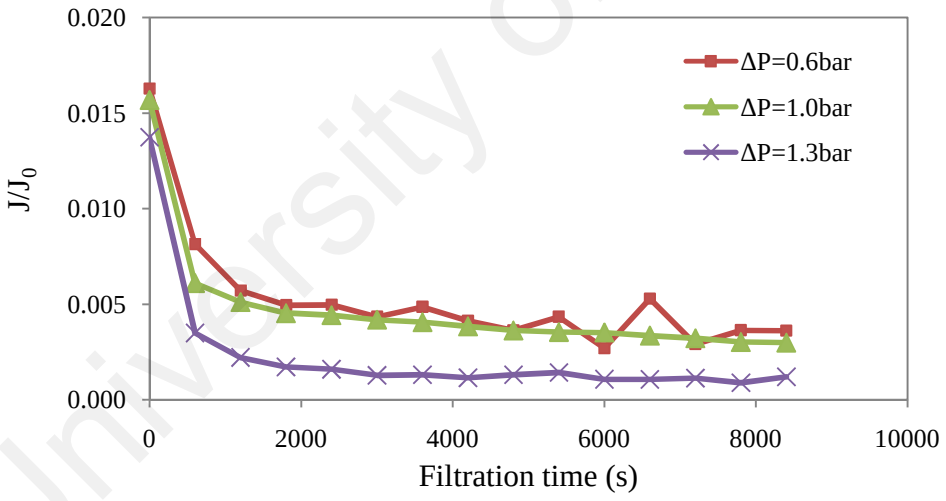

Fig. 2. Normalized filtration permeate flux time course during filtration of skim latex at constant crossflow velocity 4.6cm/s.

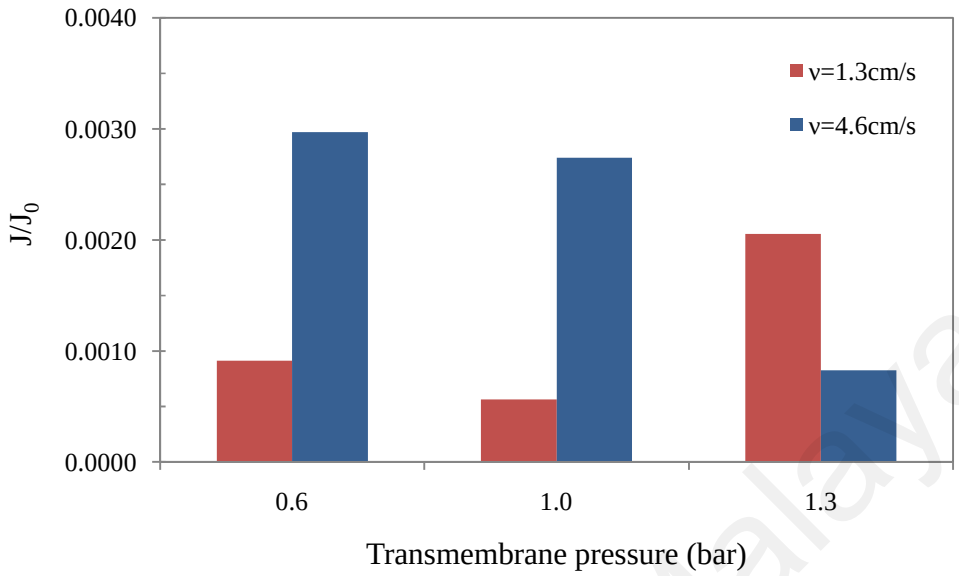

Fig. 3. Variation of normalized permeate flux at pseudo steady state during filtration of skim latex at constant crossflow velocity 4.6cm/s.

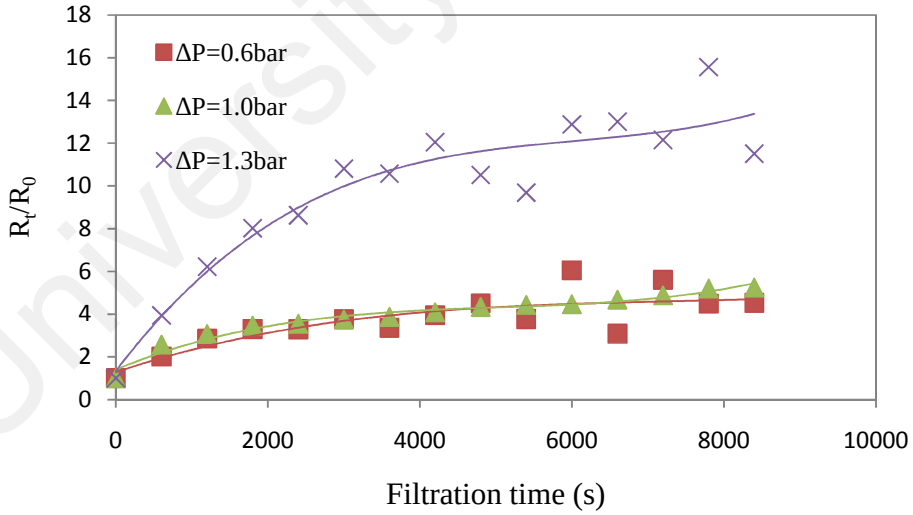

Fig. 4. Normalized filtration resistance time course during filtration of skim latex at constant crossflow velocity 4.6cm/s.

In ultrafiltration process, fouling is contributed to the combination of different fouling mechanisms [22]. Reversible and irreversible fouling resistance is studied by measure the membrane resistance after ultrafiltration of skim latex. As in table 1, the analysis of fouling resistance showed that reversible fouling is predominant (>99% of total resistance), which is mainly contributed to the formation of cake layer, compare to irreversible fouling resistance (<1%) [20]. Reversible fouling resistance in increased with transmembrane pressure at crossflow velocity 4.6cm/s. Thus, the increase in filtration resistance is mainly due to the change in reversible fouling instead of irreversible fouling. However, the effect of transmembrane pressure on irreversible fouling resistance is not significant.

A plot of the d*t/dv* versus *v* was shown in fig. 5. The curve at transmembrane pressure 1.3bar shaped concave downward, i.e. the curve of slope is increased rapidly initially and then slowly decreases. The curve at transmembrane pressure 0.6bar and 1.0bar give an almost linear curve. The slope of the regression line of the linear region is taken as the value of membrane fouling index (MFI). Resistivity, I, can be calculated from membrane fouling index values obtained using equation as shown below:

$$MFI = \frac{\eta . I}{2\,\Delta P . A^2}$$

where MFI is the membrane fouling index obtained, η is the solution viscosity, I is the resistivity, ΔP is the pressure gradient and A is the effective membrane area. The analysis of *dt/dv* versus *v* (filtration volume) shows that MFI and I are increased as applied pressure increased (table 2). MFI is increased upon the increase of pressure implies that fouling potential is higher as transmembrane pressure increased. The result is in parallel with the analysis of permeate flux performance and fouling resistance results obtained. The increase in particles convection forces with transmembrane pressure has caused more particles to foul on membrane surface and increases the fouling potential. Thus, fouled layer resistivity is higher as fouled layer is increased with transmembrane pressure.

Table 1

Resistance analysis of the ultrafiltration of skim latex at crossflow velocity 1.3cm/s and 4.6cm/s.

Crossflow velocity (cm/s)	Transmembrane pressure (bar)	R_c/R_m	%	R_f/R_m	%
1.3cm/s	0.6bar	272.81	99.5	1.25	0.5
1.3cm/s	1.0bar	1756.39	99.9	1.59	0.1
1.3cm/s	1.3bar	1071.25	99.8	1.90	0.2
4.6cm/s	0.6bar	207.49	99.1	1.81	0.9
4.6cm/s	1.0bar	370.41	99.7	1.29	0.4
4.6cm/s	1.3bar	1003.75	99.9	1.35	0.1

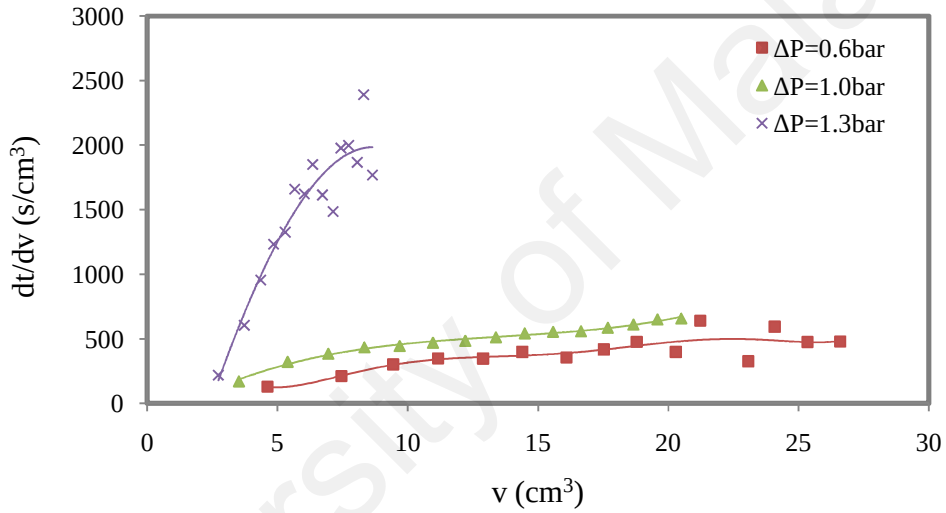

Fig. 5. MFI analysis of the ultrafiltration of skim latex at constant crossflow velocity 4.6cm/s.

Table 2

Membrane fouling index at various operating parameter.

CFV (cm/s)	TMP (bar)	MFI ($s.cm^{-6}$)	Resistivity, I x 10^{11} (cm^{-2})
1.3	0.6	550.0	8.14
	1.0	480.0	12.24
	1.3	7.1	0.24
4.6	0.6	16.7	0.59
	1.0	18.2	1.10
	1.3	400.0	31.53
1.3	0.3	708.3	5.42
3.6		62.5	0.96
4.6		229.2	4.17
1.3	1.0	480.0	12.24
3.6		278.9	14.33
4.6		18.2	1.10

3.3. Effects of transmembrane pressure on filtration performance at crossflow velocity 1.3cm/s

At crossflow velocity 1.3cm/s, initial permeate shows different trend compare to as at crossflow velocity 4.6cm/s. Initial permeate flux is increasing upon the increase of transmembrane pressure at crossflow velocity 1.3cm/s (fig. 6). This may because the increase in transmembrane pressure had increased the particles convection force to pass though the membrane. The result obtained is different from that at higher crossflow velocity (4.6cm/s) is probably due to the fact that increase of crossflow velocity also tend to increase the internal pressure in the module and cake layer formed faster [23]. Experimental result as shown in fig. 2 indicates that permeate flux at pseudo steady state is decreased slightly and then increased upon the increases of transmembrane pressure. As in previously studies, permeate flux is inversely dependence on filtration resistance. Filtration resistance is increased as transmembrane pressure increased from 0.6bar to 1.0bar (fig. 7). However, as transmembrane pressure exceeds 1.0bar, filtration resistance tends to decrease. As mentioned before, the change in filtration resistance is mainly due to the change in reversible fouling resistance as in table 1. Meanwhile, irreversible is

almost constant throughout the range of transmembrane pressure. Reversible fouling is increased as transmembrane due to more particles were brought to the membrane surface to form cake layer. However, as transmembrane pressure increased further, the average fouled layer particles size is increased and thus cake layer porosity also higher. SEM images of fouled membrane surface at transmembrane pressure 0.9bar and 1.3bar and constant crossflow velocity 3.3cm/s were shown in fig. 8. The images show that fouled layer porosity is more obvious to be seen at higher transmembrane pressure. Low porosity cake layer impedes lower filtration resistance.

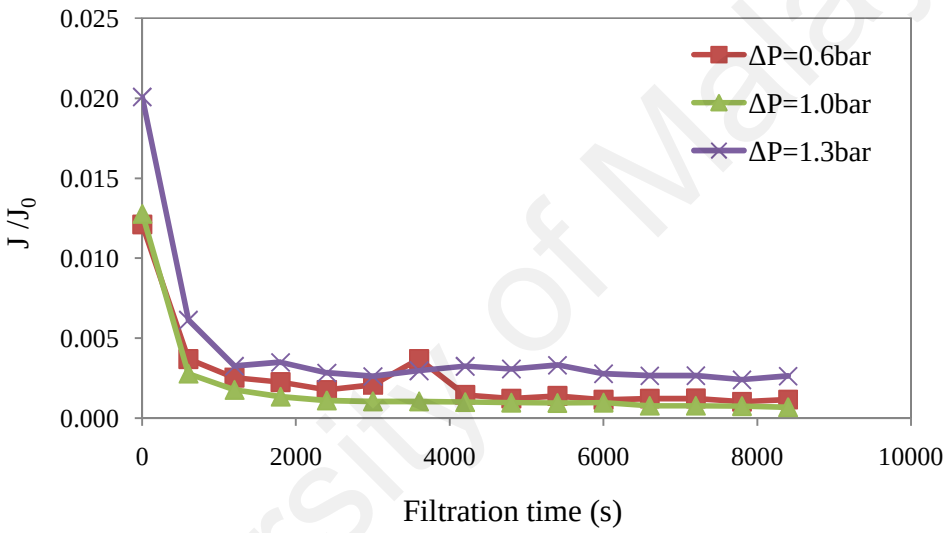

Fig. 6. Normalized filtration permeate flux time course during filtration of skim latex at constant crossflow velocity 1.3cm/s.

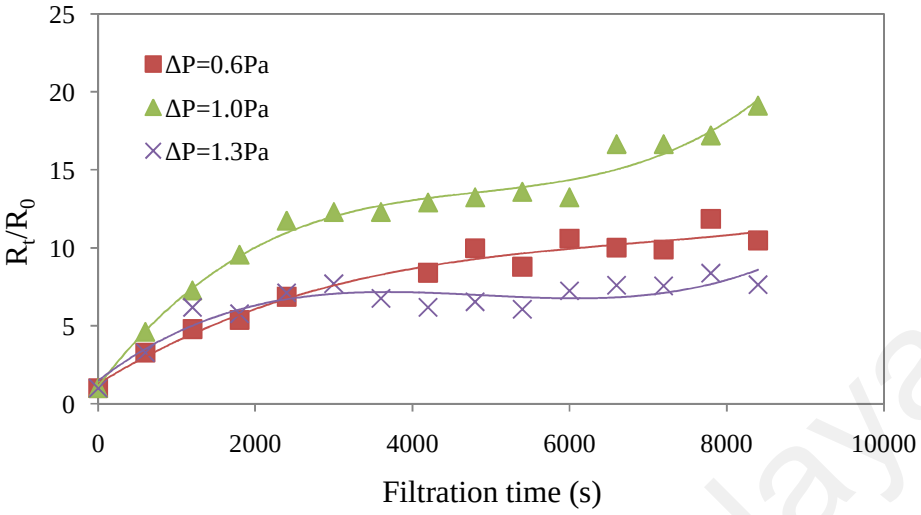

Fig. 7. Normalized filtration resistance time course during filtration of skim latex at constant crossflow velocity 1.3cm/s.

(a) (b)

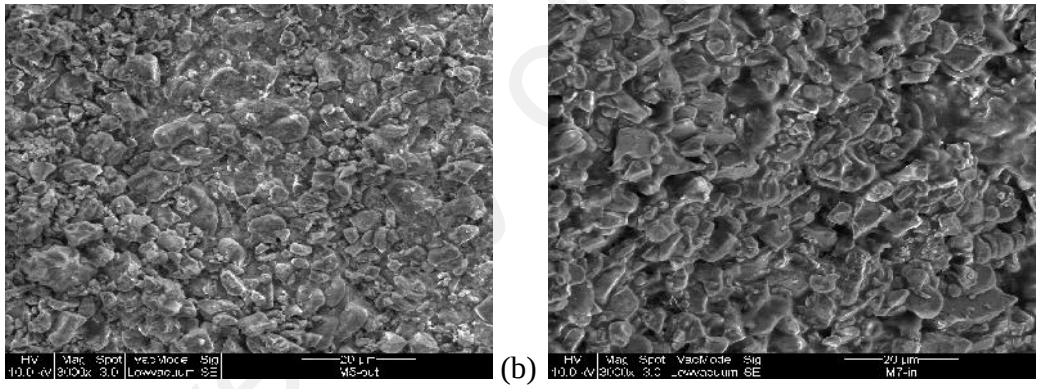

Fig. 8. SEM images of fouled membrane surface under crossflow velocity 3.3cm/s and transmembrane pressure (a) 0.9bar and (b) 1.3bar.

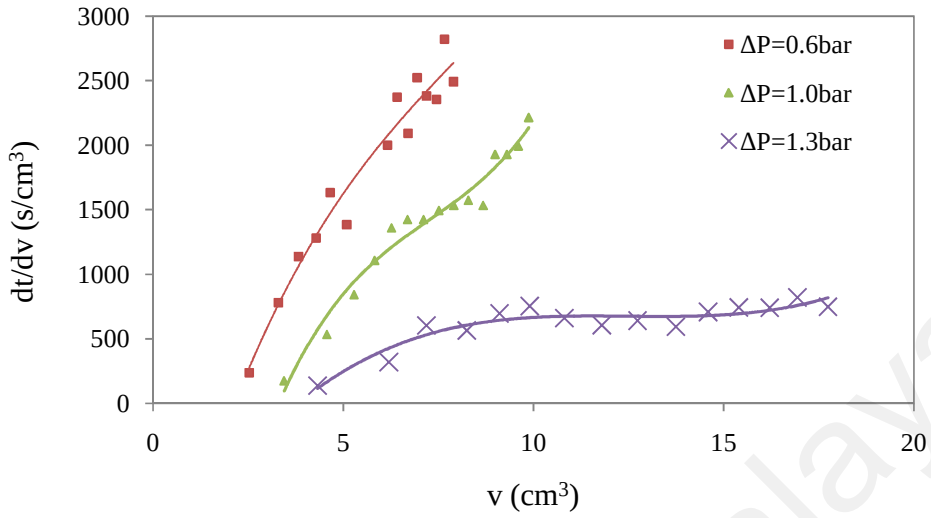

Fig. 9. MFI analysis of the ultrafiltration of skim latex at constant crossflow velocity 1.3cm/s.

A plot of the *t/V* versus *V* at crossflow velocity 1.3cm/s was shown in fig. 9. MFI is decreased slightly as applied pressure increases from 0.6bar to 1.0bar and then decrease drastically as transmembrane pressure increase further to 1.3bar. The result implies that fouling potential of cake layer is decreased with pressure. However, resistivity is increased as applied pressure increase from 0.6bar to 1.0bar. As transmembrane pressure increased further, resistivity starts to decrease due to more porous fouled layer formed. The result is consistent with the analysis of fouling resistance previously. Thus, at crossflow velocity 1.3cm/s, as transmembrane pressure increases, fouling potential is decreased. However, resistivity might change due to the structure of cake layer formed.

4. Conclusion

The effect of transmembrane pressure and crossflow velocity in ultrafiltration performance of skim latex were studied. The filtrations performances have similar trends, i.e. filtrations start with high initial permeate flux, and then decrease rapidly with time and reached pseudo steady state where permeate flux is almost constant. It had been shown that transmembrane pressure and crossflow velocity do affects the ultrafiltration process in terms of initial permeate flux, decay rate and filtration at pseudo steady state. However, the effect of transmembrane pressure in slightly different as in crossflow velocity 1.3cm/s and 4.6cm/s. At crossflow velocity 4.6cm/s, initial permeate flux and flux at pseudo steady state is reducing with the increase of transmembrane. This is because the increases of transmembrane pressure had caused the increase in filtration resistance as particles convection force increased with transmembrane pressure. It had caused the more particles to foul on membrane surface. The rate of cake layer formation also increases with transmembrane pressure. Thus, the analysis of MFI also implies that fouling potential and resistivity is positively dependent on transmembrane pressure.

At crossflow velocity 1.3cm/s, the trend is slightly different due to the change in fouled layer structure with transmembrane pressure. It was found that as transmembrane pressure exceeds 1.0bar, large particles tends to fouled in cake layer and thus increase the fouled layer porosity. As a consequences, filtration resistance is decreasing and permeate flux is improved. It can be observed in the analysis of fouling index, although fouling potential is increasing with applied pressure, resistivity might changed due to the change in fouled layer structure.

As a conclusion, both transmembrane pressure and crossflow velocity do affect the ultrafiltration performance of skim latex. However, further studies need to carry out in order to understand the fouling mechanism and to optimize the filtration performance.

References

[1] S.A. Mourouzidis-Mourouzis, A.J. Karabelas, Journal of Membrane Science 282 (2006) 124-132.

[2] D. Veerasamy, N.M. Sulaiman, J. Nambiar, Y. Aziz, pp.1 - 7.

[3] H.N. Sulaiman, M.K. Arous, Songklanakarin J. Sci. Technol. 24 (2002) 947-953.

[4] D. Datta, C. Bhattacharjee, S. Datta, IE(I) Journal-CH Vol 89 (2008) 45 - 50.

[5] M.O. Lamminen, H.W. Walker, L.K. Weavers, Journal of Membrane Science 237 (2004) 213.

[6] V. Veerasamy, A. Supurmaniam, Z.M. Nor, Desalination 236 (2009) 202-207.

[7] D. Veerasamy, N.M. Sulaiman, J. Nambiar, Y. Aziz, (2003) pp.1 - 7.

[8] S. Novalic, G. Heisler, J. Lahnsteiner, Journal of Membrane Science 130 (1997) 1-5.

[9] K. Konieczny, M. Bodzek, Desalination 104 (1996) 75-82.

[10] R.G. Holdich, G.M. Zhang, The Chemical Engineering Journal 60 (1995) 31-37.

[11] K.J. Hwang, P.Y. Sz, Journal of Membrane Science 347 (2010) 75 - 82.

[12] A. Waniek, M. Bodzek, K. Konieczny, Polish Journal of Environmental Studies Vol. 11 (2002) 171-178.

[13] E.E. Chang, S.-Y. Yang, C.-P. Huang, C.-H. Liang, P.-C. Chiang, Separation and Purification Technology 79 329-336.

[14] P. Blanpain-Avet, N. Doubrovine, C. Lafforgue, M. Lalande, Journal of Membrane Science 152 (1999) 151-174.

[15] M.K. Purkait, P.K. Bhattacharya, S. De, Journal of Membrane Science 258 (2005) 85-96.

[16] P. Mikulasek, R.J. Wakeman, J.Q. Marchant, Chemical Engineering Journal 69 (1998) 53-61.

[17] M.K. Purkait, S. DasGupta, S. De, Journal of Colloid and Interface Science 270 (2004) 496-506.

[18] J.K. Thomassen, D.B.F. Faraday, B.O. Underwood, J.A.S. Cleaver, Separation and Purification Technology 41 (2005) 91-100.

[19] K.-J. Hwang, P.S. Huang, Separation and Purification Technology 68 (2009) 328-334.

[20] I. McGuire, K. Coyle, G. Foley, Journal of Membrane Science 344 (2009) 14-16.

[21] G.T. Vladisavljevic, P. Vukosavljevic, B. Bukvic, Journal of Food Engineering 60 (2003) 241-247.

[22] D.-O. Chase, W. Li, C.-C. Ho, Journal of Membrane Science 280 (2006) 856-866.

[23] Y.-S. Chen, S.-S. Hsiau, Chemical Engineering and Processing: Process Intensification 48 (2009) 988-996.